Cellular and Gene Therapies for the Enhancement of Peripheral Nerve Regeneration through Bio-Engineered Nerve Conduits

Mel Patrick Tohill BMedSc(Hons) MB BCh BAO MRCS(Ed)

A Thesis submitted for the Degree of Doctor of Philosophy (Plastic Surgery)

The Blond McIndoe Centre

The Royal Free and University College Medical School

University College London

ProQuest LLC
789 East Eisenhower Parkway
P.O. Box 1346
Ann Arbor, MI 48106-1346

To my wife, Jacqueline,

for her constant love, support, encouragement and patience.

To my son, Malachy, the light of my life.

And to my Parents,

for their love and for giving me every opportunity in life.

ABSTRACT

Despite optimal surgical management the functional outcome following peripheral nerve injury remains poor. Experimental adjuvant treatments have been developed to enhance peripheral nerve regeneration including the use of bio-engineered conduits, cellular transplantation, the addition of growth factors and modulation of the extra-cellular matrix.

Transplantation of cultured Schwann cells (SCs) improves regeneration through bio-engineered conduits. To improve the localisation of transplanted cells in combination with fluorescent immunohistochemical techniques SCs were retrovirally transduced with green fluorescent protein (GFP). GFP-SCs were found to have similar growth and vitality characteristics in comparison with non-transduced cells and following *in vivo* transplantation were easily identified and enhanced nerve regeneration.

Bone marrow stromal cells (MSCs) are capable of unorthodox plasticity. Their abundance, ease of access and culture make them potential substitutes for SC transplantation. Following exposure to glial growth factor, MSCs exhibited phenotypical and morphological characteristics of SCs. Following *in vivo* transplantation these cells were also found to confer a beneficial effect on nerve regeneration.

Neurotrophic factors enhance nerve regeneration however delivery at the site of injury is problematic. The use of gene therapy to provide growth factors at the site of injury may overcome this problem. A splice variant of the IGF-1 gene, Mechano-Growth Factor (MGF) was delivered to the site of peripheral nerve injury and functional and histological measures of regeneration were assessed at 14 weeks. It was found that delivery of the MGF cDNA at the site of injury improved target muscle function and total axon number in regenerating nerves.

Extracellular matrix macromolecules are important constituents of the peripheral nerve. The addition of fibronectin, laminin, and collagen substrata were found to enhance SC growth *in vitro*. Coating nerve guidance fibres with these molecules within a peripheral nerve conduit was also found to enhance nerve regeneration and influence the expression of the cell adhesion molecules NCAM and N-cadherin.

DECLARATION

I, Mel Patrick Tohill, confirm that the work presented in this thesis is my own. Where information has been derived from other sources, I confirm that this has been indicated in the thesis.

CONTENTS

CHAPTER 1

Introduction

CHAPTER 2

Materials and Methods

LIST OF FIGURES

LIST OF TABLES

LIST OF ABBREVIATIONS

α-MEM	α-modified Eagle medium
Ara C	Cytosine-ß-D-arabinoside
BDNF	Brain derived neurotrophic factor
cAMP	Cyclic adenosine monophosphate
cDNA	Complementary deoxyribonucleic acid
CNS	Central nervous system
CNTF	Ciliary neurotrophic factor
DMEM	Dulbecco's modified Eagle medium
DMSO	Dimethylsulphoxide
DRG	Dorsal root ganglia
ECMM	Extracellular matrix
EM	Electron microscopy
FCS	Fetal calf serum
FGF	Fibroblast growth factor
GFAP	Glial fibrillary acidic protein
GFP	Green fluorescent protein
GGF	Glial growth factor
IGF-1	Insulin-like growth factor
LIF	Leukaemia inhibitory factor
LVM	Low viscosity mannuronic acid
MGF	Mechano-growth factor
MMLV	Moloney Murine Leukaemia Virus
MSC	Marrow stromal cell
MVM (alginate)	Medium viscosity mannuronic acid
NT-3/4/5	Neurotrophin-3/4/5
ntSC	Non-transduced Schwann cell
NCAD	N-cadherin
NCAM	Neural cell adhesion molecule
NGF	Nerve growth factor
PBS	Phosphate buffered saline
PDL	Poly-D-lysine
PDGF	Platelet-derived growth factor
PGP	Protein gene product
PHB	Polyhydroxybutyrate
PKA	Protein kinase A
PNS	Peripheral nervous system
SC	Schwann cell
TA	Tibialis anterior
Trk	Tropomyosine kinase

ACKNOWLEDGEMENTS

I owe a great debt of gratitude to my supervisor, Professor Giorgio Terenghi, for giving me the opportunity to work in his laboratory, for his inspiration, guidance, support, friendship and endless patience. It has been a privilege to have worked in the Blond McIndoe laboratories.

I would like to thank Professor Mikael Wiberg (Umeå University, Sweden) for his invaluable guidance, insight and constructive criticism. I am also grateful for the warm hospitality shown by Professor Wiberg and his staff during my visits to Sweden.

I would also like to thank the following people:
Miss Cristina Mantovani: For her technical expertise and help in the laboratory, for her time, dedication, attention to detail, and kindness.

Dr Elizabeth James and Mrs Dawn Mann (Queen Victoria Hospital, East Grinstead): For their help and instruction in all aspects of tissue culture.

Professor Geoffrey Goldspink, Dr ShiYu Yang and Mr David Sutton (Department of Anatomy, Royal Free and University College Medical School): For the use of their laboratory and assistance in recording and interpreting myophysiological data.

Dr Susan Shawcross: For her technical help and advice in all things scientific, for her assistance in the laboratory, and above all, friendship.

Dr Jan Egil Melvik (Pronova Biomedical, Oslo, Norway): For instruction in manufacturing alginate beads.

The Blond McIndoe Research Fellows: Andrew Wilson, Pari Mohanna, Martin Thornton, Magda Simon (Post-doctoral Fellow), Ash Mosahebi, Bernadine Idowu, and Jenny Caddick, for their help, support and friendship.

Chapter 1

Introduction

"There is a single light of science, and to brighten it anywhere is to brighten it everywhere"

Isaac Asimov

1.1 The clinical importance of peripheral nerve injury

In England alone in the period 2005-2006 there were approximately 4,300 peripheral nerve injuries requiring emergency hospital admission and subsequent surgical intervention within the NHS (Hospital Episode Statistics 2005-2006, Department of Health – www.hesonline.nhs.uk). These injuries are most commonly seen in young adult males following accidental and self-inflicted lacerations, road traffic accidents, penetrating trauma, falls and industrial accidents, with nerves of the upper limb especially at the level of the wrist, palm and digits being more frequently affected than those of the lower limb (Evans, 2001; Noble et al. 1998). It is unfortunate that the greatest expansion in our knowledge of the clinical presentation of peripheral nerve injury, the development of surgical management paradigms and the prognosis of functional recovery is as a result of modern warfare when serious injuries present more frequently (Sunderland, 1978). Despite great technical developments in surgical technique, functional recovery from such injuries remains poor, often leading to economic implications for an otherwise fit and healthy individual. Peripheral nerve injuries require specialist care by plastic surgeons who perform over 50,000 nerve repairs each year in the United States alone (Evans, 2001). In the most severe nerve injuries it is necessary to replace irreparably damaged nerve tissue with an autologous graft. In a series of over 1,000 peripheral injuries treated at a regional plastic surgery unit in the south-east of England it was found that approximately 7% of the total number of injuries assessed required nerve grafting. It was also shown that when there was a delay in referral of a nerve injury to a specialist

centre up to 63% of these injuries required either a primary or secondary grafting procedure (McAllistair et al. 1996).

1.2 Anatomy of the peripheral nerve

The peripheral nervous system is a highly specialised and organised structure which is responsible for relaying information to and from the central nervous system. The fundamental unit is the peripheral nerve fibre which is composed of a cytoplasmic extension of a sensory, motor or sympathetic neuron (the axon) supported by Schwann cells, and extracellular matrix components which compose the basal lamina and an inner endoneurial sheath. Axons vary from a few millimetres to a metre in length and from 0.2μm to 20μm in diameter. An axon consists of a cytoskeleton formed by neurofilaments and neurotubules, contained within a membrane, the axolemma. Within this there is a viscous fluid, the axoplasm, and a number of subcellular structures including mitochondria, endoplasmic reticulum, and granular vesicular structures. Axons not only conduct electrical impulses from and to the central nervous system but they also permit the retrograde or anterograde transport of proteins to and from the cell body respectively (Sunderland, 1978). Schwann cells (SCs), the glial cells of the peripheral nervous system, surround and support axons. In unmyelinated axons, chains of SCs support and separate multiple small diameter axons by enveloping them with extensions of the cell cytoplasm. In a myelinated fibre SCs produce a multilayered sheath of myelin which surrounds an individual axon. The SC nucleus and cytoplasm lies outside the myelin sheath and rests externally on a basement membrane. At regular points the SC cytoplasm comes into direct

contact with the axon, slightly constricting the axon at these points to form the nodes of Ranvier. Nodes of Ranvier provide entry points for extracellular ions which facilitate the saltatory propagation of impulses from node to node (Sunderland, 1978). Nerve fibres, separated by endoneurial sheaths, are grouped together to form fascicles that are surrounded by a perineural sheath. Each nerve trunk is composed of a number of fascicular bundles which are themselves surrounded by the epineurium, a loose connective tissue which also supports blood vessels and lymphatic vessels (Lundborg, 1988). Fascicular bundles are segregated into afferent motor fibres and efferent sensory fibres, correct apposition of these fibres is important following axotomy (Terzis & Smith, 1990). Nerve fibres can be classified according to their thickness and conduction velocities, namely an *A* group of large myelinated fibres, a *B* group of small thinly myelinated fibres and a *C* group of unmyelinated fibres (Erlanger & Gasser, 1924).

1.3 Pathophysiology following peripheral nerve injury

A complex chain of events follow traumatic peripheral nerve injury which, depending on the severity of the injury, leads to Wallerian degeneration and ultimately axonal regeneration.

1.3.1 Classification of peripheral nerve injuries

The consequences of damage to a nerve fibre depend on the nature, site and severity of the injury. Localised damage to nerve fibres was originally classified by Seddon in 1947 and Sunderland in 1951 and has now been expanded to include

6 categories (Brandt & Mackinnon, 1997). The underlying principle behind the classification is whether or not the connective tissue surrounding fibres remains intact. *First-degree injury (neuropraxia)*: A localised conduction block in which axon integrity is maintained although there may be focal demyelination. Full recovery is expected. *Second-degree injury (axonotmesis)*: Axonal injury occurs, however overall connective tissue architecture and continuity is maintained. The distal segment undergoes Wallerian degeneration followed by regeneration from the proximal segment. Complete recovery is expected unless end-organ atrophy ensues prior to reinnervation. *Third-degree injury*: As for a second degree injury although regeneration impeded by partial scar formation. *Fourth-degree injury*: As for a second degree injury but scarring completely impedes regeneration. *Fifth-degree injury (neurotmesis)*: Complete division of a peripheral nerve, requires surgical apposition for regeneration to proceed. *Sixth-degree injury*: A combination of any of the above levels of injury at multiple sites in the course of a nerve.

1.3.2 Wallerian degeneration

The term Wallerian degeneration has been used to describe the histological changes seen in the peripheral nerve following crush and axotomy injuries after the observations of Waller (1850) and other pioneers in this field including Ranvier, Von Bünger and Cajal. A complex cascade of events occur which involve changes in the neuronal cell body, the axon and its associated SCs. Upon disruption of an axon at the site of injury axoplasm leaks from the cut ends, axolemmal membranes collapse and the proximal and distal stumps retract. By

12-48hrs mitochondria collect in the nodal regions, myelin retracts from the node, neurofilaments become disarranged and the axoplasm becomes filled with granular material (Williams & Hall, 1971). Wallerian degeneration describes the degeneration of axonal architecture extending proximally to the first node of Ranvier and distally throughout the entire course of the nerve the purpose of which is to provide a permissive environment for nerve regeneration (Waller, 1850; Stoll et al. 1989). Following the breakdown of axonal and myelin constituents at the site of injury SC de-differentiation and proliferation occurs. Cellular debris is removed initially by local proliferating SCs, however this is accelerated by the infiltration of macrophages (Hall, 1993). Proliferating SCs align to form bands of Bünger between the proximal and distal stump, in addition to this they upregulate the synthesis of a number of important neurotrophic factors (cf. 1.8).

Following injury chromatolysis occurs in the neuronal cell body, this is characterised by cytoplasmic swelling, displacement of the cell nucleus to the periphery and the appearance of Nissl's granules (Sterman & Delannoy, 1985). If repair is not performed promptly up to 40% of sensory neuronal cells may die through apoptosis, this has long-term implications for functional recovery (Hart et al. 2002).

1.3.3 Axonal regeneration

Axons have intrinsic growth capacity following injury. If a neuronal cell body survives the initial insult of axotomy upregulation in the synthesis of cytoskeletal elements such as actin, tubulin and neurofilaments occurs in preparation for the onset of regeneration. At the site of injury several axonal branches sprout from the first proximal node of Ranvier within 24hrs. Following nerve injury cAMP levels rise which in turn stimulate PKA which in turn promotes the transcription of genes responsible for the assembly of cytoskeletal elements (Neumann et al. 2002). Injury also has a direct effect on the expression of c-Jun which leads to increased levels of integrin expression (Raivich et al. 2004). At the front of each regenerating axon a 'regeneration front' consisting of mobile filopodia (Seckel, 1990) responds to neurotrophic cues (cf. 1.8) and makes contact with the basal lamina and the SCs composing the bands of Bünger. Such dependence on chemical and physical cues imparts high tissue specificity for regenerating nerve fibres (Lundborg et al. 1986). Elongation of the proximal axon and distal progression of the regeneration front is associated with the production of cytoskeletal elements such as neurotubules and axolemmal membrane (Popov, 1993). Each axon produces several sprouts, but only one of these sprouts matures upon target organ contact, the remaining sprouts degenerate in a process described as 'pruning'. Sustained axonal regeneration is dependent on the creation of a 'permissive' environment. Regeneration within the CNS is poor as the presence of certain proteins e.g. myelin-associated glycoprotein (MAG) inhibits axonal regeneration. Within the PNS the scavenging of these proteins by SCs and

macrophages improves the 'permissive' nature of the environment for axonal regeneration.

1.3.4 Schwann cells and regeneration

An interdependence exists between regenerating axons and SCs. The latter provide structural and trophic support to regenerating axons, whilst axon-SC contact promotes proliferation, differentiation and maturation of SCs (Maurel & Salzer, 2000). It has been shown that preventing SC proliferation at the site of injury impairs axonal regeneration (Hall, 1986). Over the first days following injury, SCs in the distal nerve stump divide and upregulate the gene expression of the low affinity neurotrophin receptor p75; the neuregulin receptors; NCAM and L1 (Martini & Schachner, 1988; c.f. 1.4); laminin; cytokines (Kurek, 1996); and neurotrophic factors (cf. 1.8.2). Collectively these changes produce a population of axon-responsive SCs which facilitate axonal growth into the zone of injury. In SCs adjacent to regenerating axons a second wave of SC proliferation occurs, this precedes the formation of myelin (Pellegrino & Spencer, 1985), and a 1:1 relationship between myelinating SCs and axons is established (Mirsky & Jessen, 1999).

1.4 Cell adhesion molecules and the extracellular matrix

Axonal growth is highly stereospecifc, depending upon receptor molecules in the regeneration front interacting with extrinsic cues. These cues include soluble factors secreted by intermediate and final targets (Lumsden & Cohen, 2004),

components of the extracellular matrix (Reichardt & Tomaselli, 1991) and glycoproteins expressed on the surface of cells (Bixby & Harris, 1991).

1.4.1 Cell adhesion molecules and nerve regeneration

Cell adhesion molecules (CAMS) are important constituents of the receptor systems present on neuronal regeneration fronts and include the integrins (Reichardt et al. 1991), the immunoglobulin superfamily (Doherty & Walsh, 1992) and the cadherins (Takeichi, 1991). During growth, axon-SC interactions are mediated by cell adhesion molecules such as neural cell adhesion molecule (NCAM), L1, and N-cadherin, whereas axon-basal lamina contact is mediated by laminin and integrin interactions (Bixby & Harris, 1991).

In the developing nerve, expression of the immunoglobulins NCAM and L1 is seen at axon-SC contact points on the plasma membrane (Rathjen, 1988). With maturation this expression is significantly reduced in myelinated fibres but it is maintained in unmyelinated fibres (Martini, 1994). Following denervation, N-CAM and L1 are upregulated on SCs where they are in contact with each other in the SC column (Jessen et al. 1987). Upon contact with axons this expression becomes localised to the plasma membrane at the point of contact followed by temporal down-regulation as myelination develops as seen during development (Martini & Schachner, 1988; Rathjen, 1988). L1 has been shown to stimulate neurite outgrowth *in vitro* (Seilheimer & Schachner, 1998).

Cadherins are a family of Ca^{2+}-dependent cell-cell adhesion molecules which bind specific cells expressing the same cadherin (Takeichi, 1991). N-cadherin has been shown to stimulate neurite outgrowth on astrocytes

(Neugebauer et al. 1988) and on SCs (Letourneau et al. 1990), and it is found localised on the plasma membranes of axons and SCs during regeneration, but not between axons and basal lamina or SCs and basal lamina (Shibuya et al. 1995).

CAMs not only mediate adhesion between SCs and between SCs and axons but their activation can also trigger cytoplasmic signals via second messengers which ultimately lead to axonal growth. Low or high levels of intracellular Ca^{2+} levels can be inhibitory for neurite outgrowth (Kater & Mills, 1991). Antagonists of Ca^{2+} channels can inhibit CAM-dependent neurite outgrowth (Doherty et al. 1992) whereas direct activation of Ca^{2+} channels mimics CAM-dependent neurite outgrowth (Saffell et al. 1992).

1.4.2 Extracellular matrix

Signalling from the extracellular matrix, and in particular the basal lamina, plays an important role in supporting SCs and axons during development and axonal regeneration (Mirsky & Jessen, 1999). The basal lamina contains physiologically active molecules such as laminin and fibronectin within a collagen matrix, with laminin being the most potent adhesion molecule for promoting axonal outgrowth (Ide, 1996). Contact of axons and basal lamina is mediated by laminin-integrin binding (Letourneau et al. 1994) which promotes adhesion and motility of regeneration fronts through intracellular signal transductions (Bixby & Jhablava, 1990).

The aim of developing any bio-engineered system is to mimic as closely as possible the internal structural and molecular characteristics of the tissue being substituted. The addition of extracellular matrix macromolecules (ECMMs) such

as laminin, collagen and fibronectin to the structural scaffolds of peripheral nerve conduits may improve SC attachment and orientation, and as a consequence or independently, improve axonal growth. Laminin-coated micropatterned surfaces improve SC attachment and significantly improve unidirectional orientation *in vitro* (Thompson & Buettner, 2001) whilst laminin-coated poly (L-lactide) fibres promote directional neurite outgrowth *in vitro* (Rangappa et al. 2000). *In vivo* studies have shown that the addition of laminin to nerve conduits improves regeneration (Bailey et al. 1993).

Collagen is an important structural constituent of the extracellular matrix and it promotes Schwann cell adhesion, basal lamina deposition and neurite ensheathment *in vitro* (Obremski & Bunge, 1995). Several studies report a beneficial effect of using collagen gel matrices and filaments to bridge long nerve gaps (Chang et al. 1990; Chamberlain et al. 1998; Yoshii & Oka, 2001; Yoshii et al. 2001).

Fibronectin is a glycoprotein constituent of the extracellular matrix and addition of exogenous fibronectin stimulates Schwann cell proliferation and directional migration *in vitro* (Baron-Van Evercooren et al. 1982; Ahmed & Brown, 1999). Addition of fibronectin to nerve conduit matrices improves long-term regeneration (Bailey et al. 1993) and augments regeneration in conduits containing a mixture of fibronectin and transplanted SCs (Mosahebi et al. 2003). Conduits formed from fibronectin mats have been successfully used to guide regenerating axons and it has also been shown that these materials can be impregnated with neurotrophic factors (Whitworth et al. 1996).

1.5 Nerve repair

Following division of a peripheral nerve (neurotmesis) direct surgical apposition of the epineurium is required. In more complex injuries where nerve tissue is extensively damaged a gap may be created which prevents direct apposition of the proximal and distal stumps. In such cases nerve reconstruction is required and at present involves the interposition of autologous nerve tissue e.g. the sural nerve. Autologous nerve grafting was first described by Albert (1878), pioneered by Huber (1919) and Bunnell (1927), and achieved widespread acceptance following the surgical challenges faced during World War II (Sunderland, 1978). The harvesting of autologous nerve tissue for such purposes presents additional problems e.g. wound infection, scarring, loss of sensibility in the distribution of the donor nerve, neuroma formation, and the fact that there is a limited number of donor sites available which can be rapidly exhausted in a patient with multiple nerve injuries. With such limitations, attention has been drawn to the concept of an 'off the shelf' bio-engineered nerve graft made of a bio-compatible/resorbable material. Whilst surgical techniques have been optimised with the introduction of the operating microscope, functional recovery in ideal conditions remains poor (Mackinnon & Dellon, 1988). Hence research has also focused on experimental adjuvant treatments such systemic pharmacotherapy, transplantation of cells, administration of growth factors, addition of extracellular matrix macromolecules and gene transfer to maximise the regenerative capacity of the peripheral nervous system. This thesis concentrates on a number of experimental manipulations involving a biocompatible nerve graft.

1.5.1 Bio-engineered nerve conduits

The development of nerve conduits to span injury gaps has provided great insights into the physiological processes that occur in nerve regeneration (Hall, 2001). The conduit confines and directs axonal regeneration and prevents the influx of inflammatory cells and scarring. Materials used to construct nerve conduits may be either biological or synthetic, the latter receiving widespread interest in recent years.

Studies of biological materials started with Glück (1880) who used a section of artery to bridge the hypoglossal nerve in a dog, this was followed by the use of a vein by Platt (1919) and more recently by Ferrari et al. (1999). The use of artery and vein grafts for nerve conduits is however suboptimal because there is a limited supply of dispensable autologous vascular material. Muscle grafts have been used because it is possible to preserve the basal lamina structure following freezing (Glasby et al. 1986), but regeneration is still inferior to autografts and is poor over long gaps.

Some non-biological materials have also limited clinical applicability due to their lack of degradation. Lundborg et al. (1982) demonstrated good axonal regeneration through silicone conduits however long-term problems occurred due to irritation and rigidity of the conduit. With the expanding field of material science a number of biodegradable materials have emerged which have been used to construct conduits including fibronectin (Whitworth et al. 1995), collagen, polyglycolic acid (Matsumoto et al. 2000) and poly-3-hydroxybutyrate (Young et al. 2002).

Poly-3-hydroxybutyrate (PHB) is a biopolymer produced from 3-hydroxypropionic acid and is found as a natural storage product in many bacteria. Following fermentation and solvent extraction, PHB is polymerised into fine fibres which can be formed into sheets which in turn can be rolled into conduits. PHB is non-antigenic and bio-compatible, being resorbed through hydrolytic degradation over a period of approximately 24 months (Holmes, 1988). A number of experimental studies have demonstrated the ability of PHB conduits to support nerve regeneration *in vivo* (Hazari et al. 1999; Mosahebi et al. 2001; Mosahebi et al. 2002; Mosahebi et al. 2003; Mohanna et al. 2003; Mohanna et al. 2005). PHB sheets have been used clinically as pericardial patches (Duvernoy et al. 1992) and at present the material is being used in a multicentre trial evaluating their use as an adjunct to peripheral nerve repair.

1.5.2 Transplantation of Schwann cells

The pivotal role of SCs in nerve regeneration is well described (cf. 1.3.4). In experimental studies of regeneration through injury gaps, SC transplantation has been shown to improve regeneration, an effect most likely due to release of neurotrophic factors, contact guidance through the expression of cell adhesion molecules, and to synthesis of extracellular matrix (Guenard et al. 1992; Levi et al. 1994; Mosahebi et al. 2001; Mosahebi et al. 2002; Mosahebi et al. 2003; Rodriguez et al. 2000). The interaction of transplanted SCs with regenerating axons and their distribution throughout the conduit has been described following the incorporation of labelling techniques (Mosahebi et al. 2001). The use of

transplanted SCs as a source of recombinant neurotrophins within conduits also represents an attractive therapeutic concept (Sørensen et al. 1998).

1.6 Cell labelling for transplantation studies

Labelling of cells transplanted in a bio-engineered system allows the assessment of their survival and integration within the host upon histological analysis. The ideal cell label would be stable for long periods of time, not be diluted with cell division and not be immunogenic. Cell labelling may be endogenous or exogenous. Endogenous cell labelling is integrated with phenotypic expression, for example, male cells in female hosts identified by their Y chromosome (O'Leary & Blakemore, 1997) allografts or xenografts identified by strain- or species-specific antigens (Jacque et al. 1986), or genes for reporter molecules such as *lacZ* introduced into the genome via DNA transfer techniques (Guenard et al. 1999; Mosahebi et al. 2001). Exogenous labelling involves chemically tagging a component of the cell such as the cytoplasm, cell membrane or nucleus with a radioactive probe or fluorescent dye such as Hoechst 33342 and PKH26. However, these labels are diluted with cell division and leaching can occur from transplanted cells resulting in labelling of the hosts cells (Iwashita et al. 2000). In addition, some labelling methods have been shown to reduce long-term cell viability (Mosahebi et al. 2000). A more stable labelling has been obtained by transfection of cultured SCs with the *lacZ* reporter gene (Mosahebi et al. 2001). However a number of problems have been reported upon histological analysis, as *lacZ* expression is confined to the nucleus. Therefore, *lacZ* expression is only detected if the cell body and the nucleus are sectioned during histological

analysis. The *in vivo* morphology of a Schwann cell is that of a small cell nucleus with disproportionate cytoplasmic processes. In histological sections, it is the SC cytoplasm that is more readily detected by immunostaining, hence the absence of a detectable nuclear cell body gives the misleading result that fewer labelled cells are seen than are actually present. A further drawback is that to identify the *lacZ* label a prolonged chemical process is required, with limited penetration into the tissue and moderate disruption of tissue architecture.

Over the past decade bioluminescent protein markers have received great interest for their use in labelling and tracking cells, proteins and for measuring gene expression. The first described and most widely studied are the green fluorescent proteins (GFPs) (Shimomura et al. 1962). To date there are few reports describing the use of GFPs as endogenous reporter molecules for transplanted SCs.

1.6.1 Bioluminescent proteins

The first written report of bioluminescence was from Pliny the Elder in the first century AD, who observed the bright glow of certain jellyfish in the Bay of Naples (Johnson & Shimomura, 1978). This chemiluminescence phenomenon requires an enzyme and has evolved independently many times in different species, as seen in bacteria, unicellular algae, coelenterates, beetles and fishes. Chemically, all involve exergonic reactions of molecular oxygen with different substrates (luciferins) and enzymes (luciferases) resulting in an energy rich intermediate, the breakdown of which provides energy for excitation of an accessory protein to produce light. Variation between species occurs in how this

energy rich intermediate is utilised to produce fluorescence (Wilson & Hastings, 1998). With the exception of bioluminescent bacteria there is no definitive explanation as to why these organisms evolved bioluminescence or fluorescent proteins. Green fluorescent protein was discovered by Shimomura (1962) as a companion protein to aequorin, a well known chemiluminescent protein that produces blue light in the *Aequorea* jellyfish. They reported that the blue light emitted from the aequorin protein caused the excitation of an accessory protein (GFP) to emit green light. To date the best described bioluminescent proteins are the green fluorescent proteins which are found in a number of marine invertebrates (coelenterates), the best characterised arising from the phylum Cnidaria which include the hydrozoan, *Aequorea victoria* (crystal jellyfish), and the anthozoan, *Renilla reniformis* (sea pansy) (Prasher, 1995). Although the biochemistry of the GFPs in these species is similar, the mechanism through which they are stimulated to emit light is different.

1.6.2 Biochemistry of Green Fluorescent Protein

GFP is a protein of 238 amino acid residues which fold to form an 11 β-stranded 'barrel' surrounding a *p*-hydroxybenzylideneimidazolidinone chromophore (Figure 1.1). Substitutions in this amino acid sequence alter folding of the protein, absorption and emission spectra (Heim et al. 1994). The emission of green light *in vivo* is due to energy transfer from either aequorin or the *Renilla* luciferase to a GFP molecule (Figure 1.2). The two bioluminescent systems are activated *in vivo* by a Ca^{2+} signal which is initiated by a mechanical or primitive neuronal stimulus. *Aequorea* bioluminescence is activated when Ca^{2+} binds to

aequorin which oxidizes bound coelenterazine, transferring the released energy to GFP. In contrast, *Renilla* biolumniscence is controlled by the luciferin-binding protein (LBP). Only on binding Ca^{2+} does the LBP permit the luciferase to oxidise coelenterazine and transfer energy to GFP. Isolated *Renilla* and *Aequorea* GFP can be made to fluoresce in the absence of these energy transfer systems by exciting the protein with light of a specific wavelength. The *Aequorea* GFP has two excitation peaks at 395nm and 470nm, while *Renilla* GFP has a single excitation peak at 470nm. It is suggested the difference is due to different apoprotein environments of the chromophores. The two GFPs have identical emission spectra in the region of green light (λ_{max}=509nm) (San Pietri et al. 1993). The quantum yield (probability of re-emitting a photon once the molecule has been excited) of GFP is greater than that of aequorin therefore the biological role of GFP may be that it is more efficient at producing light from transferred energy (Morise et al. 1974).

GFPs are stable proteins meaning their spectral properties are unaffected by denaturing conditions. The 'barrel' of β-strands surrounding the central chromophore protects this light-emitting region of the protein. They are resistant to strong acids, alkalis, proteolytic enzymes and temperatures of up to 80°C and can even be renatured to functional protein (Prasher, 1995).

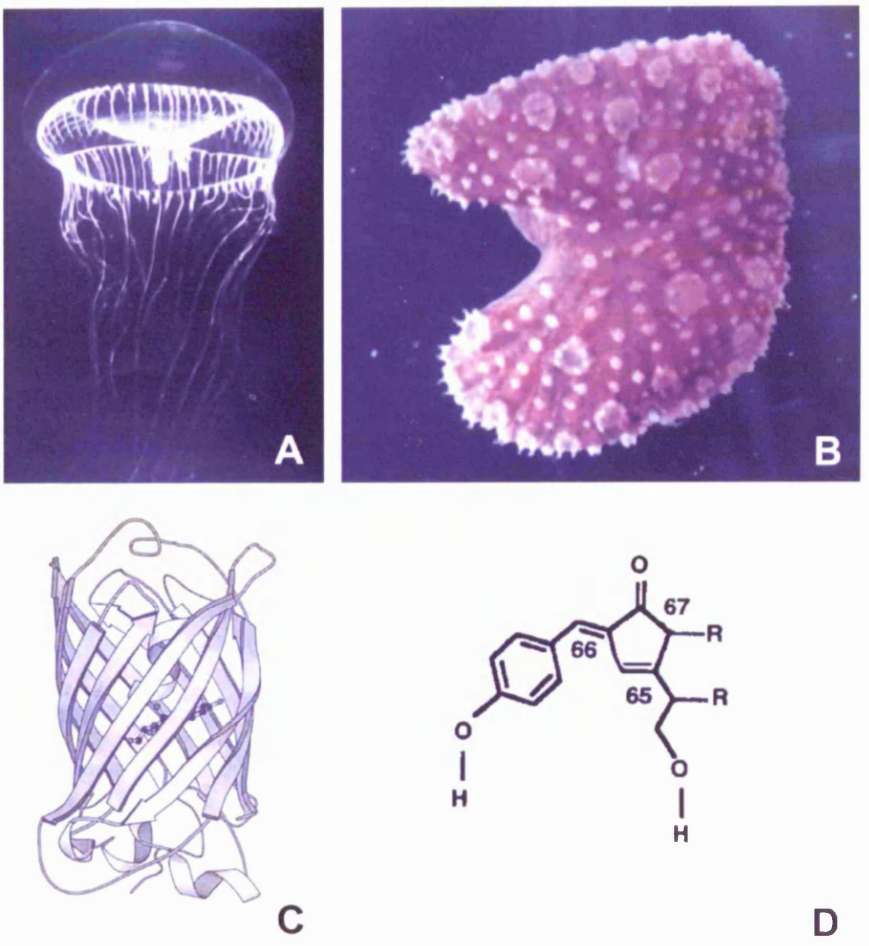

Figure 1.1 (**A**) The bioluminescent jellyfish *Aequorea victoria*. (**B**) *Renilla reniformis* (sea pansy). (**C**) The three dimensional structure of GFP illustrating the central chromophore surrounded by a 'barrel' of 11 β-strands of amino acids. (**D**) The central chromophore structure (Tsien et al. 1993).

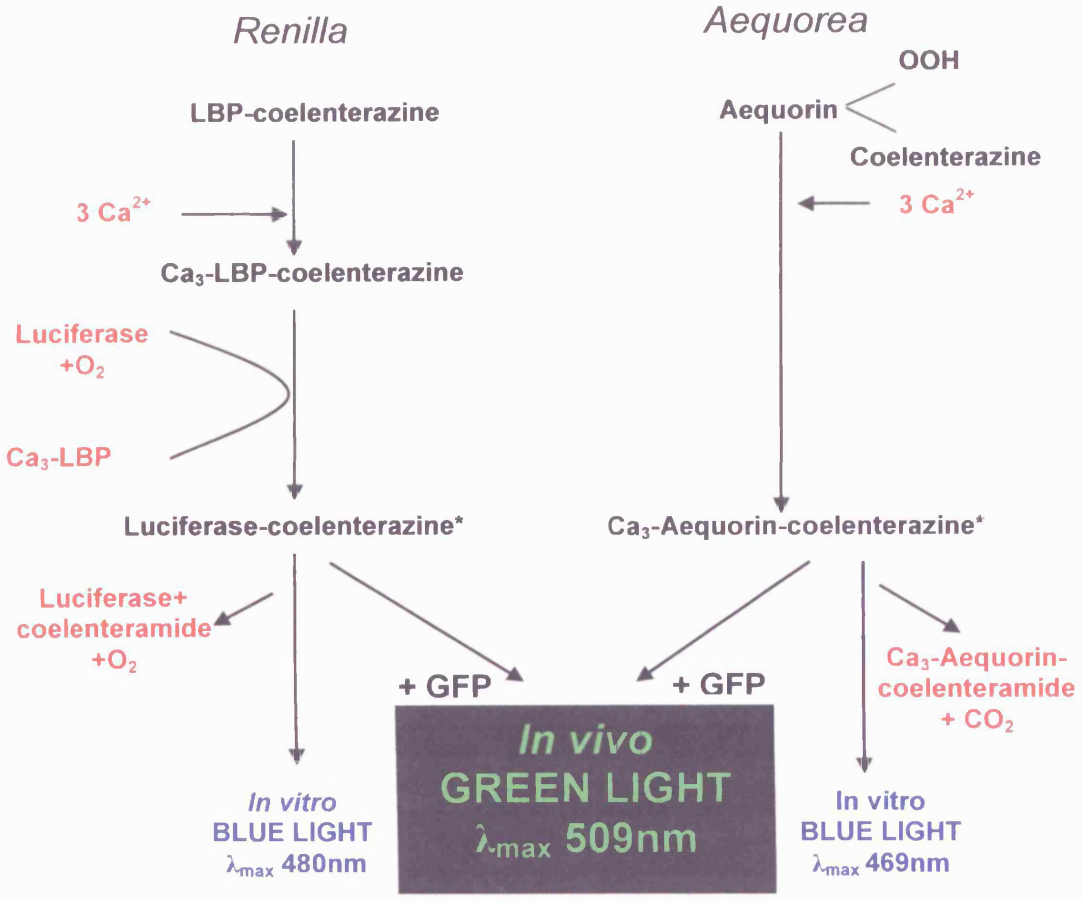

Figure 1.2 The bioluminescent pathways of *Renilla* and *Aequorea*. In *Renilla*, coelenterazine acts as a luciferin which when exposed to Ca^{2+} can be oxidised by luciferase. In *Aequorea*, the photoprotein aequorin oxidises coelenterazine on exposure to Ca^{2+}. In both cases the energy released on oxidation of coelenterazine stimulates green fluorescent protein to emit green light *in vivo*. The asterisks show an excited state luciferin. After Prasher (1995).

1.6.3 Applications of GFP

The first cloning of GFP cDNA was performed by Prasher (1992). Following this, a great deal of interest was generated in GFP when it was shown that expression of the cloned gene produces fluorescent protein in a variety of cell types (Chalfie et al. 1994; Inouye & Tsuji, 1994). The GFP gene therefore contains all the necessary information for the post-translational synthesis of the chromophore with no specific enzymes being required to initiate fluorescence. GFP has been successfully used as a reporter gene and cell marker (Chalfie et al. 1994; Ikawa et al. 1999; Takada et al. 1997), as a fusion tag to monitor protein localization and fate (Cubitt et al. 1995), and to monitor protein-protein interactions using fluorescence resonance energy transfer (FRET) (Tsien et al. 1993). For histological purposes the biochemical stability of GFP is advantageous as it makes the protein resistant to a wide range of temperatures, pH and enzymes which may be encountered in various staining protocols. The protein is highly soluble and therefore requires formaldehyde fixation prior to cryostat sectioning and staining (Jockusch et al. 2003). The use of GFP is advantageous in such techniques as transplanted labelled cells can be visualised in combination with other fluorochrome-labelled antigens.

Fluorescent protein technology has great potential for the study of bio-engineered cellular systems. Developments have been aimed at producing a range of spectrally distinct fluorescent proteins to allow simultaneous multicolour tracking of separate genes, fusion proteins or labelled cells. Mutants of GFP are now available with enhanced fluorescence (EGFP) and emission spectra corresponding to blue (BFP), cyan (CYP) and yellow light (YFP) (Zimmer, 2002).

More than 25 fluorescent proteins have been isolated from different marine organisms (Labas et al. 2002). These technologies have far-reaching applications for the study of bio-engineered nerve grafts. For example, cells could be labelled with one fluorescent protein for cell tracking following transplantation whilst secondary proteins could be tagged to a particular growth factor(s) enabling the measurement of gene expression within transplanted cells.

1.7 Stem cell therapies for peripheral nerve injury

Stem cells are the fundamental cellular building blocks of life, in addition to coordinating organ growth from embryo to adulthood they also play an important role in tissue regeneration and repair. A large body of literature exists describing embryonic stem cells, haematopoietic stem cells, and epithelia which display a rapid turnover i.e. the skin and intestinal epithelium (reviewed by Tohill & Terenghi, 2004). Discrete stem cell populations have now been identified in more static adult tissues such as adipose tissue and neural tissue. Notwithstanding the biological complexities of characterising such cells, there is qualified excitement at the potential of stem cells to revolutionise our approach to tissue engineering. One such area is that of regeneration in the peripheral nervous system.

The transplantation of cultured SCs into bio-engineered conduits has been shown to improve nerve regeneration in experimental models of peripheral nerve injury (Guenard et al. 1992; Mosahebi et al. 2001; Rodriguez et al. 2000). However, the use of autologous cultured SCs for the treatment of acute injuries may be impractical due to the technical difficulties and time required in harvesting and expanding such cells which may take up to 10 weeks (Mosahebi et al. 2001).

Such a delay in performing a primary nerve repair following injury would be deleterious to clinical outcome. Indeed, it has been shown that the longer the time lag between injury and repair the greater the neuronal cell death in the dorsal root ganglia and therefore a reduced potential for recovery (Hart et al. 2002).

The ideal 'transplantable cell' should be easily accessible, capable of rapid expansion in culture, immunologically inert, capable of long-term survival and integration in the host tissue, and amenable to stable transfection and expression of exogenous genes (Azizi et al. 1998). In a search for such a cell attention has been drawn to the possible use of stem cells.

1.7.1 Basic biology of stem cells

A minimalist definition of the stem cell describes it as a clonogenic cell capable of self-renewal and multi-lineage differentiation (Till & McCulloch, 1961). The semantics of stem cell biology can cause confusion as there is no universally accepted definition of what a stem cell is and no unified theory describing their origin, plasticity and function in the adult organism. A number of criteria have been proposed to help identify a stem cell. These dictate that the cell must be (i) undifferentiated (i.e. lacking a tissue-specific differentiation marker), (ii) capable of proliferation, (iii) self-renewable, (iv) able to produce a large number of differentiated functional progeny and (v) able to regenerate tissue after injury (Loeffler & Potten, 1997).

Multi-potential cells are stem cells of tissues that are capable of developing into a restricted number of cell types specific to that tissue (Alison et al. 2002). There are two populations of cells within a tissue, those which are post-

mitotic and responsible for physiological activity, and stem cells which are responsible for organ and tissue growth and repair following injury. As an organism matures from embryo to adult the number of post-mitotic cells increase and the number of stem cells decrease. The proportion and activity of stem cells within adult tissue depends on tissue type, i.e. depending on whether the tissue is renewing e.g. intestinal epithelium, or static e.g. the CNS (Marshak et al. 2001). Under steady-state conditions the stem cell pool remains constant but following injury or during disease it can expand rapidly. The haematopoietic system displays regenerative capacity more dramatically than any other tissue as huge numbers of cells are continuously produced throughout life. It is possible to re-establish the entire haematopoietic compartment following complete ablation as is seen following cytotoxic therapy for haematological malignancies, and it is this property which has been exploited to successfully treat such conditions (Thomas, 1991). Embryonic stem cells can be propagated in culture (Thompson et al. 1998) however obtaining such cells faces practical, ethical and legislative difficulties (McLaren, 2000; Shapiro, 1999). The identification, isolation and expansion of truly multipotent adult-derived stem cells remains problematic. Toma *et al* (2001) (Toma et al. 2001) described the isolation and expansion of multipotent stem cells from skin however it was not possible to determine the origin of the cells with absolute certainty. The problem of isolating clonal stem cells from adult tissues is probably the greatest obstacle faced in this field (Donovan & Gearhart, 2001; Vogel 2001).

The control of self-renewal and differentiation is most probably influenced by *extrinsic* factors i.e. the environment or niche, and *intrinsic* cellular factors.

The environment influences the biochemical and morphological properties of stem cells. Stem cells adjust their properties according to their surroundings and select specific lineages according to the cues they receive from their niche (Fuchs & Segre, 2000). Extrinsic factors include cell-cell interactions (Henderson et al. 1994; Kopan et al. 1994), locally secreted factors (Reynolds & Weiss, 1996; Gritti et al. 1996; Shah et al. 1994; Shah et al. 1996) and the extracellular matrix (Quesenberry & Becker, 1998; Jensen et al. 1999).

Intrinsic factors determining self-renewal and division exist. Under similar conditions it has been observed that subpopulations of haematopoietic stem cells have different capacities for self-renewal depending on telomerase activity, with increased telomerase expression correlating with an increased capacity for self-renewal (Morrison et al. 1996). Maintenance of the undifferentiated state may be determined by the asymmetric inheritance of certain proteins which influence gene expression, for example the nuclear protein PIE-1 inhibits embryonic genes which are responsible for somatic lineage differentiation (Seydoux et al. 1996). The role *in vivo* of asymmetric kinetic genes may be of fundamental importance as intrinsic factors controlling self-renewal, however it is believed the predominant form of self-renewal in mammals detectable so far is symmetric division (Morrison et al. 1997). Manipulation of asymmetric genes *in vitro* may enable great advancement in stem cell expansion (Sherley, 2002).

The control of differentiation is a complex event requiring exit of the cell from the undifferentiated state and entry into a determined developmental pathway. At present cell determination is seen as a stochastic event initiated by intrinsic factors with an outcome biased by extrinsic factors. The challenge at

present is to identify further intrinsic and extrinsic regulatory mechanisms which determine stem cell fate and to define the relationship between these systems.

Developmentally the components of the peripheral nervous system originate from the neural crest. In looking for alternatives to SC transplantation in bio-engineered conduits it is useful to briefly review reports utilising neural progenitor cells in peripheral nerve regeneration.

1.7.2 Neural progenitor cells

There are a limited number of reports describing the use of stem and progenitor cells in peripheral nerve transplantation. SCs are derived from the neural crest of the neuroectoderm and differentiate and migrate into the peripheral nervous system with development (LeDouarin, 1991). The use of neural derived progenitors from the fetal rat hippocampus to seed a conduit spanning a 15mm gap in the rat sciatic nerve has been described. Significant morphological and functional evidence of regeneration with integration and differentiation of transplanted neural progenitors into Schwann-like cells was reported (Murakami et al. 2003). Neural stem cells have been identified in the adult CNS (Reynolds & Weiss, 1992). Such adult-derived stem cells and those isolated from fetal tissues have been successfully propagated and differentiated *in vitro* into all major cell types of the nervous system (Morrison et al. 1999). The use of fetal or adult-derived neural progenitors fails to avoid the problems encountered with SCs i.e. source of donor tissue and the time taken to expand such cells. Morrison et al. (1999) identified populations of SC progenitors within the rat fetal sciatic nerve, but there has been little evidence to suggest the presence of a stem cell population

within the adult peripheral nerve, although their existence has been postulated within populations of the neurons of dorsal root and autonomic ganglia (Geuna et al. 2000). The absence of a population of peripheral nerve stem cells may be explained by the inherent plasticity of mature SCs to dedifferentiate and proliferate in response to injury (Bunge, 1993).

1.7.3 Olfactory ensheathing cells

Olfactory ensheathing cells (OECs) can be described as peripheral nerve progenitor cells as they develop from a peripheral origin, the olfactory placode, and retain the ability to self-renew and differentiate. In the adult organism they continually regenerate from a long-term pool of progenitors to myelinate the olfactory nerves (Ramon-Cueto & Avila, 1998). OECs are considered an intermediate glial cell type as they express a number of Schwann cell-specific marker molecules including p75, NCAM, GFAP and P0 but not GalC (Wewetzer et al. 2002). They have been found to stimulate axonal regeneration in the spinal cord (Ramon-Cueto & Nieto-Sampedro 1994; Navarro et al. 1999) and to form myelin constituents *in vitro* (Santos-Silva & Calvacante, 2001) and *in vivo* following peripheral nerve transplantation (Verdu et al. 1999), this indicates their peripheral origin as they do not myelinate small diameter olfactory axons. The potential for the therapeutic transplantation of OECs as a surrogate for SCs in peripheral nerve injury is still debatable, as there are many pragmatic difficulties to overcome when applied to the clinical setting. However, OECs do merit attention as at present they are the only PNS-progenitor type cells known to exist.

1.7.4 Bone marrow stromal cells

Until recently, dogma dictated that organ-specific stem cells were restricted to differentiate only into cell types from the tissue from which they originate. Unlike embryonic cells, organ-specific stem cells were believed to have lost the capacity to generate other somatic lineages. However, recent reports have suggested that stem cells from one tissue can cross lineage boundaries to differentiate into cells of other lineages either *in vitro* or *in vivo* after transplantation. This plasticity, or ability for cells to trans-differentiate, has aroused great interest for its therapeutic potential in tissue engineering. A promising candidate to display such plasticity is the bone marrow stromal cell.

Bone marrow contains two distinct populations of progenitor cells: haematopoetic progenitors and bone marrow stromal progenitors. Marrow stroma has been identified as the site of origin for mesenchymal progenitors for bone, cartilage, tendon, adipose tissue and muscle (Caplan, 1994). In addition, the stroma has been identified as a supportive tissue for the haematopoietic system, enhancing cytokine-induced proliferation of haematopoietic precursors (Verfaillie, 1993). Marrow stromal cells are easily accessible through the aspiration of the bone marrow cavity. They readily adhere in tissue culture in comparison to their non-adherent haematopoietic counterparts (Bianco, 2001). A number of mitogenic factors have been identified which stimulate colony formation and proliferation such as PDGF, EGF, bFGF, TGFβ and IGF-I (Gronthos, 1995). Bone marrow stromal cells have been shown to be inherently heterogeneous in terms of growth kinetics, morphology and phenotype. This may be due in part to

the fact that the actual number of true stem cells is small, being estimated at 2-5 per 1 x 10^6 mononuclear cells, with the majority of cell growth arising from expanding differentiated colonies under mitogenic influence. With the development of specific antibodies such as STRO-1 (Simmons, 1991) and characterisation ($CD45^{-ve}$, $CD34^{-ve}$, $CD105^{+ve}$, $CD73^{+ve}$) (Pittenger et al. 1999) for human mesenchymal stem cells, their expansion and properties can be studied and defined with more certainty.

Marrow stromal cells differentiate according to a hierarchical paradigm into osteoblastic, chondroblastic and adipocytic progenitors (Muraglia et al. 2000). Orthodox plasticity between these lineages has been reported from adipocytic and chondrocytic lineages to osteogenic differentiation (Beresford 1992; Gentili, 1993). Recent reports have described unorthodox plasticity of haematopoietic progenitors (Orlic et al. 2001; Lagasse et al. 2000) and bone marrow stromal cells in that they have been shown to cross oligolineage boundaries which were previously thought to be uncrossable. The potential of marrow stromal cells to trans-differentiate from mesenchymal lineages has aroused great interest. An early report by Ferrari et al. (1998) described the migration of labelled marrow stromal cells to areas of damaged skeletal muscle. Trans-differentiation was detected due to the stromal cell expression of myogenic markers and their participation in the regeneration of damaged muscle fibres. Gojo et al. (2003) demonstrated mesenchymal differentiation into cardiomyocytes, endothelial cells and smooth muscle cells following direct injection into adult heart, it has also been shown that these cells will migrate to zones of myocardial injury following systemic delivery (Barbash et al. 2003)

although neither authors described any functional improvement. Jiang et al. (2002) identified marrow-derived cells in all somatic lineages in chimaeric mice following injection of labelled cells into 3-5 day old blastocysts and engraftment into many adult tissues following systemic infusion. There is evidence that marrow stromal cells are capable of neuronal antigen expression *in vitro* (Kim et al. 2002; Wislet-Gendebien et al. 2003; Dezawa et al. 2001) and *in vivo* (Kopen et al. 1999; Mezey et al. 2000). They have been shown to differentiate into astrocytes following direct transplantation into the rodent brain (Azizi et al. 1998 45; Kopen et al. 1999). Studies have also reported the ability of such cells to transdifferentiate into cells displaying similar characterisation to those of neuroectodermal cells (Kopen et al. 1999; Mezey et al. 2000). Akiyama et al. (2002) described remyelination of spinal cord lesions following intravenous delivery of marrow stromal cells and Hofstetter et al. (2001) showed that local delivery of MSCs at the site of spinal cord injury was associated with the formation of neurofilament bundles at the interface between scar tissue and graft. It is not clear what mechanisms govern the *in vivo* differentiation and migration of MSCs within zones of injury however it is likely that the local milieu of growth factors, cytokines and local stem cells have some influence. The potential for these cells to undergo unorthodox differentiation may be capitalised in the repair of peripheral injury.

Two recent reports have described the use of marrow stromal cell transplantation in models of peripheral nerve injury. Dezawa et al. (2001) described the *in vitro* expression of the glial cell markers p75 and S100 by rat mesenchymal stromal cells following exposure to a cocktail of growth factors, and

integration of such cells in the regeneration front upon transplantation into a blind-ending tube grafted to the proximal stump of the rat sciatic nerve. Cuevas et al. (2002) described the migration and differentiation of marrow stromal cells following the injection of cultured undifferentiated cells into the site of a sciatic nerve axotomy repair.

1.7.5 Immunotolerance to allogeneic stem cells

An important problem which faces all studies of transplantation is that of host rejection of transplanted tissue. In the clinical setting of organ transplantation this problem is overcome with the use of immuno-suppressants with the benefits of a functioning heart, lung, liver or kidney outweighing the potentially serious systemic side-effects of immunosuppression, such as susceptibility to opportunistic infection and skin cancer. A number of experimental reports have shown that there is an unexpected and fortuitous level of immune-tolerance to transplanted stem and progenitor cells. Marrow stromal cells have been shown to block the proliferation of allogeneic T-cells *in vitro* and prolong skin graft survival *in vivo* (Bartholomew, 2002). Saito et al. (2002) demonstrated immune tolerance to xenogeneic cells following transplantation in addition to the retainment of their ability to engraft and differentiate. The ability of marrow stromal cells to induce tolerance may be due to cytokine secretion such as TGFβ or due to their phenotypical immaturity as they lack MHC class II and other T-cell stimulatory surface proteins (Deans & Moseley, 2000; Tse et al. 2001). With respect to studies in the nervous system, Hori et al. (2003) has shown that CNS progenitor cells may not express MHC class I and II *in vitro* and that no short

term evidence of rejection is seen after allogeneic transplantation within the CNS. These observations are seemingly a local effect of stem cell transplantation and are distinct from the recognized phenomenon that infusion of bone marrow donor cells can improve allograft survival and reduce the need for short-term immunosuppression. Such macrochimaeric models require significant host conditioning prior to transplantation such as central and peripheral T-cell deletion (Rifle & Mousson, 2003; Wekerle et al. 2003).

One problem which may be faced when considering host tolerance to progenitor cell allografts is the consequence of the up-regulation of immunoreactive surface markers following *in vitro* or *in vivo* differentiation due to the effects growth factors or cytokines. Such effects may offset the benefits of immune tolerance to immature cells. Marrow stromal cells might be used as primary engrafting cells for differentiation into cells of a *de novo* tissue, and they might also be used as cellular vehicles for transgene expression for the production growth factors or cytokines which could ameliorate the immune response to more differentiated and functionally mature allogeneic cells (Bartholomew, 2001; Studeny, 2002).

1.7.6 Characterisation of MSC *in vivo*

With growing evidence to support the apparent plasticity of marrow stromal stem cells, it seems likely that these cells may become important components of bio-engineered systems in the future, because of their accessibility, abundance, and ease of culture *in vitro*. There is no doubt that such cells can express neuronal cell immunoreactivity under specific mitogenic influences both *in vitro* and *in*

vivo. Micro-array analysis has revealed over 2000 genes expressed by marrow stromal cells, many of these genes unrelated to mesenchymal lineages (Tremain et al. 2001), hence unlocking dormant genes may be the key to induce plasticity. At present there are no universally established protocols to induce neuro-glial differentiation of marrow stromal cells. Wislet-Gendebien et al. (2003) recently reported that the expression of nestin is a prerequisite for GFAP expression in rat MSCs and that this ability is directly proportional to passage number. It is important to examine the effects of cellular microenvironments on cell differentiation as *in vitro* experiments have identified a mitogenic effect of a large number of unrelated cytokines and growth factors on marrow stromal cells (Conget & Minguell, 1999). It is also necessary to identify the factors influencing differentiation, such as intrinsic and extrinsic mechanisms, and the interaction between the two.

1.8 The role of growth factors in peripheral nerve regeneration

A large number of cytokines and growth factors are involved in the physiological processes governing peripheral nerve regeneration. Of principal importance are the neurotrophic factors and the neuregulins. The utilisation of such peptides as adjuvant treatments to augment nerve regeneration has been studied extensively. A consistent problem faced however is how to deliver growth factor peptides over a sufficiently long period of time at the site of injury without using delivery vehicles that would be clinically impractical. Secondly, with such a large and ever expanding range of growth factors identified as to having neurotrophic

effects it is increasingly difficult to choose which growth factor when applied exogenously will have the most beneficial overall effect.

During regeneration a key function of proliferating SCs is the production of neurotrophins (Heumann et al. 1987) which exert a trophic influence on the regenerating axons of the proximal stump (Reynolds & Woolf, 1993). Neurotrophins include nerve growth factor (NGF), brain-derived neurotrophic factor (BDNF), neurotrophin-3 (NT-3), neurotrophin-4/5 (NT-4/5), glia-derived neurotrophic factor (GDNF), ciliary neurotrophic factor (CNTF) and leukaemia inhibitory factor (LIF). NGF, BDNF, NT-3 and NT-4/5 all share similar amino acid sequencing (Maness et al. 1994) and similar affinity for the p75 low-affinity nerve growth factor receptor. Specific trk receptors exist for certain neurotrophins, trkA is specific for NGF (Kaplan et al. 1991), trkB for BDNF and NT-4/5 (Klein et al. 1992) and trkC for NT-3 (Lamballe et al. 1991). All 3 trk receptors are found in subpopulations of sensory neurons (McMahon et al. 1994) whilst trkB and trkC are found in spinal motoneurons (Funakoshi et al. 1993). Neurotrophins play an important role in maximising neuronal cell survival following axotomy. Following peripheral nerve injury up to 40% of the sensory neurons of dorsal root ganglia die through apoptosis (Groves et al. 1997), in addition trk receptor expression downregulation occurs due to a reduction in local neurotrophin availability (Krekoski et al. 1996). SCs at the site of injury upregulate the synthesis of some neurotrophins and the p75 receptor however this is insufficient to prevent significant neuronal cell death (Funakoshi et al. 1993). Sensory neuronal cell death can be reduced and receptor downregulation reversed by the exogenous administration of neurotrophins such as GDNF (Munson &

McMahon, 1997), NGF, NT-3 (Ljungberg et al. 1999), and LIF (Thompson et al. 1998). Motonueron survival is enhanced by the administration of BDNF (Novikova et al. 1997), NGF (Rich et al. 1989), CNTF (Sendtner et al. 1997) and GDNF (Li et al. 1995). CNTF, LIF, NT-3 and GDNF have also been shown to enhance neurite outgrowth following axotomy and to enhance target organ muscle reinnervation leading to preservation of muscle mass and fibre type expression (Sterne et al. 1997).

Neuregulins are a family of proteins that are secreted by developing neurons and include the glial growth factors (GGFs) and heregulin. They are Schwann cell mitogens and survival factors (Minghetti et al. 1996). They have also been shown to play a role in restricting neural crest precursors to a glial cell fate (Shah et al. 1994). Recombinant human GGF II has been shown to increase Schwann cell motility and proliferation *in vitro* and to indirectly increase neurite outgrowth *in vitro* (Mahanthappa et al. 1996). Mohanna et al. (2003) showed that delivery of GGF at the site of peripheral nerve injury dramatically increases the rate of regeneration at early time points. The mechanisms of actions of the neurotrophins and the neuregulins demonstrates an important reciprocal arrangement between developing or regenerating axons and SCs and the specificity of target organ reinnervation. This apparent symbiosis probably exists to produce an organised peripheral nerve that has axons matched to the appropriate number of SCs, whilst target organ-derived neurotrophins maintain the specificity of regeneration.

1.8.1 Insulin-like growth factors

Insulin-like growth factors (IGF-1/2) are single chain polypeptides that belong to the insulin gene family. They are derived from muscle and nerve, act predominantly through an IGF receptor and have neurotrophic properties which play an important role in the development of the central, autonomic and peripheral nervous system and its regeneration following injury (Hansson, 1993; Ishii et al. 1993; de Pablo & de la Rossa, 1995). IGF-1 enhances neurite outgrowth from DRG explants *in vitro* (Akahori & Horie, 1997), stimulates Schwann cell proliferation *in vitro* (Cheng et al. 1996) and prevents Schwann cell apoptosis *in vitro* and *in vivo* during embryonic nerve development (Syroid et al. 1999). Following axotomy Schwann cell IGF-1 gene expression for both the peptide and receptor increases for up to 7 days, thereafter the predominant source of IGF-1 comes from macrophages (Cheng et al. 1996). Administration of IGF-1 improves peripheral nerve regeneration following axotomy by stimulating axonal sprouting (Skottner et al. 1987; Kanje et al. 1989) and by promoting motor and sensory neuron survival (Neff et al. 1993; Vergani et al. 1998). IGF-1 indirectly enhances nerve regeneration by stimulating fibroblasts and macrophages to produce a number of neurotrophic factors, adhesion molecules and cytokines (Caroni & Grandes, 1990). In addition to a mitogenic effect on SCs it stimulates their differentiation through IGF binding protein-5 (IGFBP-5) which increases the myelination markers P0 and myelin basic protein (Cheng & Feldman, 1997). Rabinovsky et al. (2002) demonstrated enhanced peripheral nerve and muscle regeneration following the targeted expression of an IGF-1 transgene to skeletal muscle in a mouse model of peripheral nerve injury.

1.8.2 Mechano-Growth Factor (MGF)

IGF-1 is a major regulator of skeletal muscle growth and maintenance. During growth IGF-1 is produced by the liver in response to pituitary-derived growth hormone. Whilst systemic IGF-1 controls growth of the body, some tissues are subject to a local system of growth regulation, as seen in skeletal muscle which becomes hypertrophic in response to overload (Goldspink, 1999). The IGF-1 gene is alternatively spliced in response to different signals resulting in different peptides which vary in their mode of action and their specific target tissues. The IGF-1 gene contains two promoters initiating at the 5′ end of the gene (Figure 1.3). Transcripts initiating at promoter 2 are common in the liver and are highly growth hormone dependent, whilst transcripts initiating at promoter 1 are expressed in skeletal muscle. Following mechanical stimulation of muscle Yang and co-workers (1996) demonstrated the expression of an isoform of IGF-1 that appears to be responsible for local hypertrophy of muscle in response to overload via paracrine/autocrine routes. Because the expression of this isoform is mechanosensitive it has been termed mechano-growth factor (MGF). The MGF isoform results from a novel splice acceptor site in the intron preceding exon 6 leading to MGF cDNA differing from its liver type counterpart by the presence of a 49 base pair insert from exon 5 in man and a 52 base pair insert in the rat. These inserts result in a reading frame shift and a different C-terminal peptide sequence (Yang et al. 1996; McKoy et al. 1999; Yang & Goldspink, 2002). MGF expression rises significantly over other IGF isoforms in skeletal muscle after high resistance exercise in young subjects (25-36 years) but not the elderly (70-82 years) which is consistent with age-related desensitivity to mechanical loading

(Hameed et al. 2003). *In vitro* studies have shown that MGF stimulates muscle satellite cell (residual myoblast) proliferation whilst inhibiting terminal differentiation. These effects are seen in the presence of IGF-1 receptor blockade indicating that MGF acts through a signalling pathway independent of the IGF-1 receptor (Yang & Goldspink, 2002).

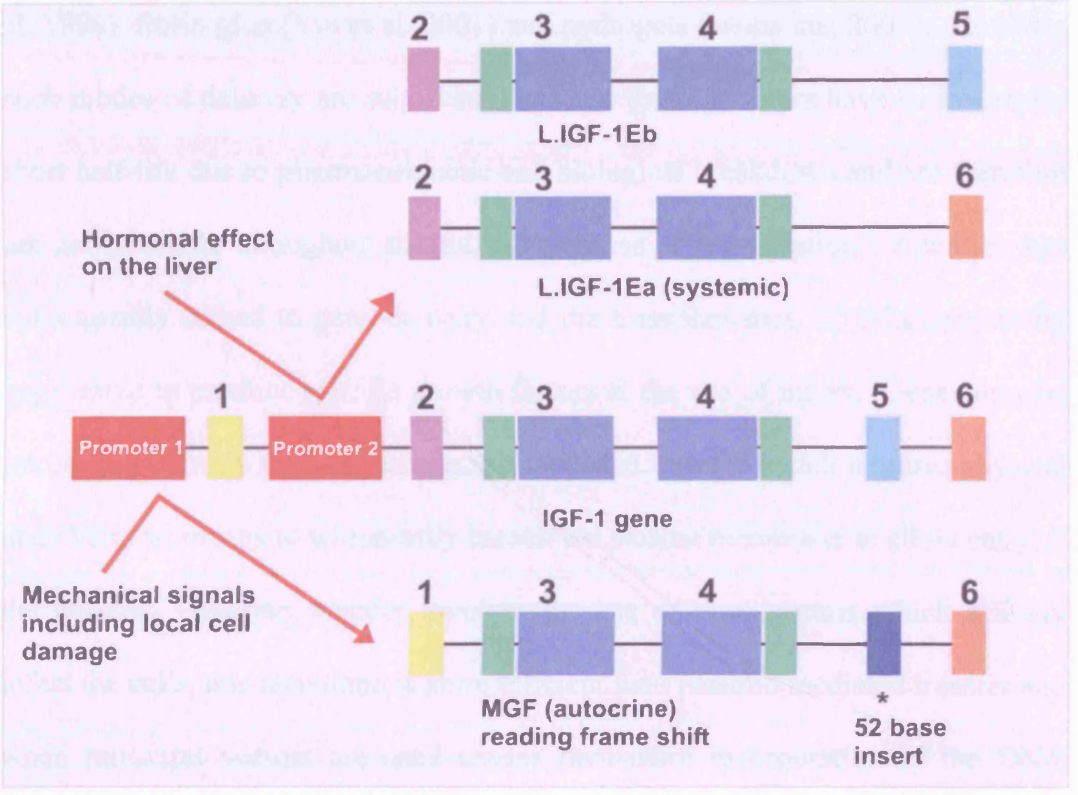

Figure 1.3 Diagrammatic representation of the alternative splice variants of the IGF-1 gene. IGF-1 (insulin-like growth factor-1), L.IGF-1 (liver insulin-like growth factor-1), MGF (mechano-growth factor). A 52 bp insert occurs in rat MGF whilst a 49 bp insert occurs in human MGF. Reproduced with permission by Dr S. Yang.

1.8.3 Delivery of neurotrophic factors

Whilst neurotrophic factors appear to be ideal adjuvant treatments for peripheral nerve injuries there are a number of practical problems faced in their implementation in the clinical setting. Systemic administration of neurotrophic factors yields undesirable side effects such as anorexia and weight loss (Penn et al. 1997). Local delivery has been achieved through the use of osmotic pumps (Santos et al. 1998), bioresorbable materials such fibronectin mats (Whitworth et al. 1996), fibrin glue (Yin et al. 2001) and hydrogels (Mohanna, 2003). However such modes of delivery are suboptimal because growth factors have an inherently short half-life due to pharmacokinetic and biological breakdown and are therefore are not available throughout the full time-course of regeneration. Attention has subsequently turned to gene delivery and the transplantation of cells genetically engineered to produce specific growth factors at the site of injury. Genes may be introduced directly to cells via plasmid mediated transfer which requires physical and chemical means to temporarily breach the plasma membrane to allow entry of the plasmid. Indirect transfer involves the use of viral vectors which actively infect the cells, this technique is more efficient than plasmid mediated transfer and when retroviral vectors are used causes permanent incorporation of the DNA within the cell's genome. Fibroblasts genetically engineered to produce NGF have been shown to increase neurite outgrowth following transplantation into the lesioned spinal cord (Tuszynski et al. 1996) whilst cultured SCs have been successfully engineered to produce BDNF and NT-3 (Sayers et al. 1998). Growth factor cDNA may also be transferred directly to the peripheral nerve via retroviral and adenoviral vehicles (Gravel et al. 1997; Glatzel et al. 2000; Young et al.

2000) however concerns have been raised about their long-term safety. Direct cDNA transfer via a plasmid delivery vehicle within a suitable matrix has been achieved and seems a more clinically acceptable alternative to viral vehicles (Andree et al. 2003). Such a delivery mechanism would be advantageous for the treatment of peripheral nerve injuries as growth factor cDNA is highly stable and therefore could be stored for prolonged periods of time. Once delivered, the cDNA is internalised at the site of injury and can potentially reach target organs and neuronal cell bodies via anterograde and retrograde transport respectively, following which the gene product can be manufactured without permanent incorporation within the genome.

1.9 Hypothesis

The transplantation of cultured SCs improves peripheral nerve regeneration, and labelling of transplanted cells is necessary to define their behaviour and interaction with regenerating axons. Hence labelling should be optimised so that it can be incorporated within the standard immunofluorescent histological techniques used to assess peripheral nerve regeneration. The use of GFP as a label for transplanted SCs has not been well documented, a great advantage of GFP over *lacZ* labelling would be the ability to assess fluorescence *in vitro* without need of a substrate, detriment to the cultures or the need for fixation. Experiments are described in this thesis which looked at the use of GFP as a label for tracking SCs in bio-engineered conduits.

Bone marrow stromal cell progenitors have shown great unorthodox plasticity in their differentiation abilities. It may be possible that these cells could be induced to differentiate along a glial cell lineage. The transplantation of marrow stromal cells *in vivo* has demonstrated their ability to integrate and differentiate within different injured tissues. These cells may be used as an alternative to cultured SCs in bio-engineered nerve conduits and therefore may have a therapeutic role in peripheral nerve regeneration.

The benefit of transplanting cultured SCs in bio-engineered nerve conduits is well established. However it is still unclear whether the culturing of SCs may effect some of their intrinsic properties, such as CAM expression. This may have important implications for their efficiency in sustaining regeneration following

transplantation. Extracellular matrix molecules play an important role in supporting axons and SCs following injury. Addition of these molecules to bioengineered nerve grafts may therefore enhance peripheral nerve regeneration. Also, it is not known if the transplantation of cultured SCs into bio-engineered conduits and the pre-coating of such conduits with ECMMs such as laminin, fibronectin and collagen influences the expression of axonal CAMs such as NCAM, L1 and N-cadherin.

A large number of growth factors have been identified as having neurotrophic effects during regeneration and may therefore be of therapeutic benefit. Administering a sustained level of growth factor peptide is problematic but may be achieved through gene transfer. The neurotrophic effects of IGF-1 have been well documented however little is known about the potential effect of MGF on peripheral nerve regeneration, however a pilot study showed that MGF may restore or maintain muscle function following injury either directly or indirectly through a neurotrophic effect on regenerating peripheral nerve.

1.10 Aims

The aims of the experiments described in this thesis are as follows:

1. Establish a protocol for labelling SCs with green fluorescent protein to aid their identification in combination with histological immunfluorescent staining used to assess peripheral nerve regeneration.

2. Assess the ability of marrow stromal cell progenitors to undergo glial differentiation *in vitro*, characterise this differentiation at a molecular, phenotypical and functional level, and to assess the ability of transplanted marrow stromal cells to support peripheral nerve regeneration through a PHB conduit *in vivo*.

3. Define the effects of the extracellular matrix macromolecules laminin, fibronectin and collagen on Schwann cell growth *in vitro*, and the effect of pre-coating PHB fibres with these molecules on peripheral nerve regeneration and cell adhesion molecule expression *in vivo*.

4. Investigate the potential of MGF to stimulate peripheral nerve regeneration and improve functional muscle re-innervation following delivery of MGF cDNA via a plasmid vector to the site of injury.

Chapter 2

Materials and Methods

2.1 Schwann cell culture

2.1.1 Nerve harvesting

Day 1 Schwann cells (SCs) were harvested from the sciatic nerves of Sprague-Dawley rats according to the following protocol (Brockes et al. 1979; Mosahebi et al. 2001). Twenty[1] 1-2 day old inbred neonatal pups were collected from between 1-2 litters giving a total of 40 nerves. Animals were terminated by cervical dislocation and then washed in alcoholic chlorhexidine solution to sterilise skin. Under an operating microscope (Zeiss, X10 magnification), a skin incision was made across the dorsum of the animal in the lumbar region, the skin was then pulled distally to reveal the musculature of the thighs and lower legs. A muscle splitting incision was then made posterior to the femur of each thigh to expose the sciatic nerve. The nerve was gently dissected from the sciatic notch to the popliteal fossa, and taking care not to incorporate any muscle or connective tissue was divided at each end, removed from the animal and then placed in chilled Dulbecco's Modified Eagle's Medium (DMEM) plus HEPES buffer with penicillin and streptomycin (cf. Appendix A). Instruments were washed in alcoholic chlorhexidene between each animal.

2.1.2 Nerve Digestion

Following collection the nerves were transferred to the tissue culture laboratory for digestion and plating. The medium was replaced with 2mls of fresh DMEM/HEPES. Five hundred μl of collagenase I and 250μl of trypsin (cf. Appendix A) was added to the suspension and incubated at 37°C for 15 minutes.

[1] An absolute minimum of 10 animals (20 nerves) are needed for successful SC harvesting as SCs are very sensitive to plating density when cultured. Low SC plating density also increases the risk of early fibroblast overgrowth.

The medium was then aspirated taking care not to remove any nerve tissue[2], and then replaced with 2ml of fresh DMEM/HEPES and fresh enzymes as before. This cycle was repeated a further 2 times (4 in total), on the 3rd and 4th cycles the medium was not discarded in order to retain the maximum number of SCs. At the end of the 4th cycle 10mls of cell growth medium (cf. Appendix A) was added to neutralise the enzymes to prevent SC damage. The mixture was triturated 3 times through a 21G needle followed by 3 times through a 23G needle and then passed through a 70μm filter (Falcon) to remove debris and undigested fragments of tissue. The resulting suspension was centrifuged at 800rpm (cf. Appendix A) for 5mins, the medium was carefully aspirated to conserve the cell pellet, replaced with 5ml of fresh cell growth medium, plated on a 25cm^2 flask coated with poly-D-lysine (Appendix A) and placed in an humidified incubator at 37°C and 5%CO_2.

2.1.3 Schwann cell purification and maintenance

Day 2 Twenty-four hours after plating the SC culture flask was checked for cell attachment and infection using an inverted microscope (Olympus). The medium was aspirated and the cells washed with DMEM/HEPES. The medium was replaced with 5ml of fresh cell growth medium containing 10μM of the cytotoxic agent cytosine-β-D-arabinoside (Arac C; Appendix A), which causes death of proliferating cells. The culture at this stage contains a mixture of SCs and fibroblasts, the latter proliferate more rapidly than SCs and are therefore more

[2] Removal of medium at this stage was performed with a manual pipette as aspiration via vacuum pump can easily cause accidental irrecoverable removal of semi-digested nerves.

sensitive to the cytotoxic effects of Arac C. With time the number of fibroblasts decreases leaving a greater proportion of SCs.

Day 3 The flask was inspected for fibroblast over-growth and the medium was replaced with fresh cell growth medium containing Arac C. This was repeated for a further 2 days. The number of days requiring Arac C addition may vary depending on the number of fibroblasts seen and SC death. If significant SC death is seen shortly after Arac C addition then the investigator should proceed directly to immuno-depletion of fibroblasts.

Day 6 Fibroblast immuno-depletion. When the SC-fibroblast culture was sub-confluent the culture was trypsinised by first aspirating the medium and washing with 5ml of Hank's medium to remove traces of serum, Mg^{2+} and Ca^{2+} which neutralise the trypsin enzyme. The Hank's medium was removed and 0.25% trypsin/EDTA (2ml for a $25cm^2$ flask, 4ml for a $75cm^2$ flask) was added and the culture incubated at 37°C for 5mins. The flask was then lightly tapped and examined under an inverted microscope to check for SC detachment, following which 5ml of cell growth medium was added to neutralise the trypsin. SCs will detach from tissue culture plastic more easily than fibroblasts, therefore vigorous tapping should be avoided as this will increase the load of contaminating fibroblasts in the trypsinised cell suspension. The cell suspension was then aspirated from the flask and placed in a 20ml universal sample bottle and centrifuged at 800rpm for 5 minutes. The supernatant was aspirated and the resulting cell pellet was resuspended in 500μl of mouse anti-rat Thy 1.1 (dil. 1:500 in DMEM) and incubated at 37°C for 10 minutes. Thy 1.1 antibodies will bind specifically with fibroblasts and cause cell lysis in combination with

complement. Fresh rabbit complement was prepared (Appendix A) and 250μl were added to the cell suspension and incubated for 30 minutes at 37°C with gentle agitation every 10 minutes. Ten ml of cell growth medium was then added to the cell suspension which was centrifuged at 800rpm for 5 minutes. The supernatant was aspirated and the cell pellet re-suspended in 5ml of SC growth medium (Appendix A) and plated in a PDL-coated 25cm^2 flask and placed in an incubator. SC purity following immuno-depletion should reach 99% (Brockes, Lemke, et al. 1980 80 /id). Fibroblast contamination is detected due to the different morphology between both cell types, SCs are spindle-shaped bipolar cells which align parallel to each other in characteristic whorls when confluent (Figure 2.1; for review of SC morphology in culture see Scarpini et al. 1993). Fibroblasts have large granular cell bodies, numerous short cytoplasmic processes and distinct nuclei under phase contrast microscopy. If fibroblast overgrowth recurred in culture the process was repeated.

When SC cultures were confluent they were washed with Hank's medium, trypsinised with 0.25% trypsin/EDTA for 5 minutes at 37°C, resuspended in 10mls of medium in a universal container and centrifuged at 800rpm for 5 minutes. Prior to centrifuging, a sample was taken to determine cell number with a haemocytometer. The cell pellet was resuspended in SC growth medium and plated on a PDL-coated flask (5 x 10^{5}cells/25cm^2 flask, 1.5 x 10^{6}cells/75cm^2 flask) and returned to a 37°C incubator. Each flask was labelled with cell type, date of harvesting, date of immunodepletion and passage (trypsinisation) number, with 'T1' denoting cells which have undergone 1 passage, 'T2' for those which have undergone 2 passages and so on.

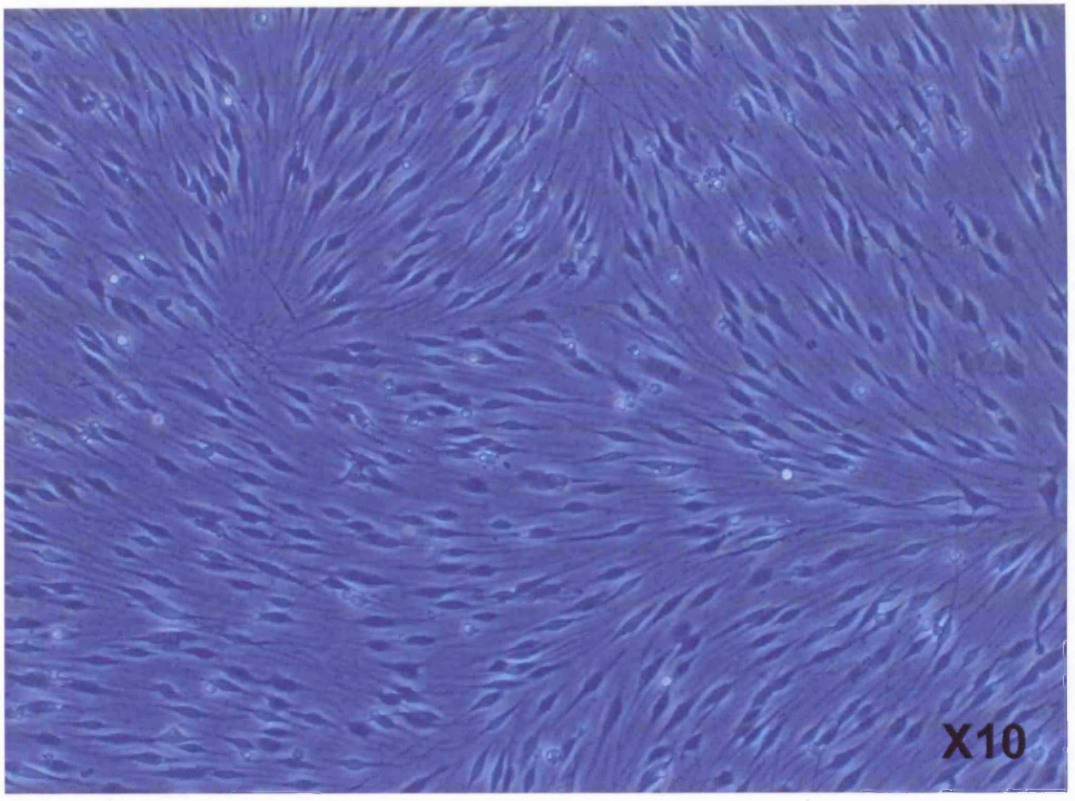

Figure 2.1 Schwann cell culture displaying characteristic 'whorled' pattern at confluence. Note the bipolar spindle shape of the cells.

2.2 Bone marrow stromal cell culture

2.2.1 Bone marrow stromal cell harvesting

Bone marrow stromal cells (MSCs) were harvested from 3 adult male inbred Sprague-Dawley rats. Following termination of the animal the lateral aspect of each hind limb was shaved and washed with alcoholic chlorhexidine. The skin of the lateral thigh was split and the muscle dissected to expose the femur and tibia of each hind limb. The capsule of the hip joint was opened and the head of the femur was dislocated from the acetabulum. Muscle was stripped from the femur throughout its length, the ligaments of the knee joint were divided and the femur was removed. Similarly with the tibia, muscles were stripped away from the bone

and the distal end of the tibia was dislocated from the talus after division of the ankle ligaments. The bones were placed in chilled DMEM/HEPES containing penicillin/streptomycin and transported to the tissue culture laboratory. In the tissue culture cabinet the distal ends of the long bones were removed with sterilised bone nibblers to reveal the marrow cavities. The marrow was flushed from each bone by aspirating 5mls of MSC growth medium (αMEM; 10% FCS; 1% penicillin/streptomycin; Appendix A) through each marrow cavity using a 5mls syringe and a 21G needle. The aspirated medium was triturated 3 times through a 21G needle followed by filtration through a 70μm filter to remove any bone fragments and other debris. The cell suspension was centrifuged in a chilled centrifuge at 800 rpm for 5 minutes. The supernatant was aspirated and the cell pellet was resuspended in 20mls of MSC growth medium with 10mls of the suspension being plated into a 75cm^2 tissue culture flask. The flasks were transferred to a 37^{o}C, 5% CO_2 incubator. After 24hrs the flasks were examined under an inverted microscope. The cells present at this stage are a mixture of adherent marrow stromal cells and non-adherent haematopoietic cells, dead cells and debris. The non-adherent cells were removed by washing the flask with DMEM/HEPES 3 times, following which 10mls of MSC growth medium was added. Washing was repeated every 24hrs until all non-adherent cells were removed. The cells were left to reach confluence (Figure 2.2), at this stage they were trypsinised, counted and re-plated at a concentration of 3.75 x 10^5 cells/75cm^2 flask. Cells were also stored at each passage stage to build cell stocks (cf. 2.4).

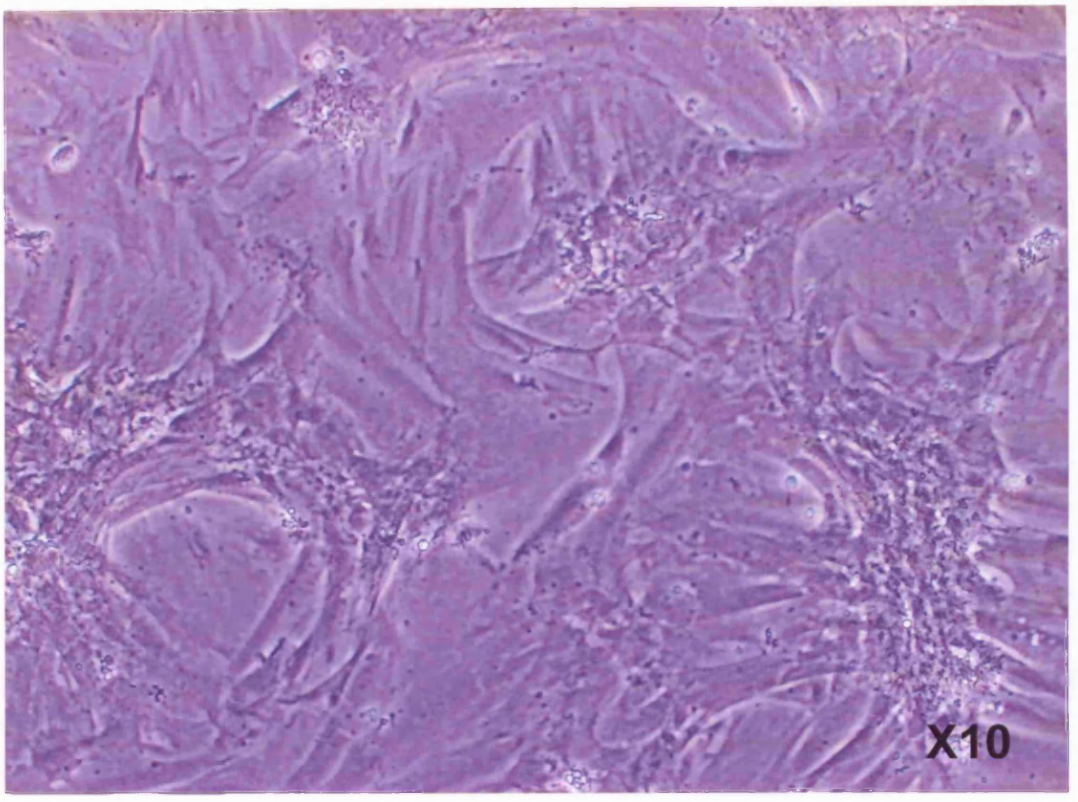

Figure 2.2 Confluent marrow stromal cells displaying typical heterogeneous morphology.

2.2.2 Stimulation of glial differentiation of bone marrow stromal cells

MSCs were stimulated towards glial differentiation through the following protocol (Dezawa et al. 2001). Sub-confluent T5 MSCs were cultured in MSC growth medium containing 1μM beta-mercaptoethanol for 24hrs. After 24hrs the cells were washed and the medium replaced with MSC growth medium supplemented with all-*trans*-retinoic acid (35ng/ml) for 3 days. The cells were washed and replaced with MSC growth medium supplemented with platelet-derived growth factor (PDGF; 200ng/ml), basic fibroblast growth factor (bFGF; 10ng/ml), 5μM forskolin, and glial growth factor (GGF; 126ng/ml) (cf. Appendix

A), and incubated for 14 days with replacement of fresh medium containing the above growth factors every 72hrs.

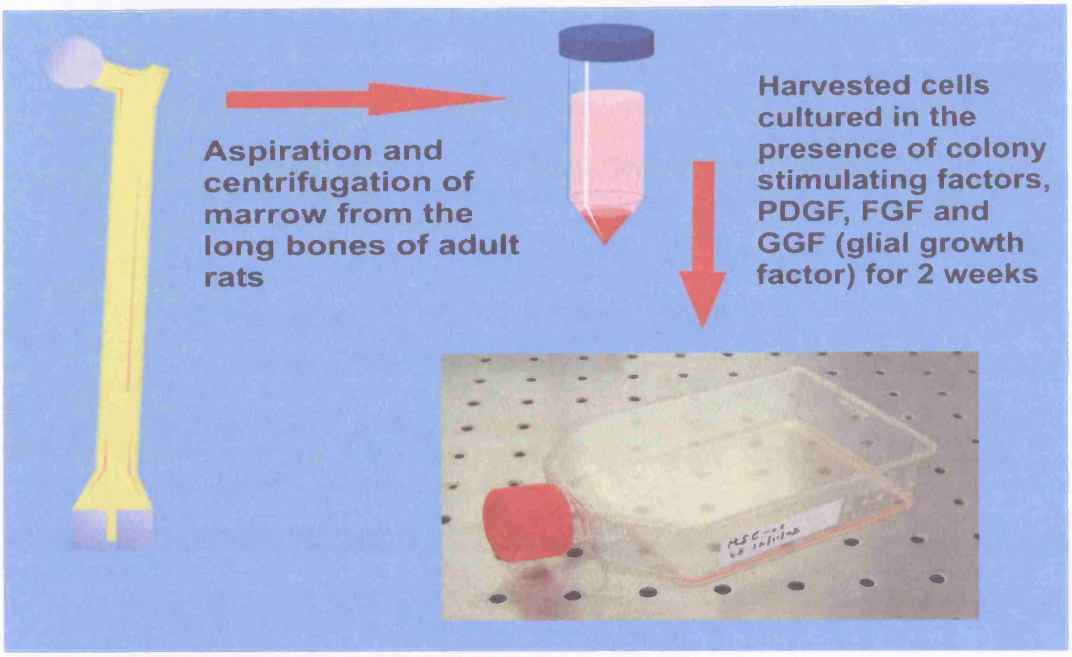

Figure 2.3 Summary of steps required to harvest and culture MSCs.

2.2.3 Clonogenic assay of bone marrow stromal cells

To determine the clonogenic ability of cultured MSCs the plating efficiency (colony forming ability) was determined where:

$$\text{Plating efficiency} = \frac{\text{No. of colonies formed}}{\text{No. of cells plated}} \times 100$$

Confluent MSCs were trypsinised with 0.25% trypsin/EDTA, suspended in 10mls of MSC growth medium and counted. MSCs were plated at various concentrations (Table 2.1) in 6-well plates and incubated for one week following which the plates were stained with 1% Azure blue (cf. Appendix C) and the

number of distinct colonies (≥ 50 cells) counted with the aid of an inverted microscope (Figure 2.4).

Cells/cm^2	*Cells/well (10cm^2/well)*
100	1000
80	800
60	600
40	400
20	200
4	40

Table 2.1 Plating densities of MSCs in each well of 6-well plates to quantify clonogenic ability (plating efficiency).

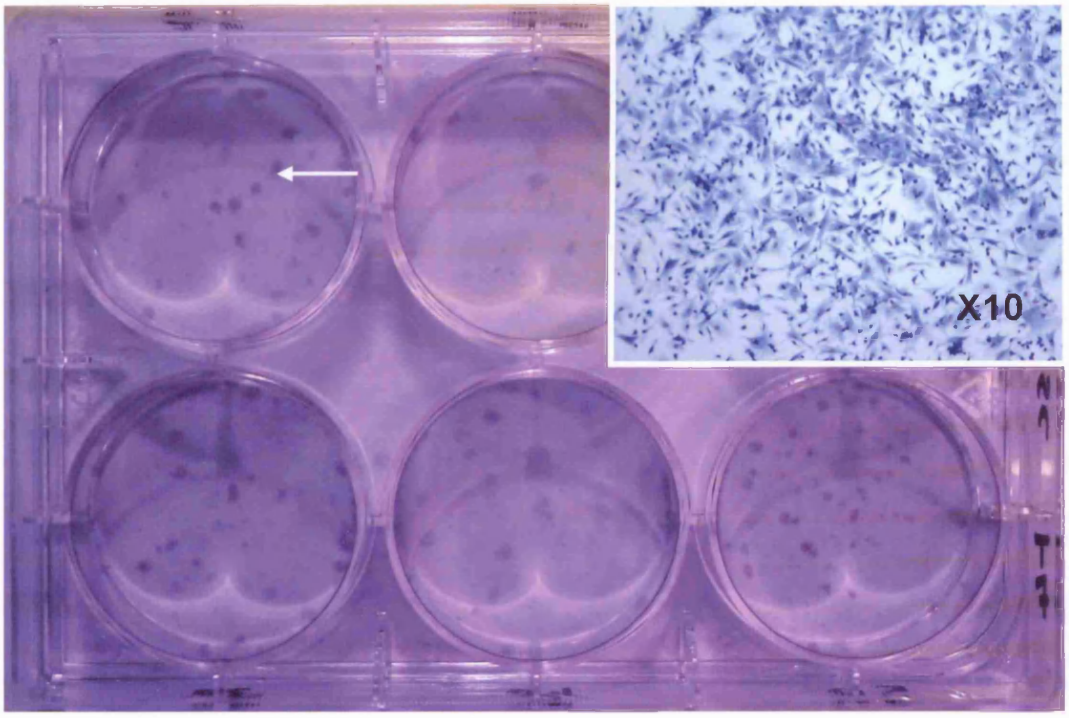

Figure 2.4 MSCs plated on 6-well plates and stained with Azure blue to quantify colony forming ability (arrow and inset).

2.2.4 Clonal selection of bone marrow stromal cells

Confluent MSCs were trypsinised with 0.25% trypsin/EDTA, suspended in 10mls of MSC growth medium and counted. The cell concentration of the suspension was reduced to 500 cells/ml by serial dilution. The cells were seeded in 96-well plates (50 cells/100µl/well) to isolate cells with clonogenic capacity. The medium was left on the cells for one week so as to not wash away any locally produced growth factors which may be involved in autocrine and paracrine growth circuits. The cells were not removed from the incubator for examination during this period as a fluctuation in temperature can arrest the cell cycle (Freshney, 2000). Wells were examined at the end of the first week and those containing single colonies (Figure 2.5) were marked, wells containing more than 1 colony were excluded. Upon the appearance of a colony in a well, the well was washed with Hank's medium, 50μl of 0.25% trypsin/EDTA was added and incubated at 37°C for 5 minutes. Following incubation, 100μl of MSC growth medium was added to the well to neutralise the trypsin following which the cell suspension was transferred to a single well of a 24-well plate with 900μl of MSC growth medium and placed in an incubator. When confluent, each well was trypsinised and transferred to a 25cm^2 flask and again left to grow until confluent.

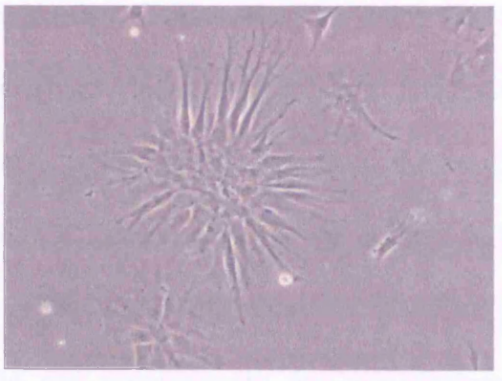

Figure 2.5 Phase contrast photomicrograph of a colony of marrow stromal cells seeded in a 96 well plate.

2.3 Cell transduction with Green Fluorescent Protein

Retroviral transduction is the most efficient means of introducing foreign genetic material into a cell. To transduce cells with green fluorescent protein (GFP) a Moloney Murine Leukaemia retrovirus (MMLV) containing the GFP sequence was used. A mouse embryonic fibroblast cell line (PT67) was used to package the virus and produce a high viral titre. The retrovirus genome consists of a single strand of RNA which is transcribed into double-stranded DNA by the enzyme reverse transcriptase. The double-stranded DNA, known as the provirus, integrates irreversibly into the cellular DNA and is hence replicated within the host's genome. PT67 cell lines contain exons for the protein core of the virus (*gag*), reverse transcriptase (*pol*), envelope proteins (*env*) and the packaging sequence (ψ), however the retrovirus produced is deficient in the packaging sequence so that when it infects a target cell it is incapable of replicating (replicative incompetent), thus preventing transduced cells from infecting other cells.

2.3.1 Production of MMLV-GFP-PT67 cell line

The MMLV-GFP-PT67 cell line was produced by D. Mann (Queen Victoria Hospital, East Grinstead, UK) using the following protocol: The ViraPort™ retroviral reporter vector pFB-hrGFP (Stratagene), containing the humanised form of green fluorescent protein from the sea pansy *Renilla reniformis*, was used to transfect a RetroPack PT67 packaging cell line (Clontech) for higher titre viral production. Co-transfection of 15μg of pFB-hrGFP and 1.5μg pSV_2neo was carried out according to the manufacturer's instructions using Lipofectamine

Plus™ reagent (Gibco). Transfected producer cells were selected for the neomycin pSV_2neo resistance marker using 800µg/ml Geneticin (G418 Sulphate; Gibco) 3 days after selection. Cells were continually cultured under selective pressure in DMEM with glutamax, sodium pyruvate and 4.5 g/ml glucose (Gibco) and 10% FCS. Fluorescent colonies were isolated, expanded and screened for the production of virus containing the hrGFP protein (Figure 2.6). PT67pFB-hrGFP Clone A2 was reselected using HAT supplements (Gibco) according to the Clontech protocol to ensure the retention of the viral genes.

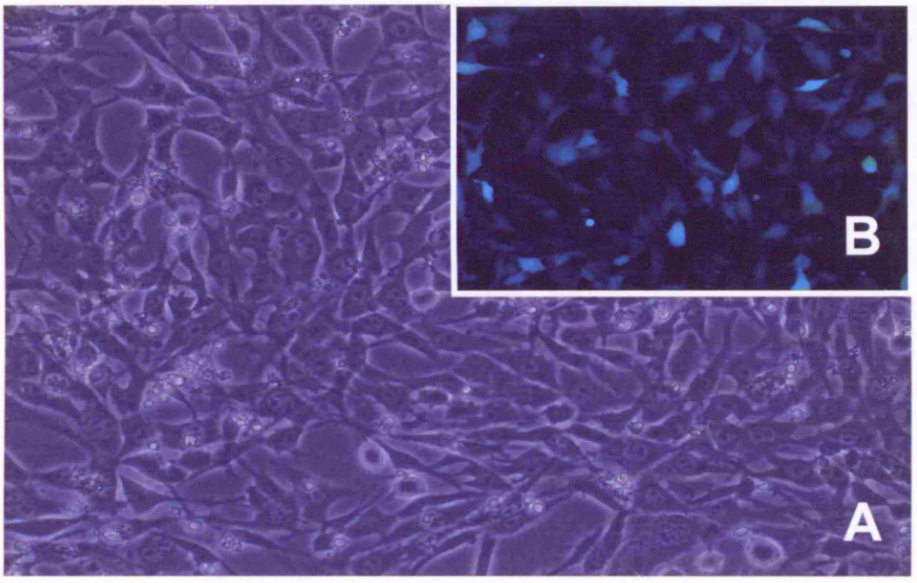

Figure 2.6 (**A**) PT67 cells under phase contrast microscopy and (**B**) green fluorescence under blue light.

2.3.2 Cell transduction

PT67 cells were grown in $75cm^2$ flasks with medium consisting of DMEM high glucose, 10% fetal calf serum and penicillin and streptomycin. At 70% confluence the medium was changed to target cell growth medium and the cells were transferred to 32°C and incubated for 72hrs. The medium (containing a high

concentration of retrovirus) was collected and filtered through a 0.45μm filter to remove any suspended PT67 cells. The filtrate was added to a 70% confluent culture of target cells (SCs or MSCs), and the cells placed in an incubator at 32°C for 24hrs. The target cells were then placed in their normal growth medium and incubated at 37°C for 24hrs. This cycle was repeated with the same target cells a further 2 times, making a total of 3 transduction cycles. Target cells were assessed for successful transduction by examining for green fluorescence under blue light with a fluorescence microscope (Olympus BX60) (Figure 2.7). Following confirmation of transduction, normal medium was added to the transduced cells and incubated for 24hrs at 32°C, the medium was removed, filtered and added to a second batch of non-transduced cells for 24hrs to ensure no transduction had taken place due to viral contamination of the conditioned medium.

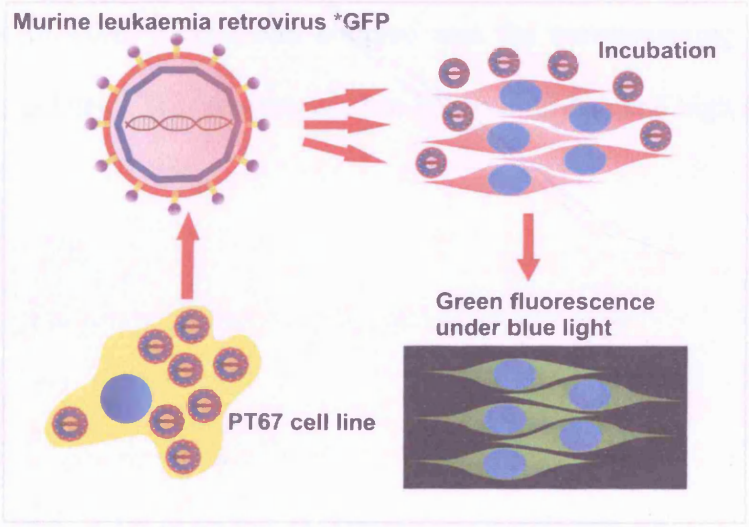

Figure 2.7 Retroviral transduction of target cells (red) using a PT67 cell line which packages a Moloney Murine Leukaemia retrovirus containing the gene for green fluorescent protein. Transduced cells are examined for green fluorescence under blue light.

2.3.3 Measurement of transduction efficiency

To measure transduction efficiency (percentage of cells transduced per total number of cells), transduced cells were trypsinised and plated on a chamber slide (Labtek) and incubated at 37°C in appropriate medium for 24hrs. The medium was then replaced with fresh medium containing 10μl/ml of Hoescht which labels cell nuclei and incubated at 37°C for 15 minutes. The chamber slide was then washed with PBS, covered with fluorescence mounting medium (Vectashield®) and a coverslip, and then examined under a fluorescence microscope (X20 high power field). A digital image was captured of cell nuclei under a rhodamine filter, the filter was then changed to blue light to capture a corresponding image of GFP-transduced cells in the same field (Figure 2.8). The images were transferred to image analysis software (Image-ProPlus®, Media Cybernetics, USA) in which the total number of cells were counted by counting blue Hoescht-labelled cell nuclei. The number of GFP^{+ve} cells was counted and the corresponding transduction efficiency calculated. This was repeated in 10 randomly picked high power fields.

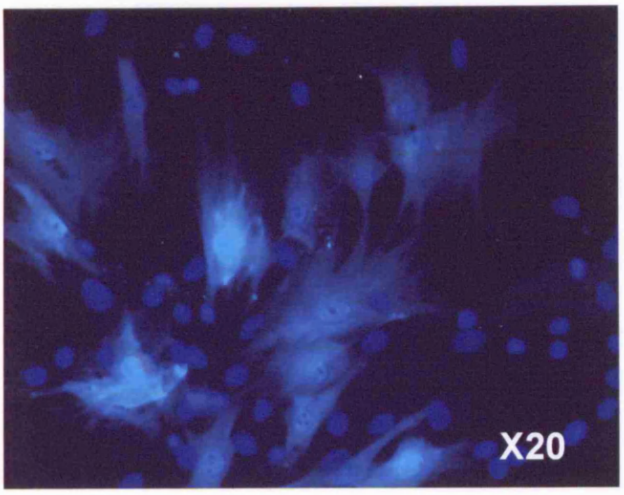

Figure 2.8 MSCs labelled with GFP (green) and the Hoescht nuclear marker (blue) to calculate transduction efficiency.

2.4 Cryopreservation of cells

Cells were frozen at regular intervals to build-up a stock for further use and analysis. When confluent, cultured cells were trypsinised (cf. 2.1.3), diluted in 10mls of cell growth medium and sampled for counting. The cells were divided into aliquots containing ~2 x 10^6 cells/aliquot which were then centrifuged at 800rpm for 5 minutes. This is the minimum number of cells/ml that should be frozen, lower concentrations yield fewer surviving cells on thawing. The resulting cell pellets were then each suspended in 1ml of chilled cell freezing medium (cf. Appendix A) and placed in cryovials for freezing. The active constituent of cell freezing medium is dimethylsulphoxide (DMSO) which prevents intracellular ice crystal formation on freezing. DMSO above 5°C is toxic

to cells and therefore should always be chilled when added to cells prior to freezing. The cryovials were transferred to an isopentane flask which was placed in a -70°C freezer overnight to allow slow freezing of the cells. Rapid freezing causes cell damage, the isopentane flask ensures slow freezing of cells at a rate of ~-1°C/min. The following day the cryovials were transferred to the gas phase compartment of a liquid nitrogen freezer for long-term storage.

2.5 Thawing of frozen cells

To thaw frozen cells, a cryovial was removed from the liquid nitrogen freezer and transferred to the tissue culture cabinet. The frozen cells were allowed to thaw at room temperature following which they were immediately transferred to a 20mls universal container. The cells were then slowly diluted with 10mls of chilled cell growth medium at a rate of 1ml/min to prevent osmotic damage to the cells. The suspension was centrifuged and washed to remove all traces of DMSO, re-suspended in suitable cell growth medium, plated in a tissue culture flask and transferred to the incubator.

2.6 Alamar Blue™ assay

Alamar Blue™ (Serotec) was used to measure the metabolic activity of non-transduced and GFP-transduced SCs *in vitro*. Alamar Blue™ is a colorimetric growth indicator solution that changes colour in the presence of REDOX reactions (blue to red) which occur during cell metabolism with colour change being quantified by measuring the difference in spectral absorbance (δ-absorbance) between 570 and 600nm wavelengths of light. Cells from each line at the same passage stage were seeded in 6 wells of a 12-well plate (PDL-coated) at a

concentration of $1x10^5$ cells per well. A further 4 wells contained media but no cells to act as a baseline control. One ml of SC growth medium containing 10% alamar Blue™ was added to each cell line well on day 1 and the cells incubated at 37°C, 5%CO_2, 99% humidity. At 4, 8, 12, 24 and 48 hours, 50μl of medium was taken from each well (including the control wells), placed in a 96-well plate and assayed with a spectrometer (Multiskan) to measure δ-absorbance, this being directly proportional to metabolic activity.

2.7 Cell growth curves

To construct a Schwann cell growth curve, cells were plated in a PDL-coated 24 well plate. Cells were plated in each well at a concentration $1x\ 10^5$ cells/ml/well. At 24 hrs (day 1) 3 wells were trypsinised and each well individually counted with a haemocytometer. This was repeated each day for a further 8 days. Data was plotted and best-fit growth curve constructed (GraphPad Prism, GraphPad Software, San Diego, California).

2.8 Preparation of PHB conduits

PHB conduits were made from sheets of sterile PHB (Astra-tech, Sweden) under aseptic conditions in a tissue culture cabinet. PHB sheets are manufactured by compressing two layers of PHB fibres together. The fibres of each layer are unidirectional (Figure 2.9A) and the layers are orientated so that when they are pressed together they run in perpendicular directions. It was therefore necessary to separate the layers before further use. To separate the layers, one corner of a sheet was gently separated using a pair of jewellers forceps (Mercian, UK) to develop a plane between the layers which were then slowly pulled apart (Figure 2.9B). One sheet is patterned from the pressing process and the other is smooth, the patterned sheet was discarded. To make a 1.4cm conduit for the rat sciatic nerve gap model a PHB sheet was cut into a rectangle measuring 1.4 x 0.8cm using a sterile scalpel blade. It is important that the direction of the fibres is parallel to the long axis of the conduit. The PHB was then soaked in sterile water to prevent excessive melting during heat-sealing. The sheets were then wrapped around a 16G intravenous cannula and welded along the points where the sheets overlap using a fine-tipped soldering iron (Figures 2.9C, D). It is important that the smooth side of the sheet forms the inner wall of the conduit. The resulting conduit is 1.4cm in length with an internal diameter of 1.6mm which allows adequate space for post-injury swelling of the rat sciatic nerve. Each conduit was then placed in an individual well of a sterile 24-well plate for storage.

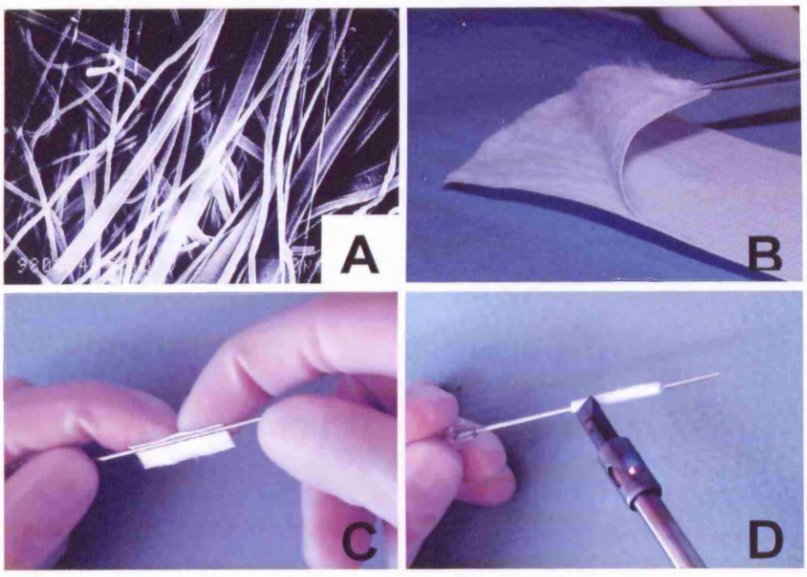

Figure 2.9 (A) E.M. photomicrograph of PHB fibres and (**B**) splitting of PHB sheet into 2 layers. (**C**) Rolling of PHB sheet and (D) welding of conduit

2.9 Silicone conduits

Pre-formed silicone tubing was used for silicone conduits (internal diameter 1mm; Philip Harris Scientific Supplies). The conduits were sterilised with gamma-irradiation (3MRad. for 50hrs) and cut to a desired length.

2.10 Loading of conduits with matrices for cell and growth factor suspension

2.10.1 Loading PHB and silicone conduits with alginate hydrogel

PHB and silicone conduits were pre-soaked in normal saline to enhance penetration of $CaCl_2$. Using a Hamilton syringe, 30μl of 1.8% alginate (Pronova, Oslo) was injected into a conduit taking care not to introduce air bubbles into the

alginate. The conduit was then placed in 0.1M $CaCl_2$ for 2 minutes to gel the alginate prior to grafting.

2.10.2 Loading of PHB and silicone conduits with collagen gel

Neutralised collagen solution (Vitrogen) was prepared (cf. Appendix A) and 2mls was placed in a 5ml bijou bottle. Empty conduits were placed vertically in the collagen and submerged until one end of the conduit rests on the surface of the collagen with the remainder of the conduit completely submerged (Figure 2.10 and 2.11). The bijou bottle was then sealed and placed in a 37°C incubator in the absence of CO_2. After 2 hrs, when the collagen surrounding the conduits was completely gelled, 30μl of collagen (with or without a suspension of cells) was injected into the conduit using a Hamilton syringe. The gelled collagen surrounding the conduits prevents leakage of the collagen solution from inside the conduit. The bijou bottle containing the conduit was then placed back into a 37°C incubator (no CO_2) and incubated for 1hr to gel the collagen within the conduits, the conduits were then removed from the bijou and transferred to the operating theatre for grafting.

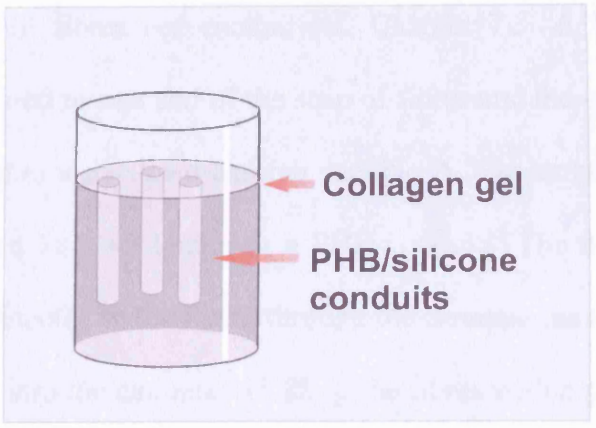

Figure 2.10 Conduits are placed in a collagen solution which is then gelled in a 37°C incubator in the absence of CO_2. When the collagen surrounding the conduits has set the conduits can be filled with collagen solution (± cell suspension) and gelled at 37°C.

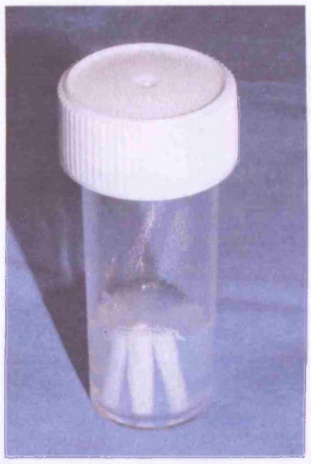

Figure 2.11
Conduits following collagen gelling.

2.10.3 Loading PHB conduits with dissociated PHB fibres

Mats of unidirectional dissociated (un-pressed) fibres of PHB were obtained from Astra-tech (Sweden). Under aseptic conditions in a tissue culture cabinet, strips of a mat were cut (2 x 20mm, varying thickness to provide a range of fibre densities) with the longitudinal axis parallel to the direction of the fibres (Figure 2.12). Conduits containing different fibre densities were assessed to define the

optimum number of fibres per conduit (cf. Chapter 7). A 9/0 ethilon suture (Ethicon) was secured to one end of the strip of fibres and the opposite end of the suture was secured to a sterilised darning needle. A 2cm length of a plastic 16G cannula was passed into the lumen of a PHB conduit. The needle was used to pass the suture connected to the fibres through the cannula, the strip of fibres were then gently drawn into the cannula. Holding the fibres with a pair of fine forceps at one end, the opposite end of the cannula was held with a pair of forceps and gently pulled out of the conduit leaving the fibres inside (Figure 2.13A,B,C and D). The fibres extending from the conduit at each end were trimmed and the conduit stored in a well of a sterile 24-well plate in preparation for grafting.

Figure 2.12 Strips of dissociated PHB fibres were cut into 2cm lengths.

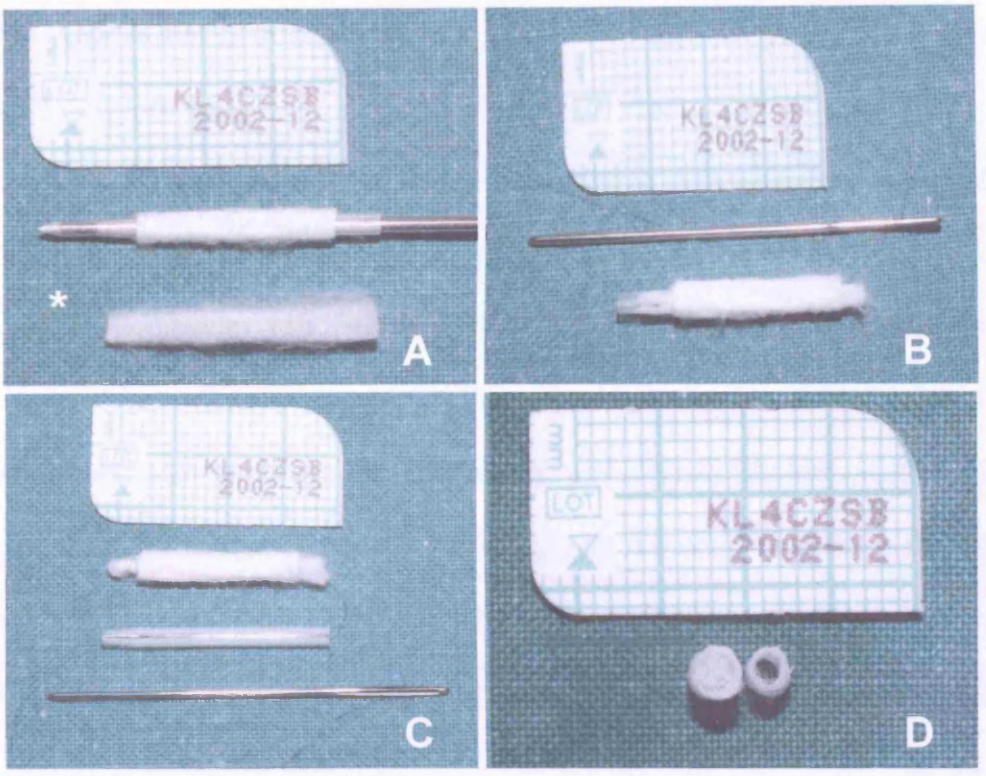

Figure 2.13 Steps involved in loading a PHB conduit with dissociated PHB fibres. (**A**) A 2cm length of 16G plastic cannula is inserted into the conduit and used to guide the entry of PHB fibres (*). (**B**) A needle connected to the fibres with a 9/0 suture is used to pull the fibres through the plastic cannula. (**C**) The plastic cannula is removed to leave the PHB fibres within the conduit. (**D**) A transverse section of the conduit demonstrating intraluminal fibres in comparison with an empty conduit.

2.11 Operative procedures

2.11.1 Anaesthesia

All procedures were carried out in compliance with the regulations specified in the Animals (Scientific Procedures) Act 1986 (UK Home Office). Inbred adult male Sprague-Dawley rats (Harlan, UK; 6-8 weeks old; weights 200-250gms) were used in all experiments. For recovery procedures animals were anaesthetised with halothane gas: The animal was placed in an induction chamber connected to an anaesthetic circuit. Oxygen was delivered at 2L/min following which 4% halothane was added for 1-2 minutes. The anaesthetised animal was then removed from the induction chamber and its left thigh was shaved and washed with alcoholic chlorhexidine. The animal was then placed on sterile drapes covering a heated mat on an operating table. Anaesthesia was maintained by reconnecting the animal to the anaesthetic circuit via a face mask with oxygen flow rate set to 500ml/minute and halothane concentration set to 1.5%. Depth of anaesthesia was regularly assessed by monitoring the animal's respiratory rate, heart rate and response to pain (tail pinch) with the halothane concentration being adjusted accordingly. Following the operative procedure to expose, axotomise and graft the sciatic nerve (cf. 2.11.3), muscle edges were re-opposed with a 4/0 vicryl suture (Ethicon) and the skin was closed with a subcuticular suture.

On completion of the operation 10mcg of intramuscular temgesic was administered, the tail was marked with an indelible pen and the animal was placed on its right side on soft bedding in an individual cage. The animal was placed in a 32°C incubator and regularly monitored until it was fully conscious, following which it was transferred to a recovery room for 24hrs prior to re-colonisation.

Animals were monitored daily for general health and morbidity associated with sciatic nerve surgery such as wound dehiscence, infection and autophagy.

2.11.2 Termination

Animals were terminated in accordance with Schedule 1 of the Animals (Scientific Procedures) Act 1986. Animals were killed by CO_2 narcosis by placing the animal in a CO_2 chamber. The concentration of CO_2 was automatically increased until the animal had stopped making any respiratory effort for more than 1 minute. Termination was then confirmed by cervical dislocation. In non-recovery procedures requiring physiological measurements (terminal anaesthesia) animals were anaesthetised with an intra-peritoneal injection of a lethal dose of sodium pentobarbitone (0.5ml/kg). After measurements had been taken the animal was terminated by cervical dislocation.

2.11.3 Gap repair (1cm) of the sciatic nerve

To expose the sciatic nerve a 4cm skin incision was made over the left gluteal region 3mm posterior to the long axis of the femur, starting at a point posterior to the level of the greater trochanter. A muscle splitting incision in the long axis of the fibres was then created in biceps femoris to expose the sciatic nerve. Muscle and skin edges were retracted to allow adequate operative exposure (Figure 2.19). Under an operating microscope (Zeiss, X10 magnification) the nerve was gently mobilised and divided 5mm from the sciatic notch. Following division, the sciatic nerve retracts to leave a gap between the proximal and distal stumps, to increase this gap to 1cm, nerve tissue (~5mm) was resected from the distal stump. A conduit of either PHB or silicone was placed in the operative field. For a 1cm gap a 1.4cm conduit is used, with each nerve end being placed 2mm into each end of the conduit, therefore leaving a 1cm gap between the nerve ends within the conduit. At each end the nerve is sutured to the conduit with a 9/0 epineural suture (Figure 2.20).

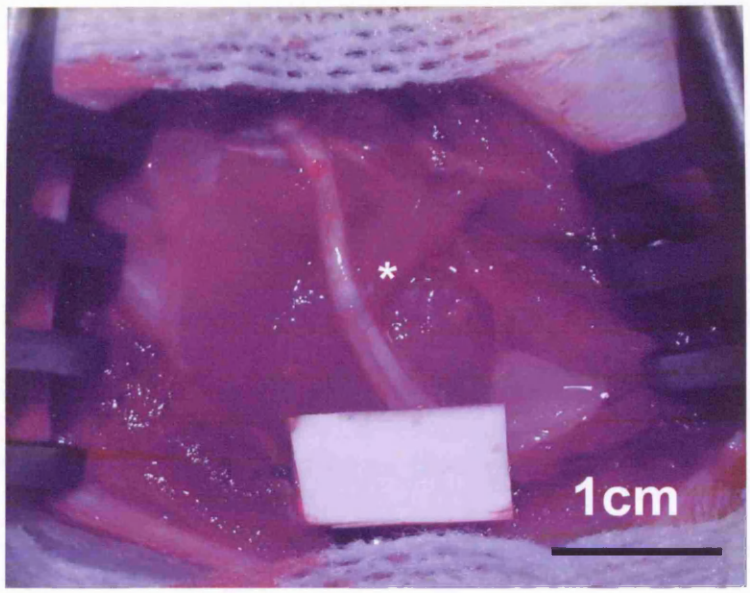

Figure 2.19 Exposure of the rat sciatic nerve*

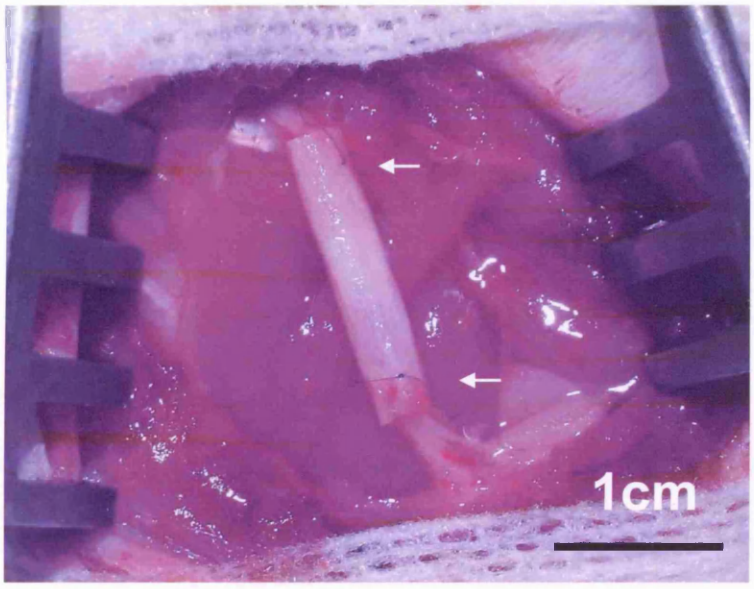

Figure 2.20 Insertion of PHB conduit and placement of 9/0 sutures (arrows).

2.12 Tissue collection

2.12.1 Tissue collection for immunostaining (nerve)

Following termination, the grafted conduit together with proximal and distal sections of nerve, were exposed using an operating microscope (Zeiss, X10 magnification). The sutures at either end of the conduit were removed to prevent tearing of tissue during cryosectioning. For immunohistochemistry the conduit and nerve at either end were removed *en bloc*, pinned out on plastic to prevent shrinkage and distortion and placed in Zamboni's fixative (cf. Appendix C) overnight at 4°C. Over the following days (~3) the specimen was washed in PBS-sucrose (Figure 2.21) until the solution became clear and the tissue had sunk to the bottom of the container. The specimen was then blocked in OCT with a piece of fixed rat liver at the proximal end to aid orientation during microscopical examination, and slowly frozen by gently immersing in liquid nitrogen. The frozen block was then stored at –40°C.

For cryosectioning, a frozen specimen block was transferred to a cryostat (Albright) and left for 30 minutes to let the temperature equilibrate between the block and the cryostat. The block was slowly trimmed in the desired orientation until the lumen of the conduit was reached in-continuity with proximal and distal nerve stumps. Cryosections were taken at 15μm thick and placed on Vectabond coated glass slides (Appendix C). The sections were allowed to dry in a 37°C oven overnight. Sections were either immuno-stained the next day or wrapped in aluminium foil and placed in a –40°C freezer for staining within a maximum of 7 days.

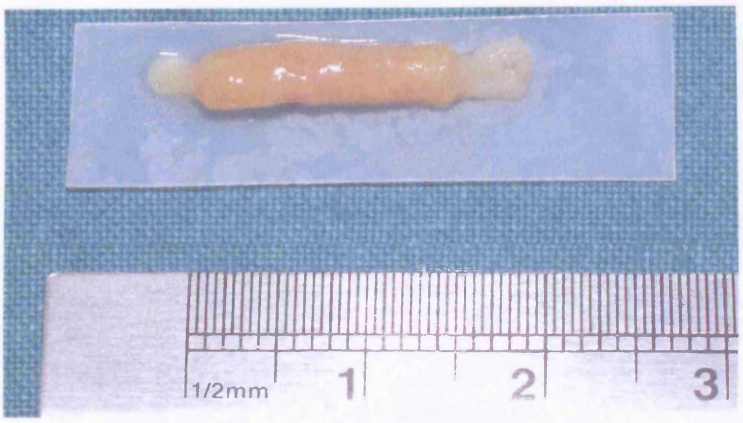

Figure 2.21 Ex-planted PHB conduit following fixation and washing.

2.12.2 Tissue collection for semi-thin sections

Semithin sections were used to assess nerve regeneration in long-term (> 6 weeks) studies. Tissue specimens from nerve distal to the nerve conduit (Figure 2.22) were placed in E.M. grade 2.5% glutaraldehyde following harvesting. The specimens were processed by the Electron Microscopy Unit, Royal Free Campus, where they underwent osmium tetroxide fixation, ethanol dehydration and resin embedding followed by staining with methylene blue-azure II and basic fuchsin (Humphrey's stain) in preparation for sectioning (1-2μm) on an ultramicrotome.

2.12.3 Tissue collection for immunostaining (skin)

Lateral paw skin was collected from the ipsilateral side to the sciatic nerve axotomy and pinned on plastic to prevent retraction. The skin specimen was placed in Zamboni's fixative and left for 24hrs at 4°C. The specimen was then washed in PBS-sucrose daily until the solution was clear of discoloration. The specimen was then blocked in OCT (cf. 2.12.1).

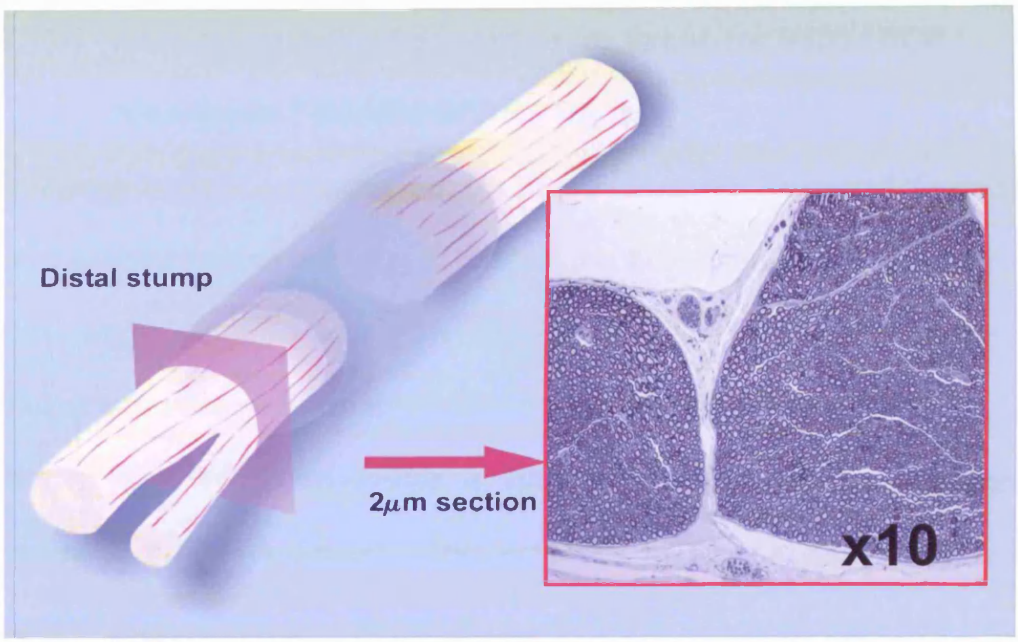

Figure 2.22 Semithin sectioning of distal nerve to assess axonal counts following regeneration through the nerve conduit.

2.13 Histological analysis

The majority of tissue collected in the experiments performed was examined using immunofluorescent histochemical techniques. As transplanted cells examined in the study were labelled with green fluorescent protein (GFP) these cells could be identified by direct fluorescence under blue light. Antigen expression was identified using antibody-mediated immunofluorescence. To prevent bleaching of fluorescence labelled antibodies and GFP in natural light, slides were kept in the dark at all times. Haematoxylin and eosin staining was carried out on random sections from each animal group to ensure correct orientation of sections prior to immunostaining and to assess general histology and morphology.

2.13.1 Immunostaining of *ex-vivo* nerve tissue for S100 / PGP / N-cadherin / NCAM / GFAP / Thy 1.1

Following cryostat sectioning (cf. 2.12.1), sections were prepared for indirect immunohistochemical analysis. If sections had been frozen they were thawed at room temperature for 3 hours. The slides were outlined with a hydrophobic pen (Dako) to prevent antibody solutions spreading and dripping off the slides. The sections were first permeabilised in 10% Triton-X-PBS for 1hr followed by washes in PBS (3 x 5mins). The sections were then incubated in a humid chamber with normal goat serum (dil. 1:100; 1hr at RT) to decrease non-specific attachment of second layer antibodies. The blocking solution was tipped off the slides and primary antibodies to either S100 (for the detection of Schwann cells); PGP9.5 (for the detection of nerve fibres), GFAP, Thy 1.1, N-cadherin or NCAM were applied (see Appendix A for details) to the sections and incubated at 4°C in a humid chamber overnight. Following 3 PBS rinses, Cy3- or FiTC-labelled secondary antibody (see Appendix A) was applied and incubated for 2hrs at room temperature in the dark. Following 3 further PBS washes, the sections were mounted with fluorescence mounting medium (Vectashield) and glass coverslips, and examined under fluorescence light using a green filter to identify Cy^3 labelling (red fluorescence) and a blue filter to identify transplanted GFP-labelled cells or FiTC secondary antibody (green fluorescence). Slides were stored at 4°C and images captured within 24hrs to attain maximum fluorescence.

2.13.2 Immunostaining of skin

Skin specimens were stained for PGP9.5, a constitutive cytoplasmic component of all nerve fibres. Following permeabilisation of the sections in Triton-X-PBS for 1 hour (cf. 2.12.1), the skin sections were counterstained in Pontamine Sky Blue for 30 minutes. Following washes in PBS (2 x 5mins) the sections were immunostained using a PGP9.5 antibody (rabbit polyclonal; see Appendix A). An FiTC-labelled goat anti-rabbit secondary antibody was then applied (cf 2.12.1). Slides were examined and images captured within 24 hours to avoid fading of fluorescence.

2.13.3 Immunostaining of cell cultures

To immunostain cultures, cells were plated on chamber slides (Labtek) pre-coated with poly-D-lysine. The chamber slides were placed in an humidified incubator at 37°C, 5% CO_2 in appropriate medium for 2 days to allow the cells to settle and adhere. Following examination under an inverted microscope to confirm adequate plating the cells were washed with PBS twice and the nuclei stained with Hoechst dye (dil. 10μg/ml in PBS) for 15 minutes at 37°C. The cells were then fixed with 4% paraformaldehyde for 20 minutes at room temperature followed by PBS washes (2 x 3mins). Primary antisera was then applied (either S100, GFAP or Thy1.1) to the cells and incubated for 30 minutes at room temperature. The cells were then washed twice with PBS, the appropriate fluorochrome-conjugated secondary antibody applied and incubated at room temperature in the dark for 2hrs. The cells were then washed twice with PBS, the plastic walls of the chamber slide and the rubber gasket were removed and a cover slip mounted with

fluorescent mounting medium (Vectashield). The slides were examined and images captured with a fluorescence microscope and stored for further use at 4°C.

2.13.4 Histochemical staining of marrow stromal cell cultures

To examine cultured marrow stromal cell (MSC) morphology, MSCs were plated in chamber slides and incubated for 2 days. Prior to staining the plastic walls and rubber gasket of the slides were removed as the protocol required exposure to alcoholic solutions. The slides were placed in a Coplin jar and the cultures washed twice with PBS, they were then dehydrated in 99% methanol for 6 minutes. The cultures were then stained with a Giemsa solution (cf. Appendix C) for between 15-60 minutes at room temperature, being washed and examined under a microscope at 15 minute intervals to prevent over-staining. The slides were finally washed with de-ionised water, allowed to air dry, and then mounted with coverslips using Canada Balsalm (Sigma) as DPX melts chamber slide plastic.

2.14 Image capture and Quantification

2.14.1 Measurement of axonal and Schwann cell regeneration distance

To measure axonal and Schwann cell regeneration distances in the grafted conduits, immunostained sections were examined. Under a X10 objective lens with a graticuled eye-piece, the distance of the most distal regenerating fibre in the regeneration front from the proximal stump (a point 2mm from the proximal end of the conduit) was measured (Figure 2.3).

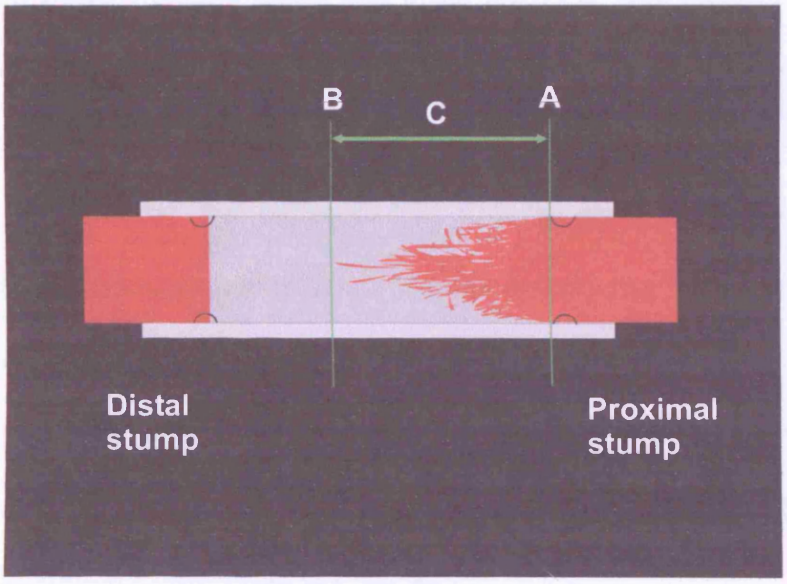

Figure 2.23 Measurement of axonal and Schwann cell regeneration distances. (**A**) Represents the starting point of the proximal stump (2mm from the proximal end of the conduit), (**B**) the point of the most distal regenerating fibre, and (**C**) the regeneration distance.

2.14.2 Quantification of NCAM and N-cadherin expression

NCAM and N-cadherin expression was quantified as intensity of staining per unit area (Thornton et al. 2005). All images were taken in monochrome to minimise loss of signal. Images were taken within 48 hours of staining to minimise decay, importantly the exposure of each section to fluorescent light was kept to an absolute minimum to prevent photo-bleaching. At a set distance (measured with a graticuled lens) from the tip of the regenerating front, images were captured at the regeneration front, proximal stump and distal stump at X40 magnification (see figure 2.24). The image capture region corresponding to the regeneration front was a point 2mm from the most distal regenerating fibre (as determined by co-staining with S100) and that corresponding with the proximal stump was 2mm from the most distal regenerating fibre. The distal stump capture area was a point 2mm from the distal stump axotomy. Images were analysed as shown in Figure 2.25. After the application of threshold values to define areas of staining, the intensity of staining per unit area within each highlighted area was calculated and expressed in arbitrary units (intensity/unit area).

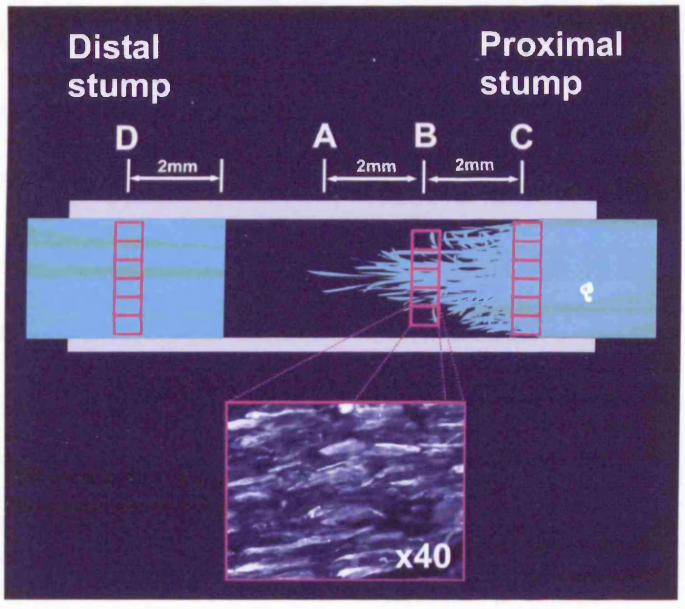

Figure 2.24 Image capturing to quantify N-cadherin and NCAM expression within a PHB conduit. The tip of the regenerating front is represented at (**A**). Images of CAM expression were captured at the regeneration front (**B**), the proximal stump (**C**), and the distal stump (**D**). A sequential set of monochrome images were taken across the width of the section at each point.

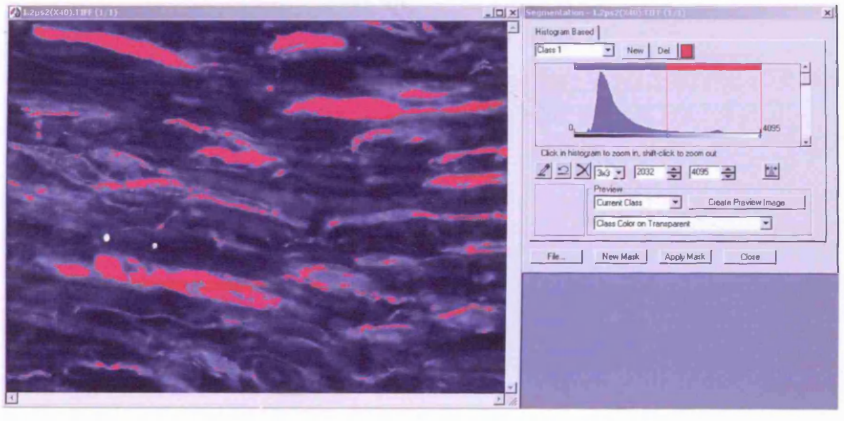

Figure 2.25 Screen capture during quantification of NCAM expression at the proximal stump. Threshold values (right panel) are set to highlight areas of NCAM expression. Areas of artefact or background staining are manually removed. The staining within the highlighted areas is then automatically analysed by the software to measure the intensity of expression per unit area (arbitrary units).

2.14.3 Quantification of semithin sections

Semithin sections were examined under bright field light microscopy using an Olympus BX60 microscope. Under low magnification (X4), an image of the complete transverse section of the nerve was captured (Figure 2.26) using a monochrome digital camera (Evolution QE, DataCell). From each section, 3 random high power images (X40) were captured. Within image analysis software (Image-ProPlus®, Media Cybernetics, USA) the low magnification image was first calibrated according to the number of pixels per unit length (μm).and the total cross-sectional area calculated (Figure 2.27). Calibrated high power images were used to measure axon number, axon diameter, myelin thickness and fibre diameter (figures 2.28-2.30). Measurement data was transferred to a spreadsheet for statistical analysis. An estimate of the total number of axons per nerve was derived from calculating the number of axons per unit area and the total cross-sectional area of the nerve.

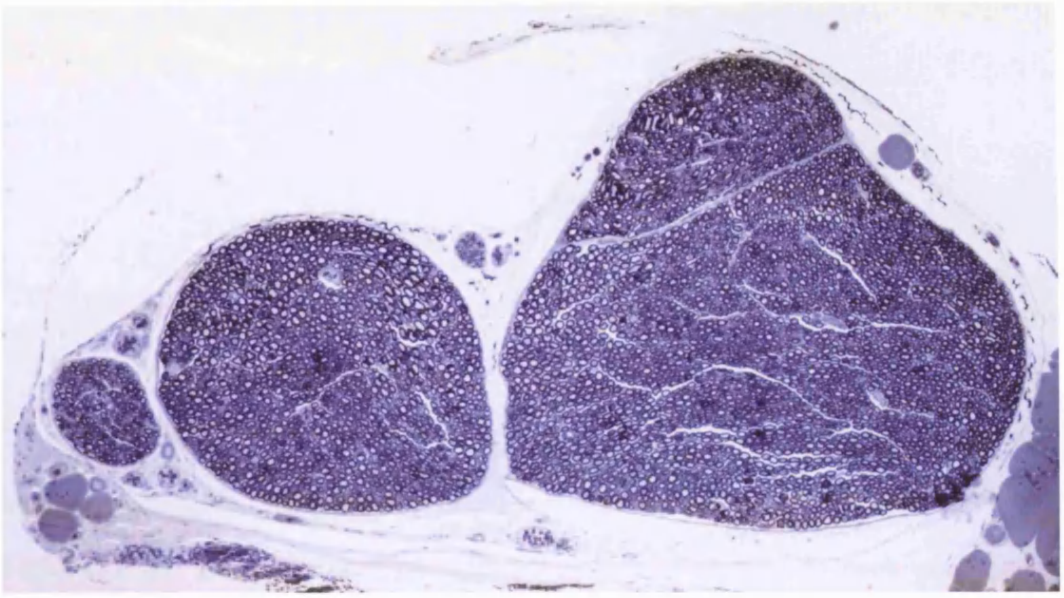

Figure 2.26 Monochrome photomicrograph of a transverse semithin section of rat peripheral nerve stained with thionine and acridine orange (X4).

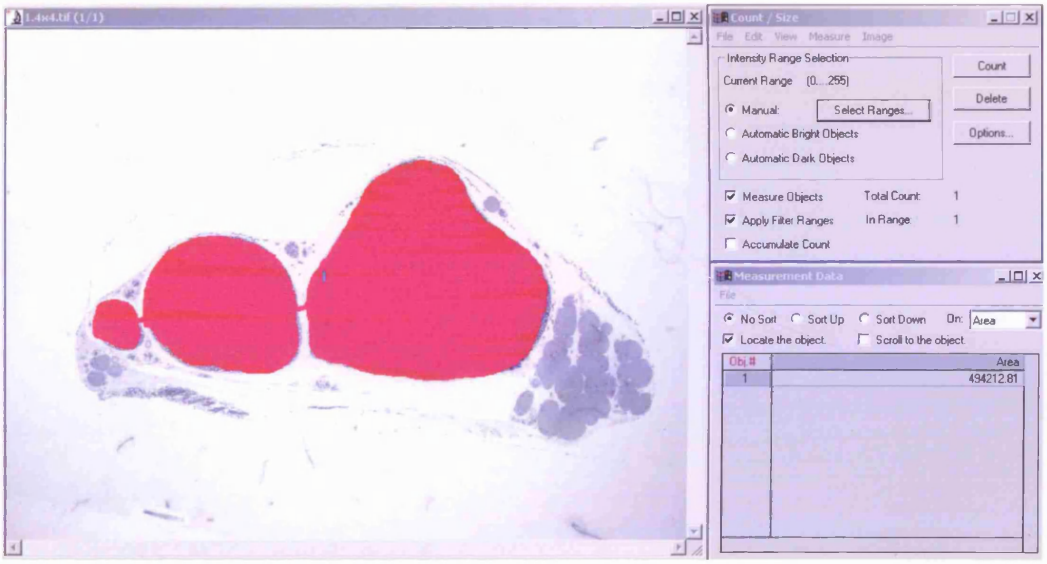

Figure 2.27 The total cross-sectional area of the nerve was calculated by manually outlining the nerve (red shading). Following calibration a value in μm^2 is obtained.

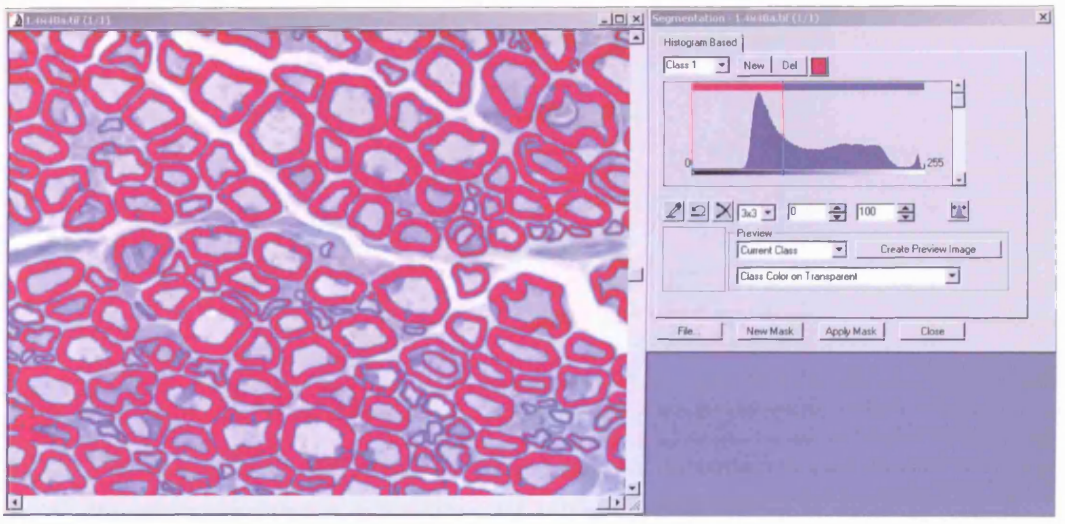

Figure 2.28 Image-Pro® Plus software assigns a number to each pixel in an image between 0 and 256, with 0 representing white, 256 representing black and the numbers between representing 255 shades of grey between white and black. The software can then be manually set (right panel) to highlight structures within an image which have a specific range of grey values, as in the above case where the myelin sheaths surrounding axons are highlighted.

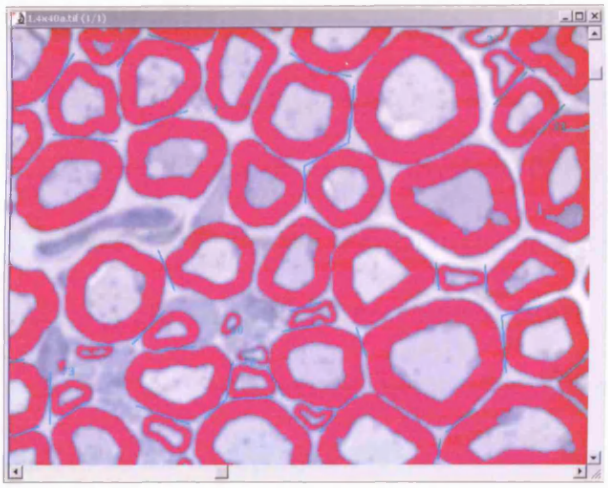

Figure 2.29 Manual editing of the selected structures was performed to eliminate highlighted background or to split two adjacent structures.

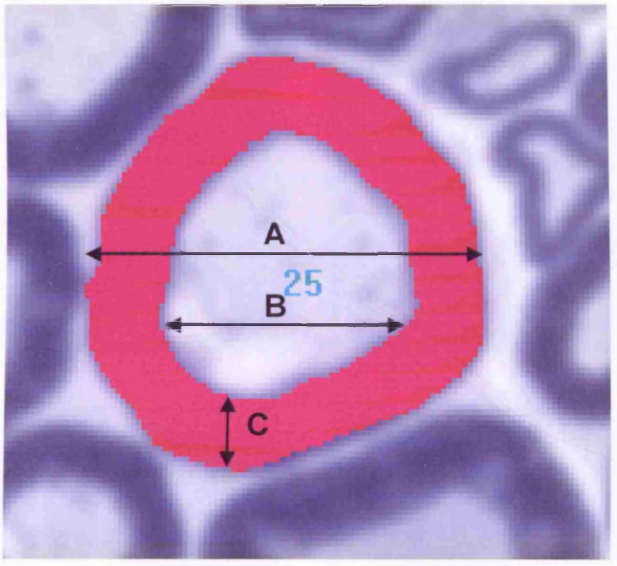

Figure 2.30 Measurements of fibre diameter (**A**), axon diameter (**B**), and myelin thickness (**C**) were automatically made by the software programme.

2.14.4 Quantification of skin immunostaining

Following staining of skin (cf. 2.13.2), fluorescence images were captured with a X20 objective lens, aligning the uppermost epidermis with the top border of the captured image field (Figure 2.31A). Six non-consecutive images were captured from each section, keeping the settings within a similar range. The images were converted to greyscale and the frame area of immunostaining manually outlined. An intensity threshold was set to highlight PGP9.5-immunostained fibres, while artefacts and background interference were manually removed and the area of staining automatically calculated (Figure 2.31B, C). The area of immunostaining was expressed as the fractional area of immunostaining.

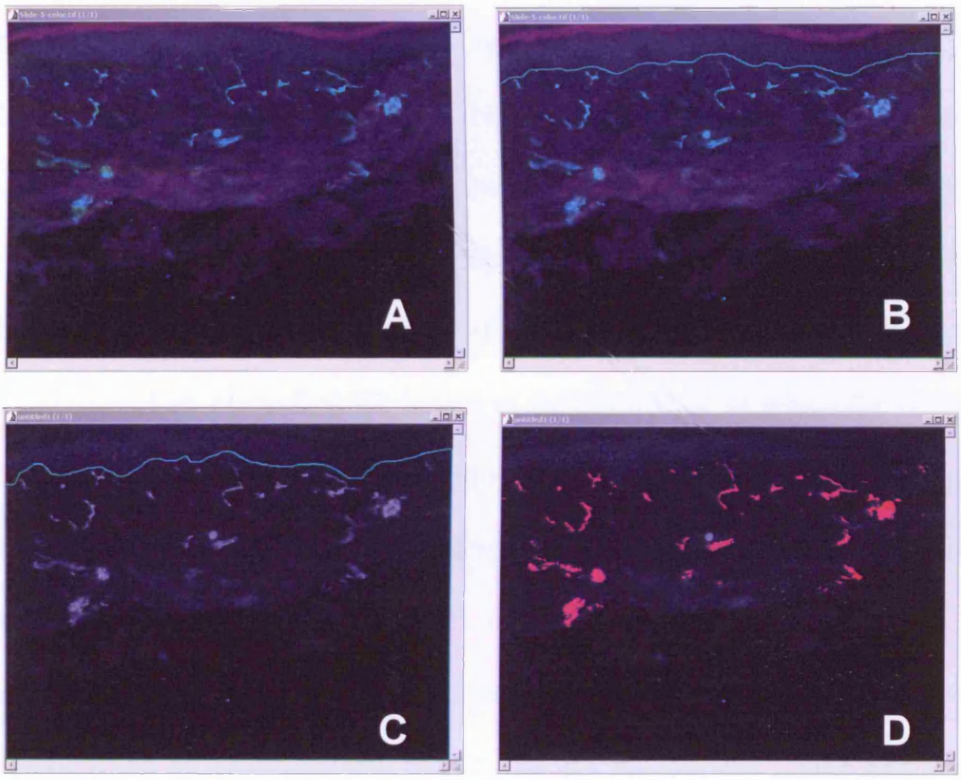

Figure 2.31 Quantification of PGP9.5 skin immunostaining. (**A**) Captured image, (**B**) selection of frame area, (**C**) conversion to greyscale, and (**D**) thresholding of stained fibres following removal of artefact.

2.15 Myophysiological measurements

Measurements of tibialis anterior (TA) muscle activity following sciatic nerve stimulation were made under terminal anaesthesia (cf. 2.11.2). The procedure was carried out in a dedicated electrophysiology laboratory (Figure 2.32) in collaboration with Dr ShiYu Yang and Professor G. Goldspink, Department of Anatomy, Royal Free and University College Medical School. Animals were placed on a platform maintained at 37°C with a temperature-controlled homeothermic blanket. The tibialis anterior (TA) muscle and tendon was dissected from its distal insertion, taking care to avoid damage to the neurovascular pedicle. The distal tendons of the TA were fixed to an isometric transducer that was linked to a PC. The muscles were activated indirectly by delivering supramaximal electrical stimuli (square pulses, 0.2-msec pulse duration, 8 V and 50 Hz) to the sciatic nerve proximal to the nerve graft. Stimuli were generated by a dual impedance research stimulator (Harvard) and delivered with a shielded bipolar silver electrode (Figure 2.33). Optimal muscle length (L_o) was determined by measuring the length of the TA muscle at which the strongest twitch contractions were generated following supramaximal stimuli. Maximum muscle tetanic force was measured and recorded using a Spike2 program (Figure 2.34; Cambridge Electronic Design Limited). Muscle fatigue resistance was determined by measuring the time to the half isometric tension of the muscles. Throughout the physiological evaluation, the TA muscle and sciatic nerve were regularly bathed in warm mineral oil. Muscle temperature was monitored and maintained between 35 and 37°C. For the purpose of comparison, all the physiological measurements from re-innervated muscle were presented as the

percentage compared to the mean values recorded from the contralateral innervated muscle.

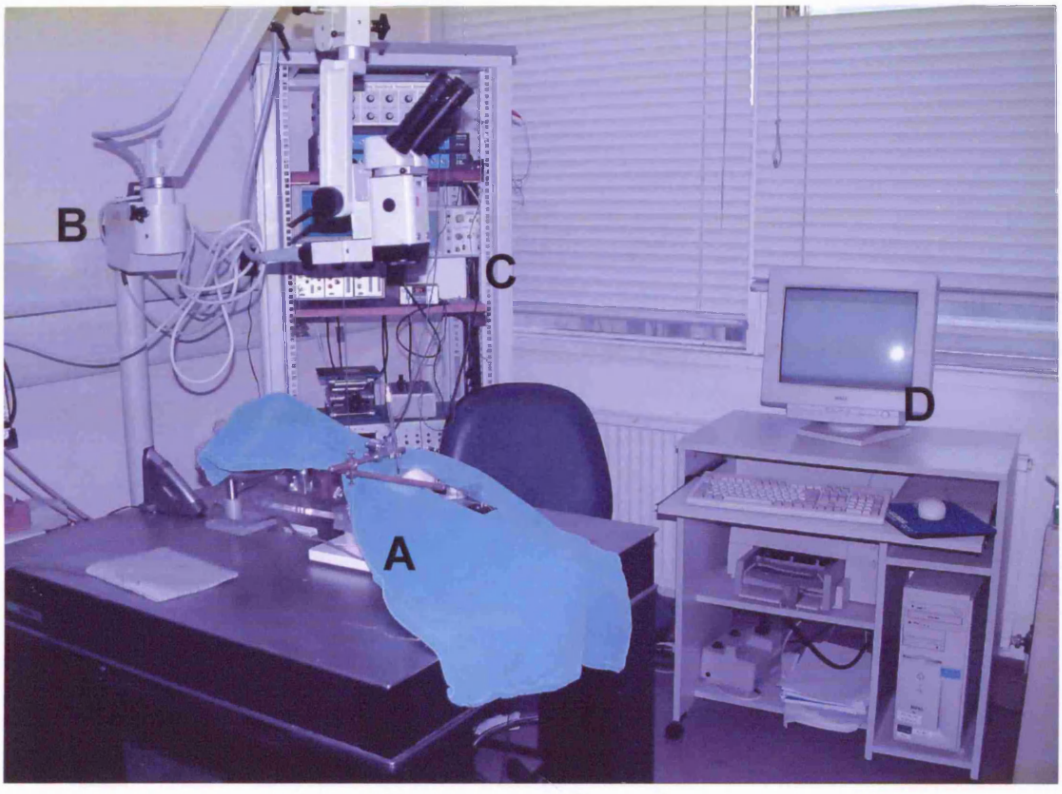

Figure 2.32 Laboratory for myophysiological measurements. (**A**) Jig to support animal containing nerve stimulator and force transducer, (**B**) operating microscope, (**C**) multichannel stimulator, (**D**) PC for recording data.

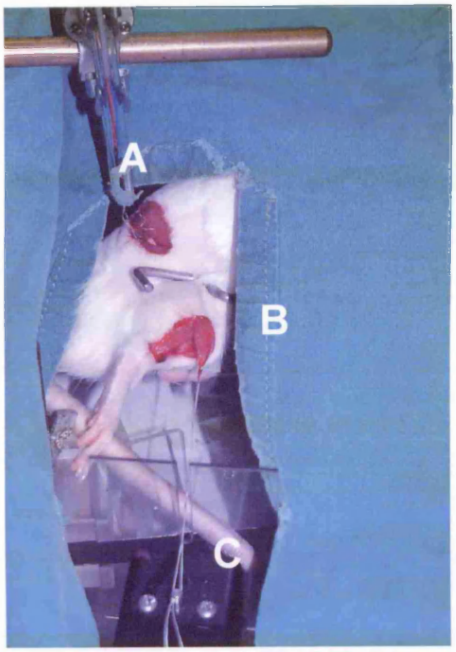

Figure 2.33 Arrangement of nerve stimulator (**A**), tibialis anterior muscle (**B**), and force transducer (**C**).

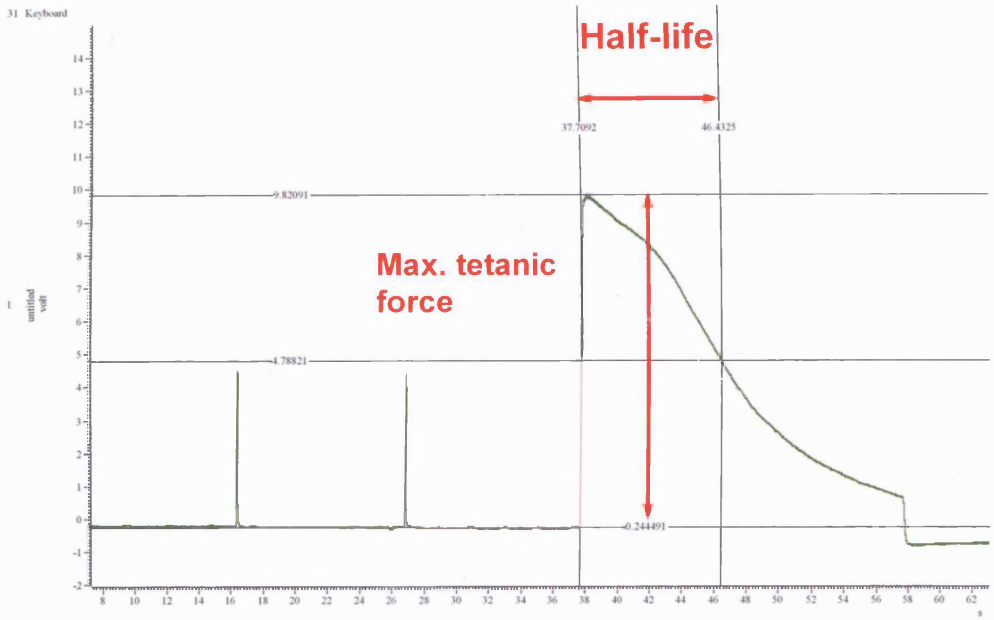

Figure 2.34 Data from the force transducer is represented on a waveform over time. The maximum tetanic force can be measured, and the half-life (fatigability) can be calculated when tetanic force falls to half its maximum value.

2.15.1 Wet muscle weights

Following termination, TA muscle was harvested from both sides and weighed immediately using an electronic balance.

2.16 Statistical analysis

Statistical analysis for each experiment was performed using a Sigmastat® software program (SPSS Science, USA).

Chapter 3

Retroviral Transduction of Schwann cells with Green Fluorescent Protein

3.1 Introduction

Following injury to a peripheral nerve, Schwann cells (SCs) play a vital role in promoting the regeneration of axons by providing both physical support and neurotrophic guidance (Hall, 1986; Sherer 1997). The addition of unlabelled cultured SCs has been shown to improve nerve regeneration through bio-engineered nerve grafts (Guenard et al. 1992; Levi et al. 1994; Rodriguez et al. 2000). A bio-engineered system containing cultured cells which is transferred from an *in vitro* to an *in vivo* setting requires initially a method of labelling the transplanted cells as a means to assess their survival and integration within the host upon *ex vivo* histological analysis. As fluorescent immunohistochemical techniques are commonly used to assess nerve regeneration through bio-engineered conduits, it would therefore be advantageous to label transplanted SCs within these conduits with a fluorescent marker that can be visualised in combination with fluorochrome labelled antibodies.

Green fluorescent protein (GFP) (Shimomura et al. 1962) is a bioluminescent protein found in a number of marine organisms such as *Aequorea victoria* (crystal jellyfish) and *Renilla reniformis* (sea pansy) (Morin & Hastings, 1971; Tsien, 1998). Depending on their species, these organisms emit green light having accepted energy from luciferases or photoproteins. Isolated GFP is excited by blue light (absorbance peak 395nm) to emit green light at an emission maximum of 508nm (Cubitt et al. 1999). Following cloning of its gene (Lorenz et al. 1991; Prasher et al. 1992) GFP has rapidly become a useful tool in many areas of cellular biology, it has been used to identify transformed cells, measure gene expression, label and locate fusion proteins, and to study intracellular protein

traffic (Prasher, 1995). The use of GFP as a label for transplanted SCs has not been well documented. This study assessed the efficiency of labelling and cell vitality after labelling *in vitro*, and ease of identification of labelled cells *in vivo* in combination with immunofluorescent histochemical protocols.

3.2 Materials and Methods

3.2.1 *In vitro* study of SC vitality and viability following retroviral transduction

SC harvesting and retroviral transduction with GFP were carried out according to the protocols set out in sections 2.1 and 2.3 respectively. Prior to transduction SCs were split into 2 cell lines, one of which was transduced, while the other cell line acted as a control for vitality and viability measurements. Non-transduced SCs (ntSCs) and GFP transduced SCs (GFP-SCs) were cultured in identical conditions. Transduction efficiency was measured at 1 week and 6 weeks following transduction (cf. 2.3.3). As a measure of cell vitality cell growth curves for ntSCs and GFP-SCs were constructed 1 week following transduction (cf. 2.7). Cell viability was assayed using an alamar Blue™ indicator solution (cf. 2.6). *In vitro* fluorescent immunohistochemistry was performed to examine SC morphology (cf. 2.13.3).

3.2.2 *In vivo* study of GFP-SCs transplanted in PHB conduits

This study was performed to determine the ability to detect GFP-SCs following *in vivo* transplantion in association with fluorescent immunohistochemical techniques. GFP-SCs were transplanted into a 1cm rat sciatic nerve gap model

spanned by a PHB conduit. Two experimental groups (a cellular group containing GFP-SCs and an acellular control group) were constructed (n=5) using adult male Sprague-Dawley rats (weights 200-250gm; Harlan). Conduits were constructed as described in section 2.10. In the cellular group conduits were filled with GFP-SCs suspended in 1.8% LVM alginate at a concentration of 80 X 10^6 cells/ml followed by gelling for 2 minutes in 0.1M $CaCl_2$ (cf. 2.10). Anaesthetic and operative procedures were carried out according to the protocols described in section 2.11. Conduits were harvested after 2 weeks and processed for fluorescent immunohistochemsitry for axonal (PGP) and Schwann cell (S100) regeneration following conjugation with a Cy3-labelled secondary antibody (cf. 2.13.1). Sections were examined under a fluorescence microscope (Olympus BX60) and images captured using a cooled digital camera (Evolution QE). Axonal and Schwann cell regeneration distances were measured to quantify regeneration (cf. 2.14.1).

3.3 Results

3.3.1 *In vitro* studies

Cultured SCs displayed classical spindle-shaped morphology on immunostaining (Figure 3.1A). SC cultures transduced with GFP (GFP-SCs) were found to exhibit bright green fluorescence *in vitro* (Figure 3.1B). The number of cells expressing GFP as a percentage of the total number of cells in culture (transduction efficiency) was 39.4% at week 1, this value being maintained at 37.9% up to week 6 (Figure 3.2). This result indicates that the transduced cells were stably transfected and that they continued to divide generating further cells

expressing GFP without significant dilution of transgene expression. The intensity of fluorescence did not qualitatively deteriorate between week 1 and week 6. It was found that the cells were susceptible to photobleaching more rapidly when exposed to blue fluorescent light than that seen with an FiTC fluorochrome, however fluorescence recovered completely if the cells were returned to dark culture conditions. When monitoring GFP-SC cultures, it was found that removing culture medium and replacing with warmed (37°C) sterile phosphate buffered saline (PBS) reduced the background auto-fluorescence seen under the microscope caused by components of the culture medium (Billinton & Knight, 2001). The PBS was replaced with cell culture medium prior to returning the cells to the incubator.

The alamar Blue™ assay (Figure 3.3) indirectly measures the metabolic activity of cultured cells. Measurements were collected over a period of 48hrs. There was a significant difference in activity between GFP-SC and ntSC cultures at t=8hrs ($P<0.05$; paired t-test) and t=12hrs ($P<0.01$; paired t-test), however at 24 and 48hrs GFP-SC activity had increased to levels comparable to ntSCs. Linear regression analysis was applied to the values plotted, no significant difference was found between the slopes of the GFP-SC and ntSC curves indicating comparable metabolic rates. Growth curves were constructed comparing the growth of ntSCs and GFP-SCs over a 7 day period *in vitro* (Figure 3.4). The exponential (rapid division) phase of growth began at day 3 in ntSCs and at day 4 in GFP-SCs. The plateau (confluence) phase of growth was reached at day 6 in ntSCs and day 7 in GFP-SCs. At confluence, ntSCs and GFP-SCs reached a comparable cell number (9.05 *vs.* $8.4x10^5$ cells/ml respectively). These measurements of vitality and

growth have shown that GFP-SCs are initially slower to establish themselves in culture following passage but that following this initial period they achieve comparable profiles to that of non-transduced cells.

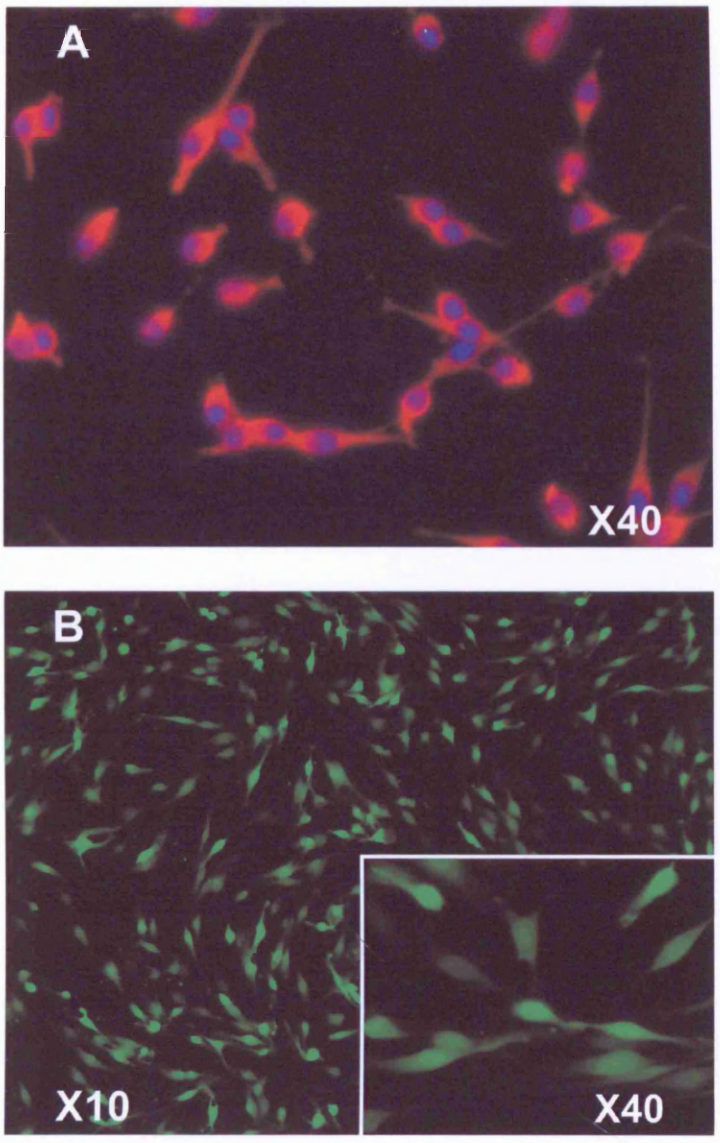

Figure 3.1 (**A**) Cultured non-transduced Schwann cells stained with an S100-Cy3 conjugate (red) and Hoechst nuclear stain (blue). The classical spindle-shaped bipolar morphology of Schwann cells is clearly visible (X40). (**B**) Cultured Schwann cells following retroviral transduction with GFP. Cells are approaching confluence and display normal morphology (X10), inset (x40).

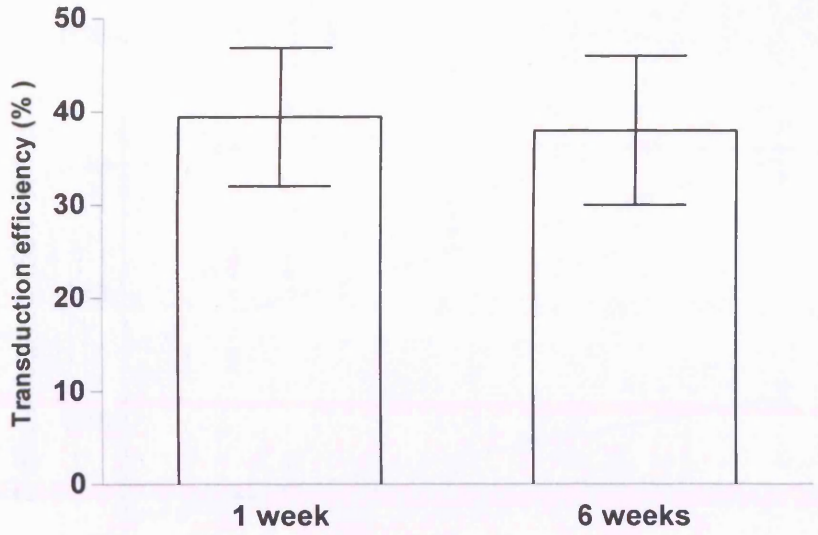

Figure 3.2 Histogram illustrating the mean transduction efficiency (% GFP labelled cells of the total number of cells per 10 high power fields) at 1 week (39.4%) and 6 weeks (37.9%) following transduction. This indicates no significant dilution of GFP transgene expression with time. Error bars indicate standard deviation.

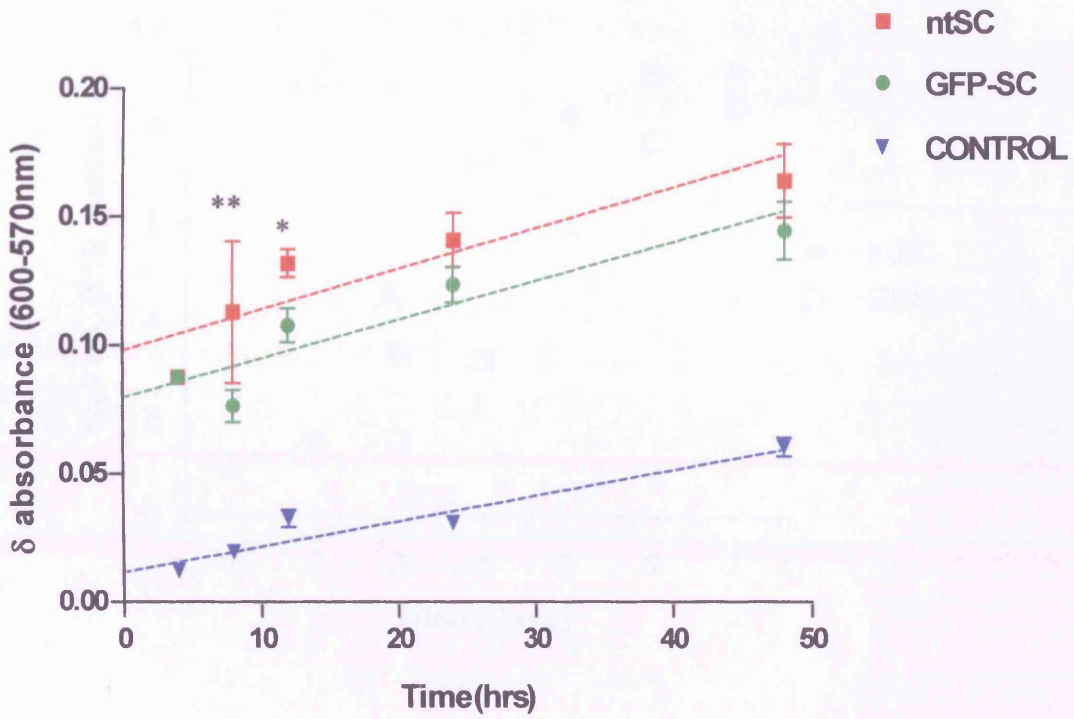

Figure 3.3 Metabolic activity over time as assessed by the alamar Blue™ assay comparing Schwann cells transduced with GFP (GFP-SC) and non-transduced Schwann cells (ntSC). Control – assay of media without cells. GFP-SCs were found to lag behind ntSCs in the first 12hrs following passage, however by 24hrs they had achieved comparable levels. Error bars indicate standard deviation. **P<0.05 at 8hrs; *P<0.001 at 12hrs, paired t-test. Linear regression analysis detected no signifiocant differences between the slopes of the GFP-SC and ntSC curves.

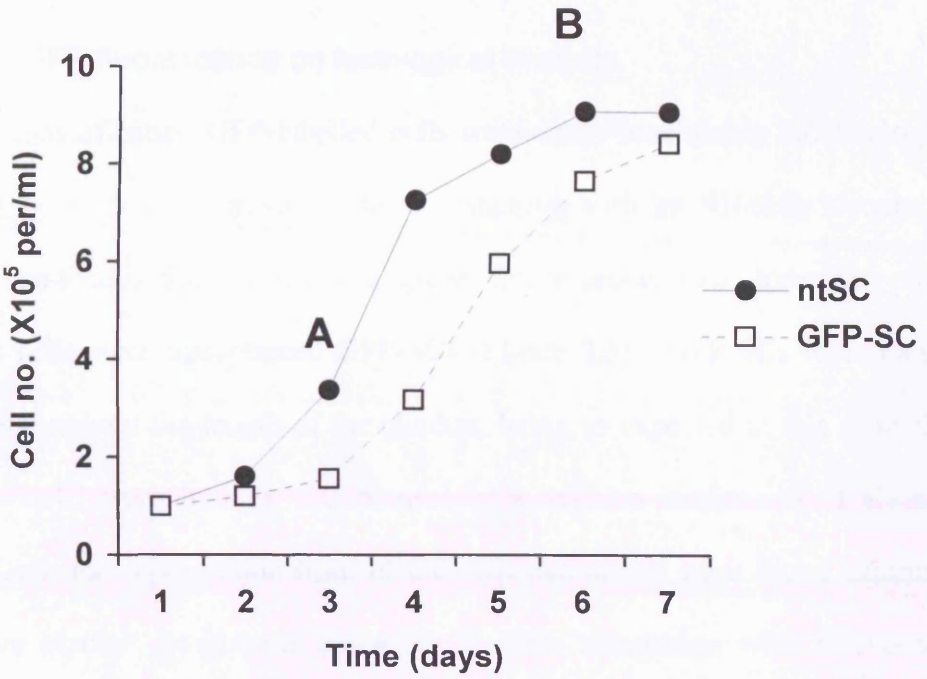

Figure 3.4 Graph illustrating growth curves of transduced (GFP-SC) and non-transduced (ntSC) cells over a 7 day period (mean values plotted). **A** – Beginning of exponential growth phase; **B** – Plateau phase (confluence). GFP-SCs take longer to reach the beginning of their exponential growth phase (4 *vs.* 3 days) and plateau phase (7 *vs.* 6 days) in comparison with ntSCs but achieve comparable confluence densities by day 7.

3.3.2 *In vivo* studies

3.3.2.1 GFP fluorescence on histological analysis

At high magnification GFP-labelled cells were easily identifiable on histological sections under blue fluorescence light. Staining with an S100-Cy3 conjugate showed co-localisation of red and green fluorescence, thus indicating GFP-labelled cells were transplanted GFP-SCs (Figure 3.5). GFP-SCs were located evenly throughout the length of the conduit, being as expected at this short time point as cells were initially transplanted in a uniform suspension of alginate. GFP-SCs at the regeneration front of the proximal stump were found exhibiting extensive bipolar cytoplasmic processes in close association with regenerating axonal fibres indicating active integration in the regenerative process. When taken in association with the significant improvement in the regeneration distances (see below) this indicates GFP-SCs were contributing to the regenerative process. The inherent fluorescence of GFP-labelled cells greatly simplified the staining procedure required to analyse sections. The MMLV is rendered replicative incompetent due to the absence of the ψ packaging signal. GFP-SCs are therefore incapable of producing functional GFP-containing retrovirus, it can therefore be assumed that visible cell labelling was restricted to transplanted cells with no contamination of surrounding tissues, as is frequently seen in chemical labelling methods (Iwashita et al. 2000).

3.3.2.2 Nerve regeneration

Regeneration was assessed by measuring axonal (PGP-staining) and Schwann cell (S100-staining) regeneration distances through the lumen of the conduits from the proximal stumps (Figure 3.6). The transplantation of GFP-SCs significantly improved the rate of nerve regeneration in comparison with the control group (Figure 3.7). Both axonal and Schwann cell regeneration distances were significantly better in the GFP-SC groups (3.3+/-0.45 *vs.* 2.4 +/- 0.14mm; $P<0.05$ and 3.55+/-0.62 *vs.* 2.55+/-0.21mm; $P<0.05$ respectively; paired t-test). Indirect comparison of the effect of GFP-SC transplants on nerve regeneration with previous studies from our laboratory which used *lacZ*-SC transplants in the same model of nerve injury (Mosahebi et al. 2001; Mosahebi et al. 2002; Mosahebi et al. 2003) showed a comparable benefit between the labelling methods used. This indicates that GFP transfection had no detrimental effect on SC physiology *in vivo* in comparison with *lacZ* labelling.

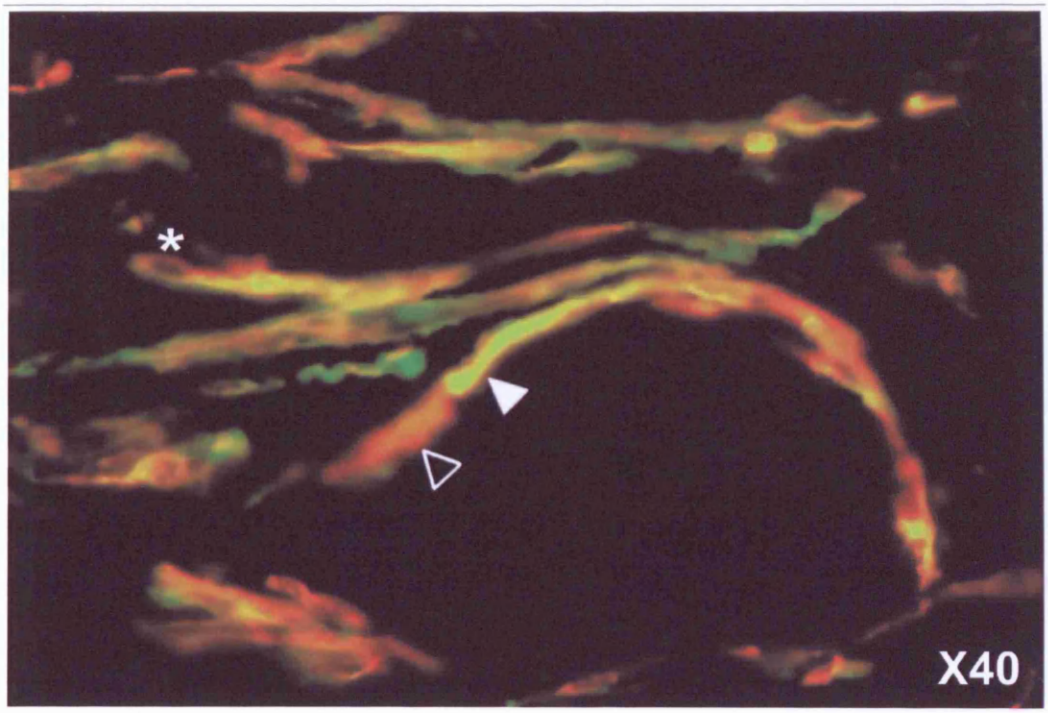

Figure 3.5 Fluorescent immunohistochemical image from within lumen of conduit containing GFP-SCs. S100 staining (red, open arrow) is seen to co-localise with the green fluorescence of transplanted Schwann cells (closed arrow). Schwann cell nucleus indicated by asterisk.

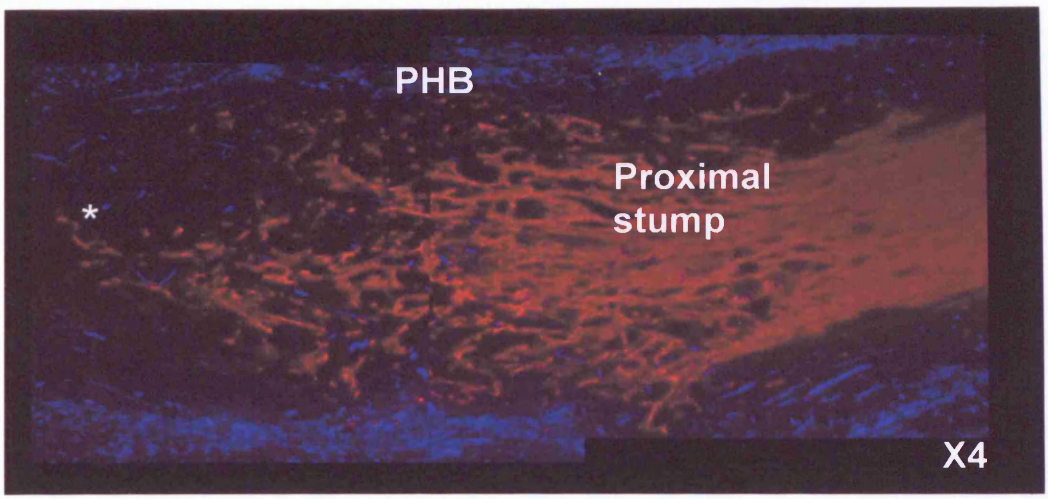

Figure 3.6 Section of a proximal stump within a PHB (blue) conduit at 2 weeks stained with S100-Cy3 to visualise Schwann cell regeneration (red). Regeneration distance is measured from the point of insertion of the proximal stump to the tip of the most distal regenerating fibre (asterisk) using a graticuled lens.

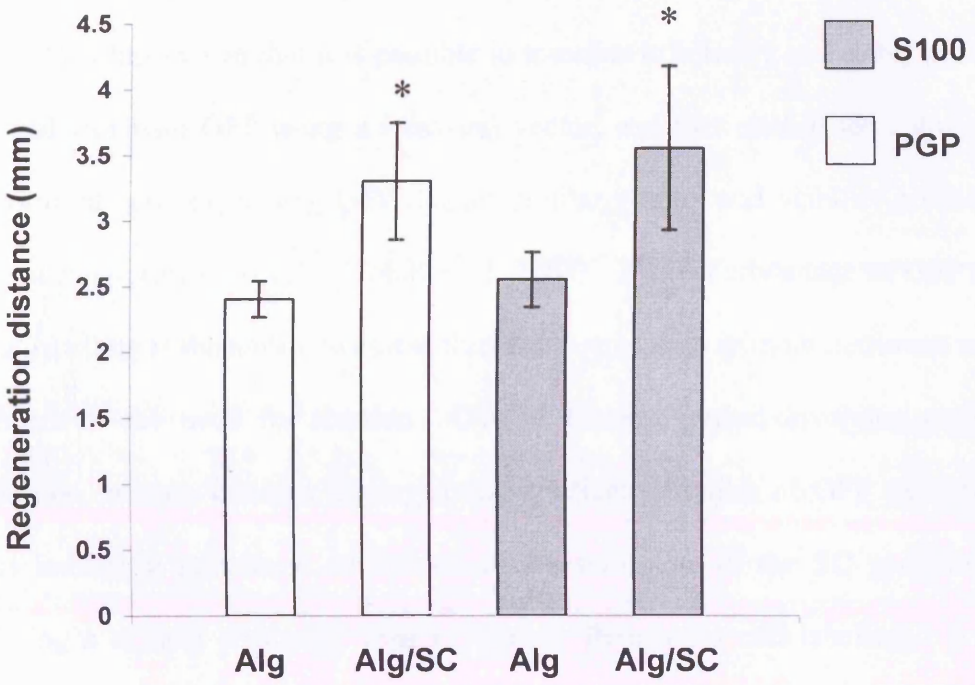

Figure 3.7 Bar chart representing regeneration distances of S100 and PGP at 2 weeks following surgical grafting of conduit. **Alg** – control group containing alginate only; **Alg/SC** – group containing alginate and Schwann cells. S100 and PGP regeneration distances were significantly better in the **Alg/SC** group in comparison to the **Alg** group. Error bars indicate standard deviation. *P<0.05, paired t-test.

3.4 Discussion

This study has shown that it is possible to transfect efficiently and stably primary SC cultures with GFP using a retroviral vector, and that established cultures of transduced cells expressing GFP display similar vitality and viability profiles to that of non-transduced cells (Tohill et al. 2004). A great advantage of GFP over *lacZ* labelling is the ability to assess fluorescence *in vitro* without detriment to the cultures or the need for fixation. Over a 6 week period involving multiple passages, primary cultures displayed no significant dilution of GFP expression, thus indicating permanent expression of the transgene in the SC genome and offering a distinct advantage over exogenous fluorescent cell labelling. It was shown that GFP-SCs lagged temporally in metabolic activity and exponential growth when compared to ntSCs. However, this effect was only seen shortly after passage *in vitro* and therefore would be negligible in longer term *in vivo* experiments. The MMLV-based retroviral vector facilitates long-term transgene expression without causing apparent significant toxicity or pathogenicity to primary SC cultures. Overall, transduction efficiency and growth kinetics were seen to corroborate with the results of previous reports which used a similar retroviral vector for GFP transfer in ovine endothelial cells (Afting et al. 2003) and corneal fibroblasts (Gatlin et al. 2003). However, this is the first study to describe oncoretroviral transduction of primary SCs with GFP. Our group has used the MMLV vector to transduce SCs with the *lacZ* reporter. On indirect comparison there was no apparent difference in growth kinetics between GFP-SCs and *lacZ*-SCs *in vitro*. Higher transduction efficiencies were seen with *lacZ* labelling (~70%) but this is more likely due to variations in transgene promoter

sequences affecting transcription activity and the addition of sequabrene in transduction cycles.

This study has shown GFP to be a suitable labelling method when used in conjunction with fluorescent immunohistochemical procedures used to assess peripheral nerve regeneration. The use of GFP is advantageous in such techniques as transplanted labelled cells can be visualised in combination with other fluorochrome-labelled antigens. For histological purposes GFP has many desirable properties as the fluorescence of the protein is unaffected by acids, weak alkalis, proteolytic enzymes and temperatures of up to 65°C (Bokman & Ward, 1981), making it versatile in a wide range of procedures. The protein is highly soluble and therefore requires formaldehyde fixation prior to cryostat sectioning and staining (Jockusch et al. 2003). Most importantly, as shown in this study, GFP-labelled Schwann cells have significantly improved sciatic nerve regeneration across a 1cm gap. This is consistent and comparable with previous transplantation studies from using alternative labelling methods and supports the fact that, physiologically, the use of GFP as a cellular label has no measurable detrimental effect on *in vivo* regeneration studies. A number of recent studies have demonstrated successful transplantation and localisation of SCs labelled with GFP (Bachelin et al. 2005; Schaal et al. 2007).

Chapter 4

Bone Marrow Stromal Cell Differentiation Following Exposure to Glial Growth Factor

4.1 Introduction

The transplantation of cultured Schwann cells (SCs) into bio-engineered conduits has been shown to improve nerve regeneration in experimental models of peripheral nerve injury (Guenard et al. 1992; Mosahebi et al. 2001; Rodriguez et al. 2000). However, the use of autologous cultured SCs for the treatment of acute injuries may be impractical due to the technical difficulties and time required in harvesting and expanding such cells. The ideal 'transplantable cell' should be easily accessible, capable of rapid expansion in culture, immunologically inert, capable of long-term survival and integration in the host tissue, and amenable to stable transfection and expression of exogenous genes (Azizi et al. 1998). A suitable candidate for such a cell may be the bone marrow stromal cell. In addition to haematopoietic stem cells, bone marrow contains cells capable of providing mesenchymal precursors such as osteoblasts, chondrocytes, adipocytes and myoblasts (Prockop, 1997; Caplan, 1991; Owen & Friedentstein, 1988). These precursors have been named colony-forming unit fibroblasts, mesenchymal stem cells or marrow stromal cells (MSCs). Such cells have displayed unorthodox plasticity in their ability to trans-differentiate across what were once thought to be un-crossable oligolineage boundaries. When transplanted into models of injury they have been reported to differentiate into a variety of cell types including retinal cells (Tomita et al. 2002), astrocytes (Kopen et al. 1999), hepatocytes (Lagasse et al. 2003), myocardium (Orlic et al. 2001), and myelinating cells of the peripheral nervous system (Dezawa et al. 2001) and spinal cord (Akiyama et al. 2002). *In vitro* studies have shown that MSCs will differentiate into cells expressing neuronal cell markers when exposed to neuronal

cell mitogens such as BDNF and NGF (Sanchez-Ramos, 2000; Kim et al. 2002) and β-mercaptoethanol (Woodbury et al. 2000). Glial growth factor (GGF) is a Schwann cell mitogen which has been shown to stimulate peripheral nerve regeneration (Mahanthappa et al. 1996), and to restrict neural crest stem cells to a glial cell fate *in vitro* (Shah et al. 1994). This study examined the effect of GGF on adult rat MSC morphology and phenotypical expression *in vitro*, and the effect of transplanting differentiated (dMSCs) and undifferentiated marrow stromal cells (uMSCs) into a nerve gap conduit.

4.2 Materials and Methods

4.2.1 *In vitro* study

Schwann cells (SCs) and marrow stromal cells (MSCs) were harvested from inbred Sprague-Dawley rats (Harlan) and cultured as described in section 2.1 and section 2.2 respectively. For identification in combination with immunofluorescent histochemical analysis, the cells were retrovirally transduced with GFP (cf. 2.3). MSCs were differentiated towards a glial cell lineage by culturing the cells in the presence of forskolin, PDGF, bFGF and GGF for 2 weeks (cf. 2.2.2) (Dezawa et al. 2001). MSCs were also cultured in the absence of GGF to produce a line of undifferentiated cells (uMSCs). The colony forming ability of freshly harvested MSCs was measured to indicate clonogenic capacity (cf. 2.2.3). At various stages of culture MSCs were plated on chamber slides for general morphology with a polychromatic blood stain (cf. 2.13.4) or fluorescent immunohistochemical phenotype characterisation with antisera to Thy 1.1 (a marker of undifferentiated MSCs), S100 or GFAP, followed by incubation with

secondary fluorochromes and a Hoechst nuclear marker to identify cell nuclei (cf. 2.3.3; 2.13.3). Transduction efficiency was measured following transfection with the MMLV-GFP retrovirus (cf. 2.3.3). Stained cell cultures were examined under a fluorescence microscope (Olympus BX60) and images captured with a cooled digital camera (Evolution QE).

4.2.2 *In vivo* study

This study used a standardised 1cm nerve gap injury rat model spanned by a PHB conduit (Hazari et al. 1999; Mosahebi et al. 2001; Mosahebi et al. 2002). The conduits contained intraluminal dissociated PHB fibres which acted as a matrix for transplanted cells. There were 4 groups (n=5) as follows:

Group 1: Acellular control conduits

Group 2: Conduits containing cultured Schwann cells (SCs)

Group 3: Conduits containing undifferentiated marrow stromal cells (uMSCs)

Group 4: Conduits containing differentiated marrow stromal cells (dMSCs)

Under aseptic conditions, conduits were constructed from a polyhydroxybutyrate (PHB) sheet to span a 1cm gap in the left sciatic nerve (cf. 2.8) (Mosahebi et al. 2003). To support cellular transplants, loose unidirectional PHB fibres of a fixed weight were threaded through the lumen of the conduits (cf. 2.10.3). Cells were suspended in DMEM (HEPES modification; Sigma) at a concentration of 80 x 10^6cells/ml (Mosahebi et al. 2001) prior to seeding within the conduit. The anaesthetic and operative procedures were performed as described in section 2.11.

Following grafting of the conduit 30μL of cell suspension was injected into the lumen of the conduit by introducing the needle of a Hamilton syringe into the distal end of the conduit until the tip of the needle had reached the middle of the conduit, the cell suspension was then very slowly injected. At 2 weeks, conduits together with proximal and distal nerve ends were harvested and placed in Zamboni's fixative in preparation for immunohistochemical staining with S100 and PGP9.5 anti-sera (cf. 2.12.1; 2.13.1). Sections were mounted in fluorescent mounting medium and examined under fluorescence light, in combination with a blue filter to identify GFP-labelled cells. Schwann cell (S100) and axonal regeneration (PGP) distances (mm) were measured at low magnification with a graticuled lens (2.14.1). ANOVA and a Tukey's test were applied using statistical analysis software (SPSS Inc.).

4.3 Results

4.3.1 Marrow stromal cell culture and phenotypical characterisation

Marrow stromal cells (MSCs) were collected by plating and culturing bone marrow aspirate. Colony formation was readily observed in the presence of β-mercaptoethanol (cf. 2.2.3). Freshly harvested MSCs showed a high clonogenic ability (plating efficiency) which increased with plating density and approached ~13% (Figure 4.1). Staining for Thy 1.1, the CD antigen expressed by undifferentiated marrow stromal cells, showed antigen expression in colony-forming cells but not by cells showing morphological signs of differentiation along one of the determined mesenchymal pathways (Figure 4.2A and B). MSCs grew rapidly in the presence of basic growth factors with a doubling time of

48hrs. Uptake of green fluorescent protein to label MSCs prior to transplantation was highly efficient (80% transduction efficiency), this being due to their high mitotic rate which increases their sensitivity to retroviral transduction (Figure 4.2C and E). Following 2 weeks exposure to GGF MSCs were found to express the glial cell markers S100 and GFAP. A number of cells (approx. 10%) displayed the classical bipolar, spindle-shaped morphology of Schwann cells (Figures 4.3B,C and D). Thus, within the MSC population exposed to GGF there were cells displaying the phenotypical and morphological characteristics of glial cells.

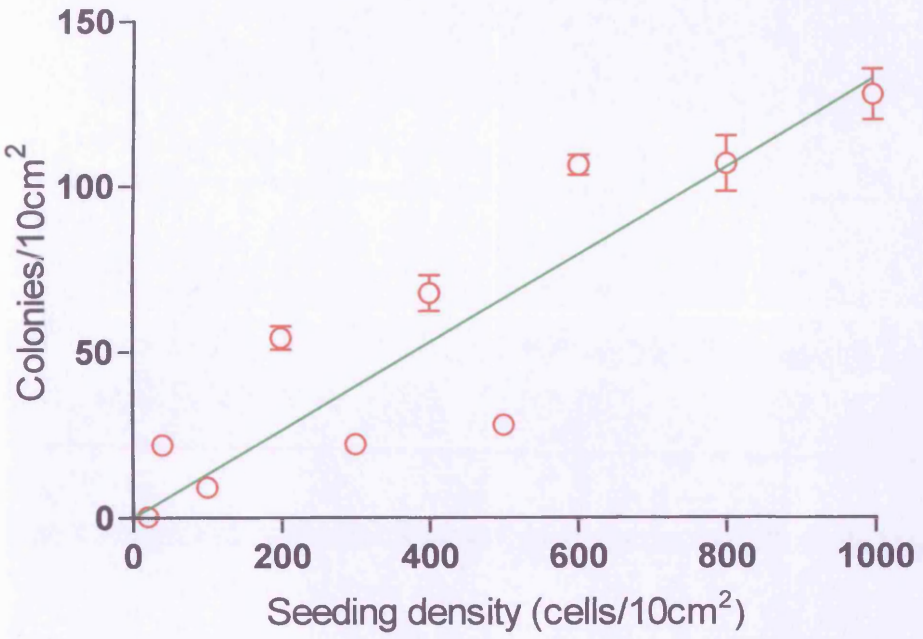

Figure 4.1 Clonogenic ability of freshly harvested MSCs in the absence of colony stimulating growth factors. Cells were seeded at set densities (x axis) and after 7 days the number of colonies per $10cm^2$ arising from each given seeding density were counted (y axis). Linear regression analysis calculated the slope of the curve (plating efficiency) which reached ~13%.

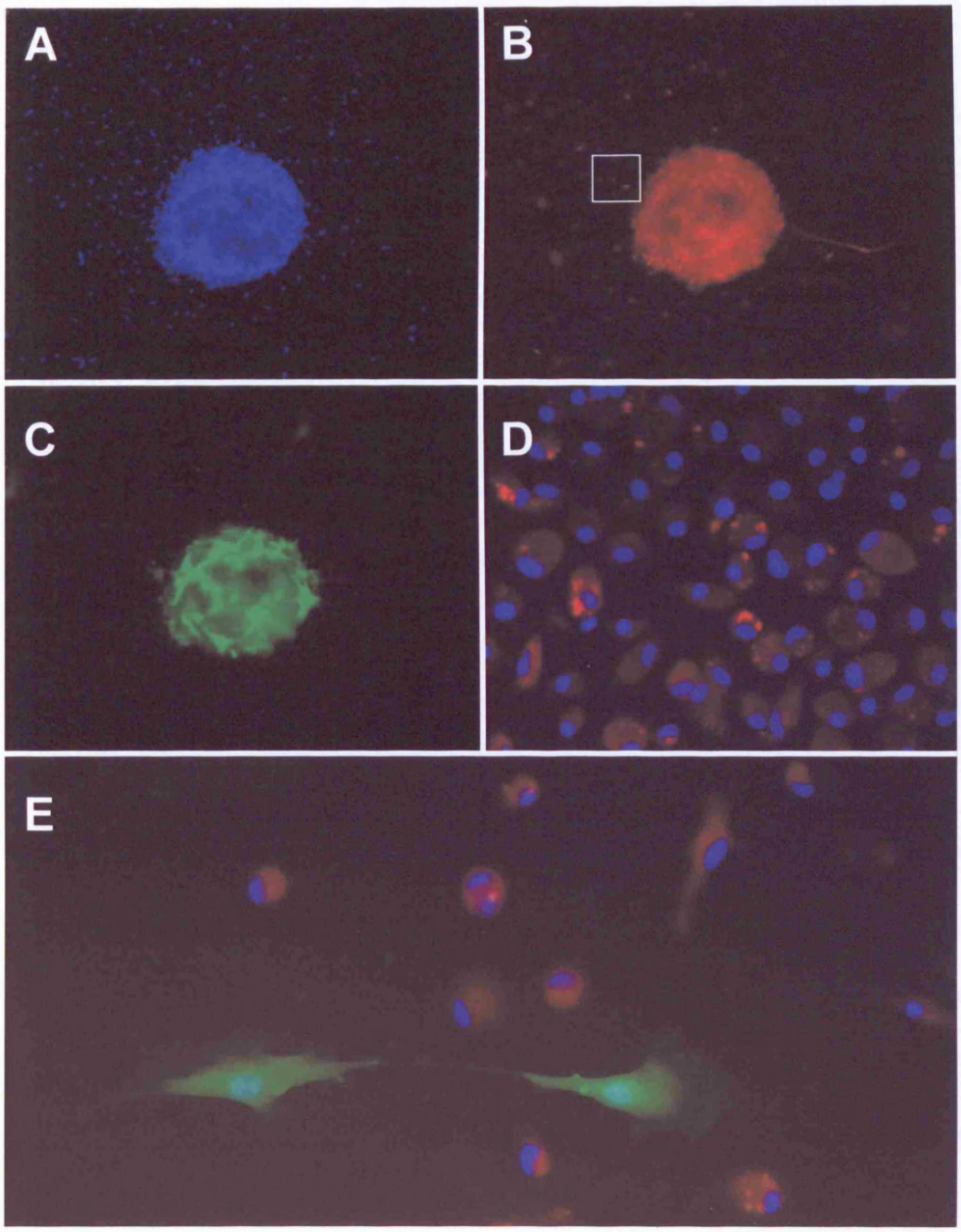

Figure 4.2 Marrow stromal cell colony immunostaining. (**A**) Colony stained with the Hoechst nuclear marker (**B**) Thy 1.1-Cy3 conjugate (red) and (**C**) green fluorescence due to GFP labelling (**A**, **B** and **C** X20 magnification). (**D**) represents the area bounded by the box in (**B**) showing undifferentiated clonal cells expressing Thy 1.1 (non-specific CD marker expressed by undifferentiated MSCs) (X40). (**E**) Illustrates daughter cells of a GFP-labelled MSC at the end of cell division. The cells display a flattened heterogeneous morphology typical of differentiating MSCs and lack the expression of Thy1.1 as displayed by the adjacent clonal cells.

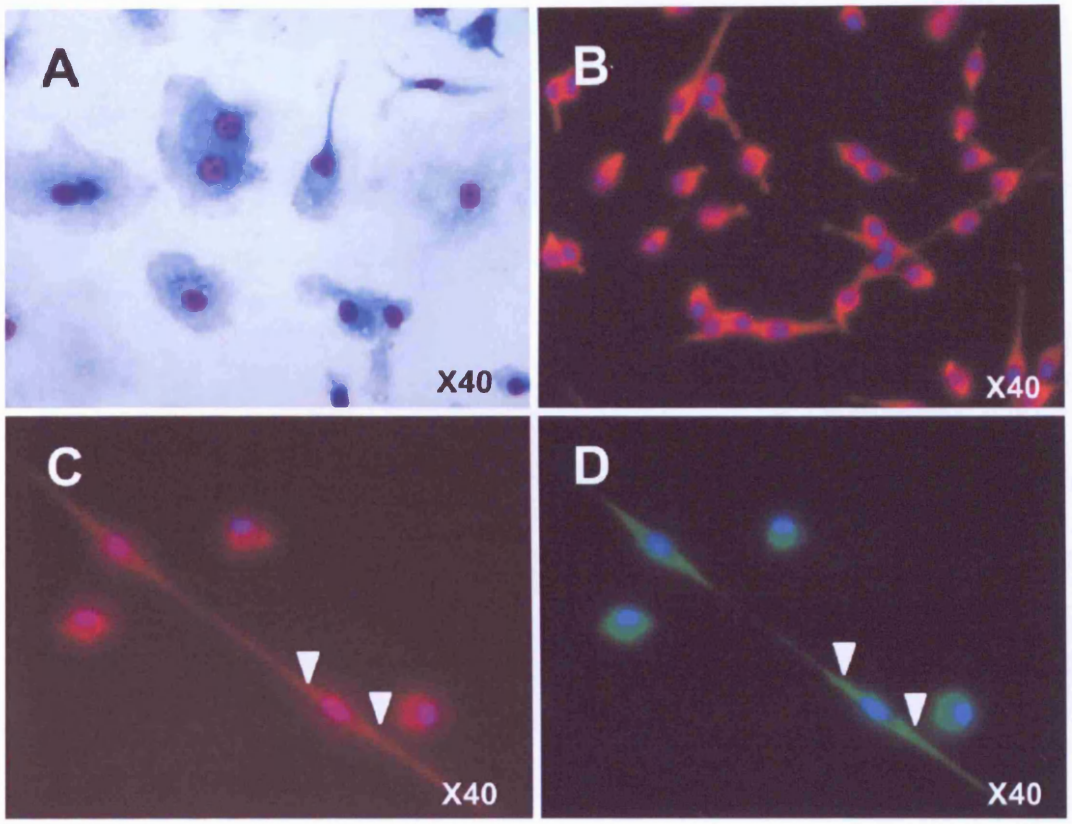

Figure 4.3 (**A**) Bone marrow mesenchymal stromal cells (MSCs) 5 days following harvesting. Large, densely staining nuclei indicate high cellular and mitotic activity. Giemsa stain (X40). (**B**) Schwann cells stained with an S100-Cy3 conjugate (red) and a Hoechst 33342 nuclear marker (blue). The characteristic spindle-shaped cell body (arrows) is clearly seen (X40). (**C**, **D**) MSCs following exposure to glial growth factor (GGF). Cells are double-stained with a GFAP-Cy3 conjugate (**C**, red) and an S100-FiTC conjugate (**D**, green). Arrows indicate spindle-shaped morphology as seen in Schwann cells.

4.3.2 *In vivo* results

Immunohistochemical analysis of the conduits containing uMSCs and dMSCs identified transplanted cells due their expression of GFP, dMSCs were found to be present evenly throughout the lumen of the conduit (Figure 4.4). At the proximal end of the conduit dMSCs were found to be adherent to intraluminal PHB fibres (Figure 4.5A and B) and to be directly involved with axonal and Schwann cell and regeneration (Figure 4.4A and 4.5C respectively). In conduits containing uMSCs a small number of transplanted cells (as detected by their GFP fluorescence) at the proximal and distal ends of the conduit were found to express S100 (Figure 4.5D) indicating a possible effect of local cellular and humoral factors on marrow stromal cell differentiation.

Axonal regeneration distance (PGP; Figure 4.6) was significantly better in the Schwann cell seeded conduits in comparison to the control (empty), uMSC and dMSC conduits. The uMSC and dMSC transplants conferred some benefit on axonal regeneration in comparison with the control however this was not statistically significant. Schwann cell regeneration distance (S100; Figure 4.6) was significantly better in the Schwann cell transplant group in comparison with the control group and the uMSC group. Schwann cell regeneration was better in the dMSC group in comparison with the control group. From these results it can be concluded that marrow stromal cells previously exposed to GGF and expressing glial cell markers prior to transplantation appear contribute to increased Schwann cell regeneration.

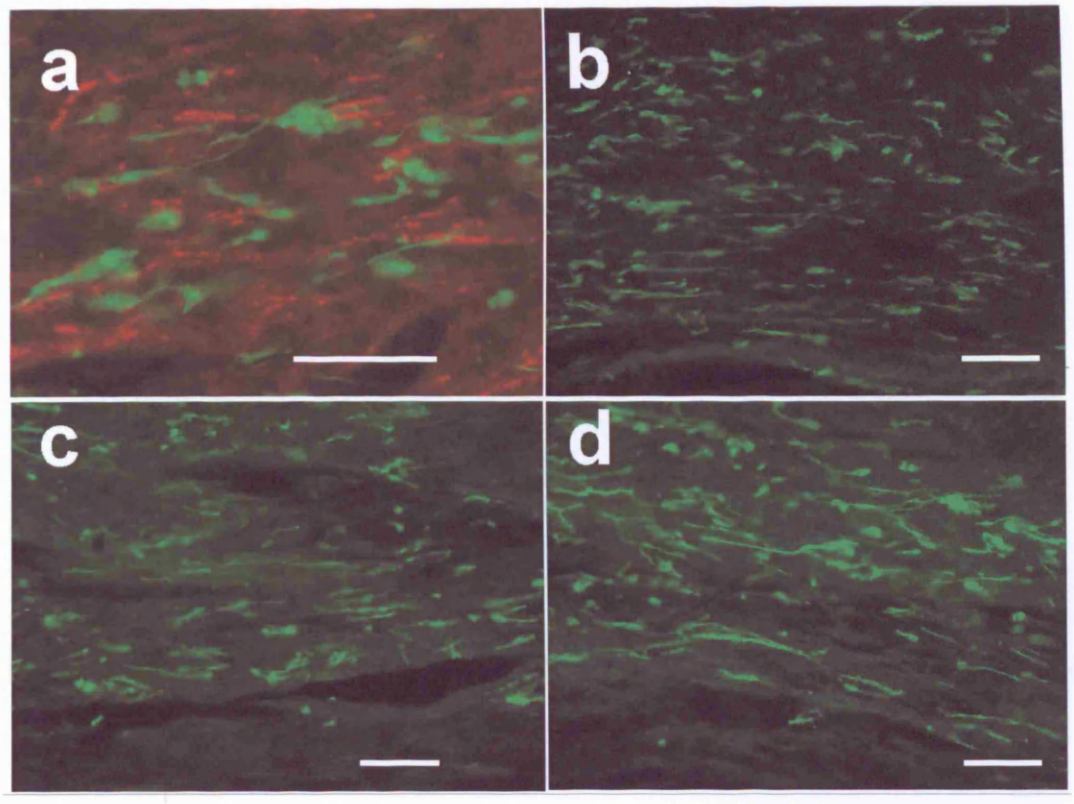

Figure 4.4 Histological sections of conduits transplanted with differentiated marrow stromal cells (dMSCs) and labelled with GFP. (a) PGP-Cy^3 staining of axons at the regeneration front of the proximal stump showing a close relationship with transplanted cells. The distribution of transplanted dMSCs with a conduit is illustrated in b,c and d. (b) Proximal end of conduit, (c) middle of conduit, and (d) distal end of conduit. Scale bar = 100μm.

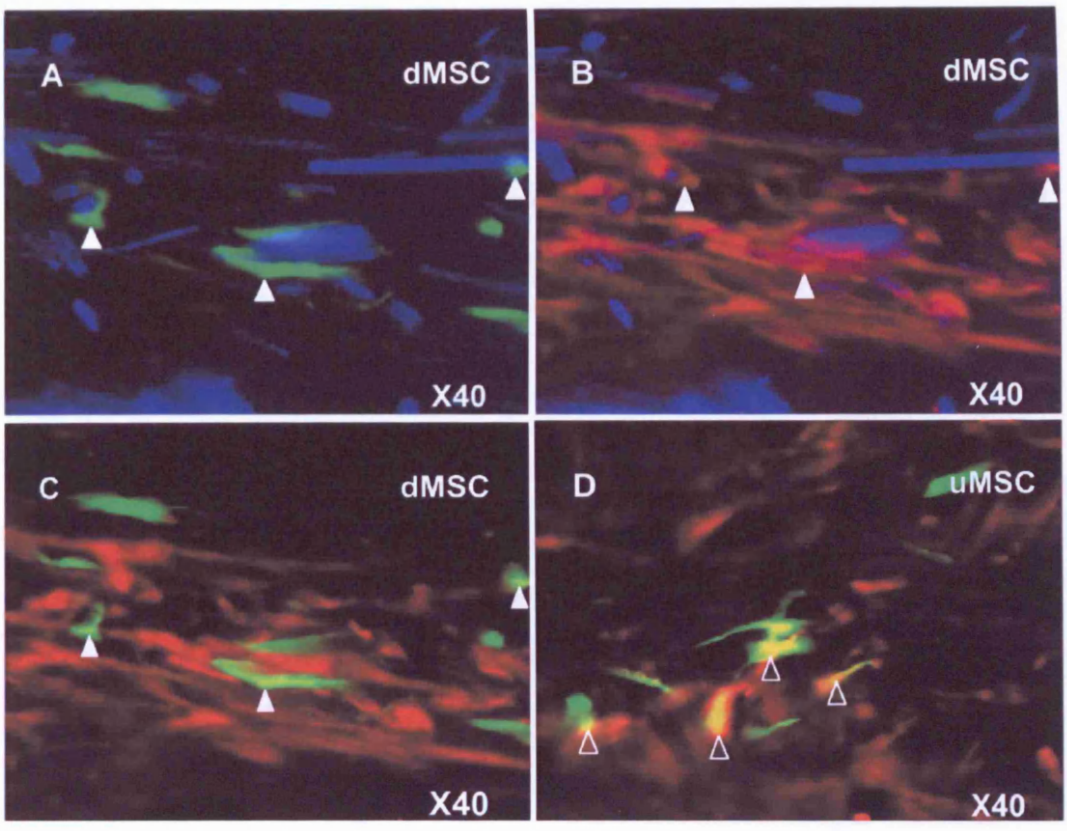

Figure 4.5 Histological sections of grafted conduits stained with S100 antibodies to detect Schwann cells. The same section shows: (**A**) GFP-labelled differentiated marrow stromal cells (dMSC; green) in close association with intraluminal PHB fibres (blue); (**B**) S100 staining (Schwann cell specific; red); (**C**) Digital combination of figures A and B, where the arrow indicates co-localisation (yellow) of S100 staining by a dMSC and involvement in Schwann cell regeneration. (**D**) Conduit containing undifferentiated marrow stromal cells (uMSC) labelled with GFP and stained with S100. Co-localisation of fluorescence (open arrow) indicates that cells are expressing S100 that was absent prior to transplantation.

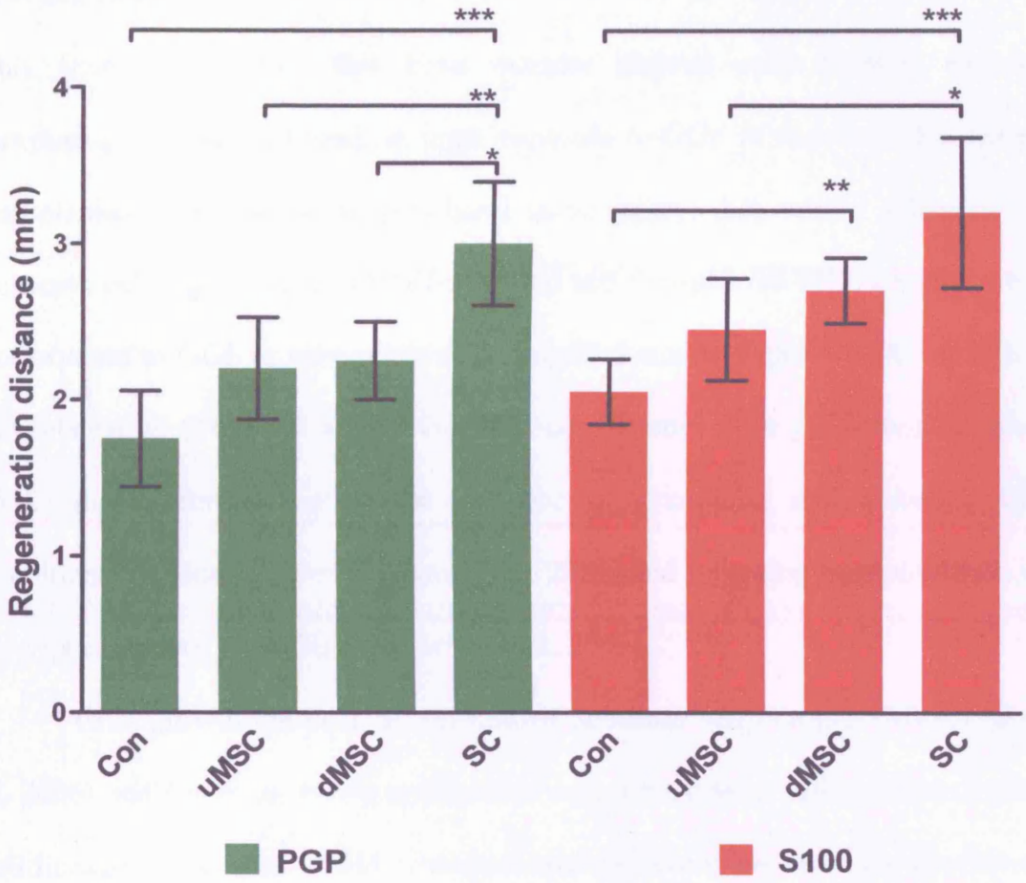

Figure 4.6 Histogram illustrating axonal (**PGP**) and Schwann cell (**S100**) regeneration distance (mean ± standard deviation) in each group. **Con** - Control – no transplanted cells; **uMSC** – undifferentiated marrow stromal cells; **dMSC** – differentiated marrow stromal cells; **SC** – Schwann cells. * $P < 0.05$; ** $P < 0.01$; ***$P < 0.001$. One way ANOVA and Tukey's post test.

4.4 Discussion

This study has shown that bone marrow stromal cells (MSCs) express morphological glial cell markers upon exposure to GGF *in vitro* and that, when transplanted into a model of peripheral nerve injury, they confer a benefit on Schwann cell regeneration. Undifferentiated and transplanted MSCs, which were not exposed to GGF *in vitro*, were subsequently found to express S100 following transplantation (Tohill et al. 2004). This corroborates with previous reports of MSC glial differentiation in the presence of neuregulin and Schwann cell conditioned medium *in vitro* (Dezawa et al. 2001) and following transplantation in a peripheral nerve crush injury (Cuevas et al. 2002).

Glial growth factor is a well known Schwann cell mitogen (Minghetti et al. 2006) and has been shown to stimulate neural crest stem cells towards a glial cell lineage (Shah et al. 1994). Previous studies have shown that growth factors can effect directed differentiation or cell selection in stem cell populations to produce cells from all germ layers but that no one factor causes differentiation exclusively to one cell type (Schuldiner et al. 2000). Therefore, GGF might act on MSCs by stimulating transcription of glial lineage genes with or without suppression of mesenchymal lineage genes or by promoting proliferation in subpopulations of truly totipotential cells while indirectly inducing death of other cell types.

Characterisation of dMSCs, and indeed all differentiated stem cells, remains problematic, and care must be taken in interpreting the results of phenotypical markers as determinants of cell differentiation. Glial fibrillary acidic protein (GFAP), present on cells of a glial lineage (Jessen & Mirsky, 1999), has

been found on a number of non-glial somatic cells, including fibroblasts (Hainfellner et al. 2001). It is still unclear how a stimulation process might direct a cell towards a given phenotype and morphological shape, and whether phenotypical and morphological expression really equates with functional ability. The interpretation of the results of this study is dependent upon the assumption that marrow stromal cells have become glial-type cells following *in vitro* differentiation and transplantation, acquiring Schwann cell marker expression and morphology. Hence, if they were functional Schwann cells, their effect on improving regeneration is consistent with studies of Schwann cell physiology following injury and transplantation (Hall, 1986; Guenard et al. 1992; Mosahebi et al. 2001). However, if we assume that differentiated cells are non-functional cells expressing glial cell markers, their benefit on nerve regeneration may be derived from some basic structural or humoral support such as the production of basement lamina, extracellular matrix macromolecules or non-specific growth factors. Caddick (2006) recently described morphological and phenotypical characterisation of MSCs following exposure to GGF. Increased expression of GFAP and p75 was detected histologically and phenotypically in comparison with cells not exposed to GGF. In addition, co-culture of glial-differentiated MSCs with chick embryo dorsal root ganglia (DRG) improved parameters of neurite growth indicating differentiated MSCs are functionally competent. The ability of MSCs to transdifferentiate into glial cell-like lineages has been confirmed by several authors (Keilhoff et al. 2006; Hou et al. 2006; Keilhoff et al. 2006 296).

It is thought that the microenvironment of a tissue has an important role to play in the control of tissue-specific adult stem cells (Morrison et al. 1997). Stem

cells are normally quiescent in tissues such as the brain, but are capable of constant renewal and replenishment in epithelia and of tissue repair following injury. The microenvironment is thought to control stem cell behaviour due to a combination of locally secreted factors (Jan & Jan, 1998), cell-cell interactions mediated by integral membrane proteins, and the extracellular matrix (Artavanis-Tsakonas et al. 1999). We cannot exclude that these factors may be responsible for some of the undifferentiated marrow stromal cells showing expression of S100 *in vivo*. Homeostatic controls, such as from the local existing population of stem cells, will also influence the behaviour of the transplanted cells. It has also been suggested that stem cell migration to zones of injury is more likely due to local depletion of progenitors than due to increased availability of survival factors (Hinks et al. 2003).

Interpretation of these results is influenced by current theories on stem cell trans-differentiation, which is conflicting with previously established laws of lineage restriction (Anderson et al. 2001). However, continued evidence for the ability of marrow stromal cells to transdifferentiate (Caddick et al. 2006) will highlight their potential use for therapeutic strategies in a wide range of injuries and diseases. Further transplantation study will need to identify more clearly the difference observed between transplants of differentiated and non-differentiated cells, and to characterise at the molecular and functional level the phenotypically transformed cell.

Chapter 5

Functional and Histological Assessment of Nerve Regeneration Following the Delivery of Mechano-Growth Factor cDNA

5.1 Introduction

Peripheral nerve regeneration has been augmented by the application of neurotrophic factors at the site of injury (Terenghi 1999; cf. 1.8). The sustained delivery of neurotrophins is hindered by their pharmokinetic profiles such as short half-life, diffusion into a large volume of distribution and biological breakdown. For maximal effect the availability of neurotrophins should run parallel to the time course of regeneration, which by definition is prolonged. The application of neurotrophin gene transfer techniques to provide sustained availability of growth factor is a promising solution to this problem.

IGF-1 is a potent neurotrophin (cf. 1.8.4) and its splice variant MGF (mechano-growth factor) has been shown to induce muscle hypertrophy following exercise (Goldspink, 1999; Yang & Goldspink, 2002; cf. 1.8.5). Prelimary data has indicated that the delivery of MGF cDNA has a neurotrophic effect on regeneration when locally delivered to nerve gap injuries at a short time point (2 weeks). The following study was performed to investigate the effect neurotrophin plasmid delivery (MGF cDNA) on nerve regeneration over a long time frame and to assess both functional and histological outcomes of regeneration.

5.2 Materials and Methods

MGF cDNA was provided by Dr ShiYu Yang and Mr David Sutton, Department of Anatomy, Royal Free and University College Medical School. A short nerve gap model (2mm) spanned by a silicone conduit was used in the study (Figure 5.1). Three experimental groups were constructed using inbred Sprague-Dawley rats (weights 175-218gms; n=6 each group) as follows:

Group 1: Alginate only group (sham treatment – control 1)

Group 2: Vector + alginate group (control 2)

Group 3: Vector containing MGF cDNA + alginate

All anaesthetic and operative procedures were carried out according to the protocols described in section 2.11. Gamma irradiated 6mm length silicone conduits were used to span the 2mm gap in the mid-thigh section of the rat sciatic nerve. Prior to grafting the conduits were filled with 1.8% LVM alginate (Pronova) containing either a suspension of vector or vector + MGF cDNA ($1\mu g/\mu L$). The conduits were then gelled in 0.1M $CaCl_2$ for 2 minutes. At 14 weeks the animals underwent terminal anaesthesia and myophysiological measurements of the tibialis anterior muscle were recorded on the denervated and contralateral sides (cf. 2.15). The conduits were harvested together with a section of distal nerve (Figure 5.2) and fixed in preparation for transverse semithin sectioning ($2\mu m$), staining (cf. 2.12.2) and quantification of distal nerve regeneration (cf. 2.14.2). Lateral foot pad skin from the denervated and contralateral sides were collected and prepared for immunohistochemical

quantification of skin innervation (cf. 2.13.2; 2.14.3). Statistical analysis used ANOVA using SPSS software.

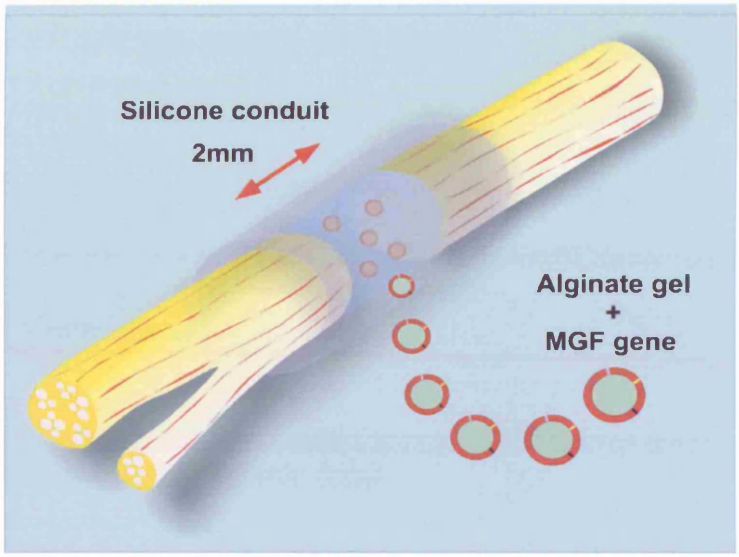

Figure 5.1 Schemmatic diagram illustrating the 2mm sciatic nerve gap model spanned by a silicone conduit containing alginate gel as a matrix for gene vector delivery.

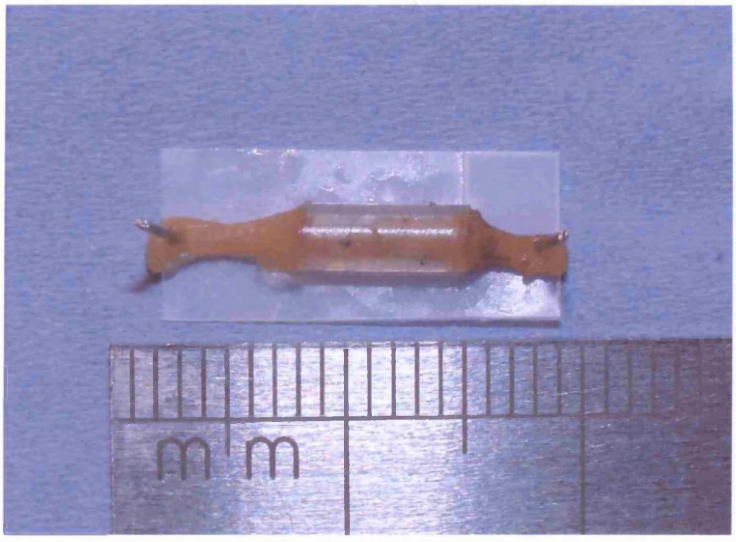

Figure 5.2 Silicone conduit and adjacent nerve stumps prior to fixation.

5.3 Results

5.3.1 Muscle physiology

5.3.1.1 Wet muscle weight

Measurement of TA wet muscle mass showed a significant reduction in all experimental groups in comparison with normal (innervated) muscle (Figure 5.3.1). The mean muscle mass in the MGF cDNA treated group (as a percentage of normal muscle mass) was 61.6% *vs.* 53.3% (control denervated muscle) and 53.0% (vector treated group).

5.3.1.2 Muscle maximum tetanic force

Maximum muscle tetanic force, which is the most definitive measurement of functional re-innervation, showed that the strength of the muscles in the MGF treated group was markedly better than that in the vector and alginate alone treated groups (Figure 5.3.2). In the MGF group the maximum muscle tetanic force of the re-innervated TA muscle was 99.4% compared to that of its contralateral innervated muscle. In the vector group in which the empty vector was included in the silicon tube, the maximum muscle tetanic force of the re-innervated TA muscle was 72.3% of its contralateral muscle; and in the alginate group in which only alginate was included in the silicon tube it was 71.5% to its contralateral side.

5.3.1.3 Muscle half-life (fatiguability)

Muscle fatigue resistance (measured as the time to half maximum isometric tension c.f. 2.34) was increased significantly within the MGF treated group compared to the vector and alginate groups (Figure 5.3.3). Although muscle fatigue resistance was increased in both control (187.9%) and vector groups (192.7%) compared to their contralateral control, this increase was significantly higher ($P<0.01$) in the MGF treated group (245.3%).

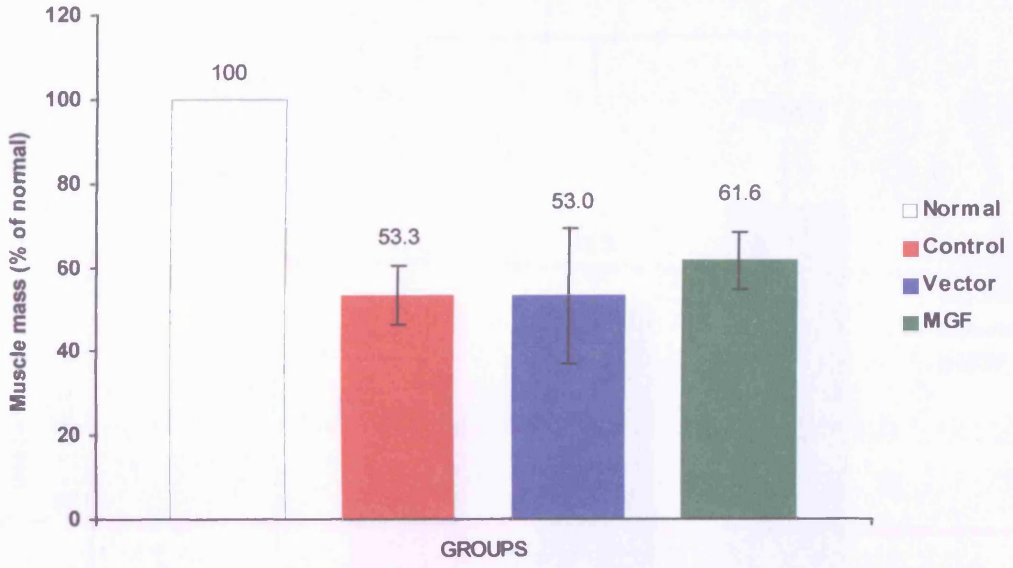

Figure 5.3.1 Denervated muscle mass (mean ± S.D.) as a percentage of the contralateral normal innervated muscle mass. All masses in the experimental groups were significantly lower than those of normal muscle ($P<0.001$).

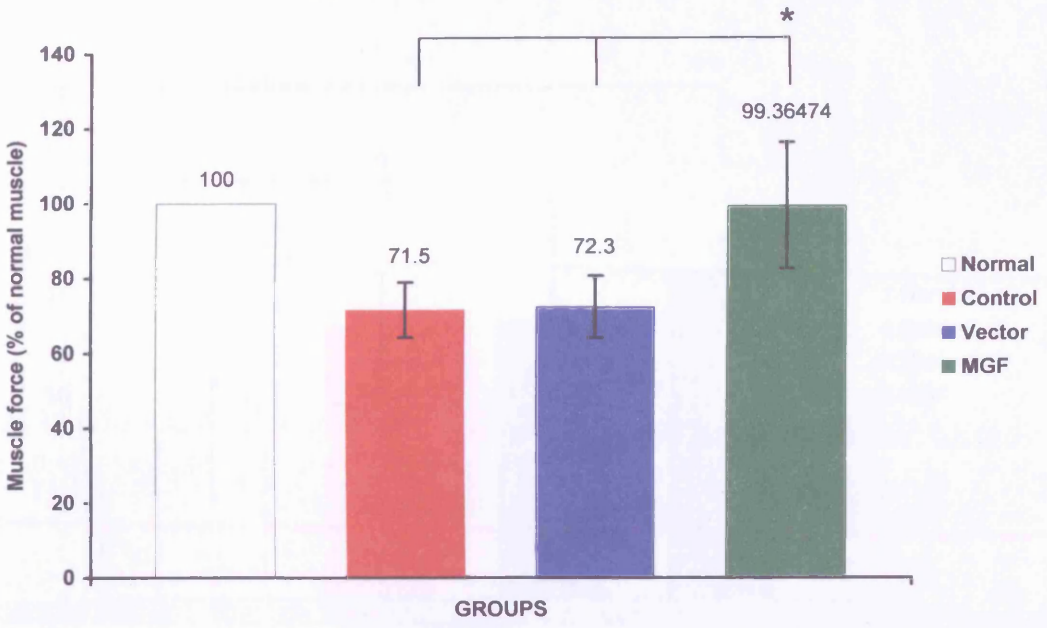

Figure 5.3.2 Muscle maximum tetanic forces (mean ± S.D.) represented as the percentage force of the contralateral normal (innervated) muscle forces. The MGF cDNA treated group approached that of normal muscle and was significantly better than the vector treated and control axotomised nerve groups (*P<0.05).

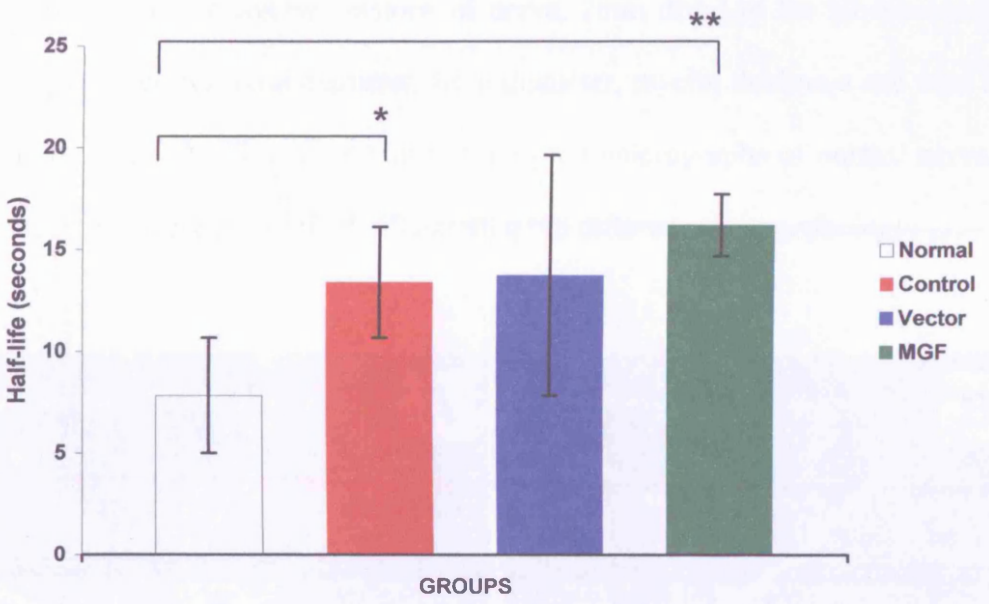

Figure 5.3.3 Histogram of half-life (fatiguability) of normal muscle and experimental groups. Half-life is calculated from the length of time taken for muscle tetanic force to fall to half maximum force (cf. Figure 2.34). All denervated muscles displayed longer half-lives than normal muscle. The control denervated muscle and the MGF cDNA treatment group were significantly longer (*$P<0.05$; **$P<0.001$). There was no significant difference between the experimental groups.

5.3.2 Semithin nerve quantification

Semithin (2μm) transverse sections of nerve, 2mm distal to the silicone conduit, were quantified for axon diameter, fibre diameter, myelin thickness and total axon count (cf. 2.14.2). Figure 5.4A and B are photomicrographs of normal nerve and regenerating nerve respectively illustrating the difference in morphology.

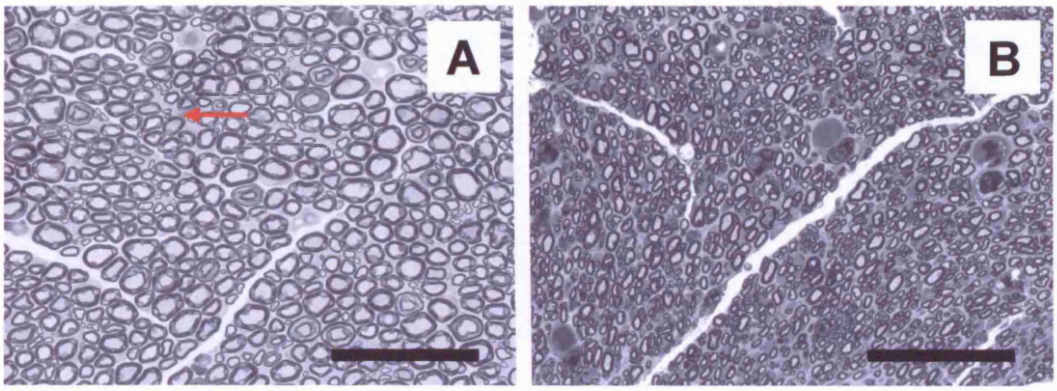

Figure 5.4 Photomicrographs of semithin (2μm) sections of peripheral nerve stained with thionine and acridine orange. (**A**) Normal nerve displaying characteristic morphology of large and small diameter fibres and unmyelinated Remark fibres (red arrow) and (**B**) regenerating nerve displaying a large number of small diameter fibres.

5.3.2.1 Axon diameter, myelin thickness and fibre diameter

The mean (± S.D.) values for axon diameter, myelin thickness and fibre diameter are shown in Table 5.1. Normal nerve contains a predominance of large diameter axons surrounded by thick myelin sheaths and therefore contains a predominance of large diameter fibres (axon diameter + myelin thickness) with a smaller number of small diameter fibres. The mean values for all these parameters were greater in normal nerve when compared to the experimental groups. Regenerating nerve contains a predominance of immature small diameter fibres with associated small diameter axons with thin myelin sheaths. With maturity regenerating nerve fibres enlarge as they reach an appropriate target organ. Figures 5.5.1-5.5.3 illustrate frequency histograms of fibre and axon diameter and myelin thickness for normal nerve and each experimental group. For each parameter normal nerve displays a bimodal distribution concentrated around small and large diameters whilst regenerating nerves display a unimodal distribution concentrated around small diameters. This is typical of both normal and regenerating nerve. The data in the Figures 5.5.1-5.5.3 is not normally distributed however following non-parametric tests (Mann-Whitney) no significant differences between the experimental groups was found.

Group	*Fibre diameter (μm)*	*Axon diameter (μm)*	*Myelin thickness (μm)*
Normal	8.02 ± 3.52	5.13 ± 2.41	1.45 ± 0.72
-ve control	3.16 ± 1.74	2.20 ±1.05	0.75 ± 0.32
Vector	4.15 ± 1.70	2.45 ± 1.29	0.85 ± 0.38
MGF	3.44 ± 1.38	2.05 ± 1.10	0.63 ± 0.29

Table 5.1 Summary data (mean ± S.D.) of measurements of transverse sections of peripheral nerve distal to conduit (with exception of normal nerve). Normal (normal nerve), -ve control (alginate only), vector (vector + alginate), MGF (MGF cDNA + vector + alginate).

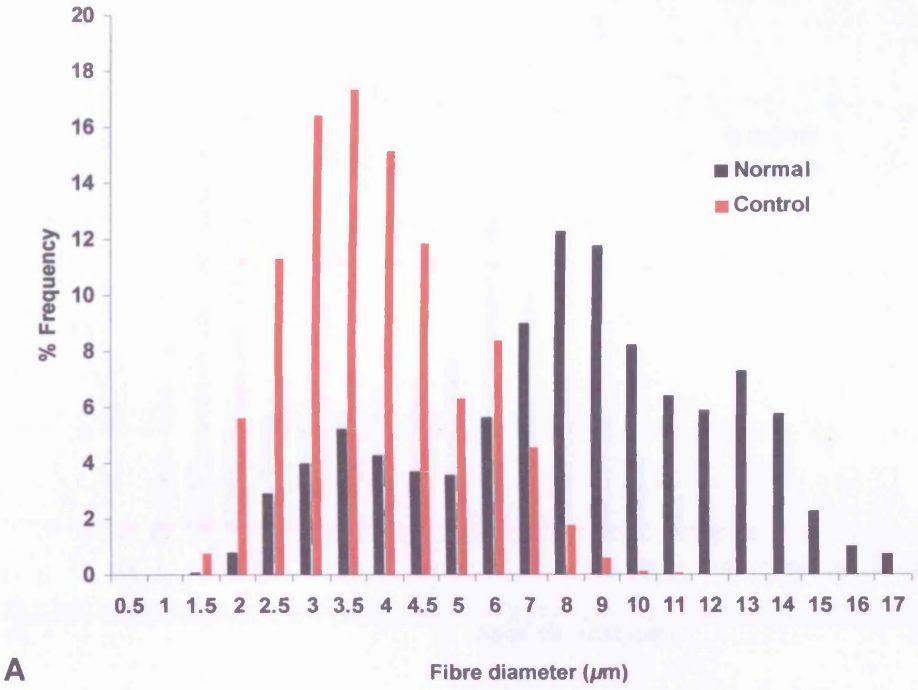

A

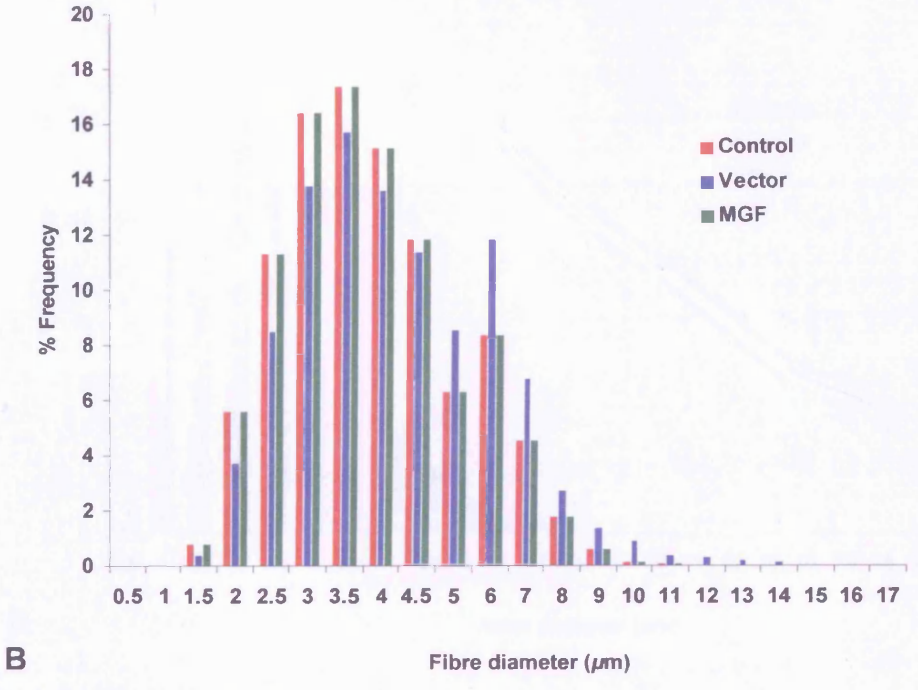

B

Figure 5.5.1 (**A**) Frequency histogram of fibre diameter in normal nerve and regenerating nerve 14 weeks following axotomy. In normal nerve a characteristic bimodal distribution of axon diameters is seen whilst in regenerating nerve there is a unimodal distribution concentrated around small diameter axons. On comparing the axotomised control, vector and MGF groups (**B**) the distribution of axon diameters was similar in all regenerating groups (cf. Figure 5.4).

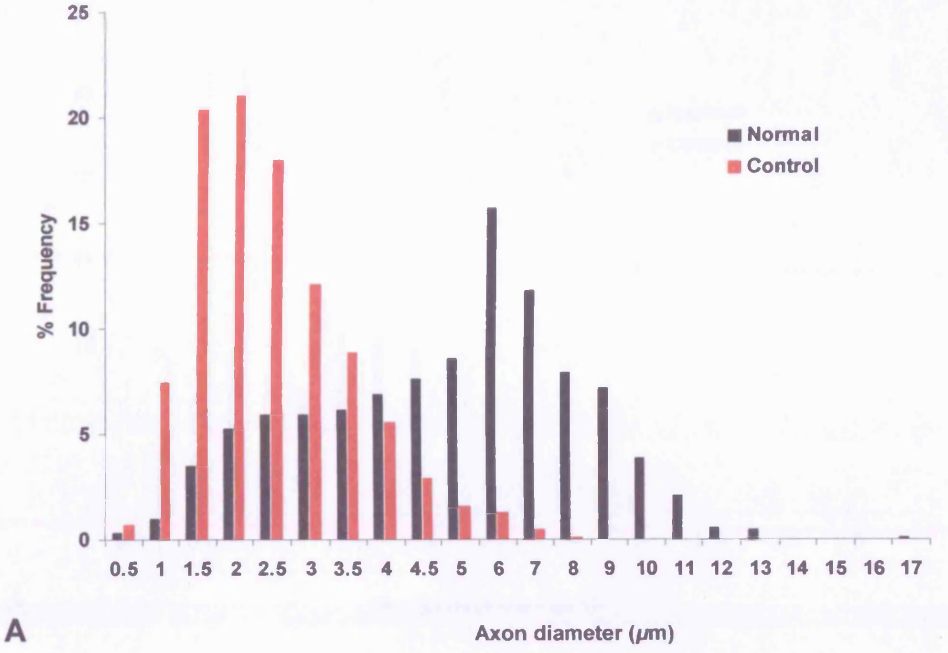

A

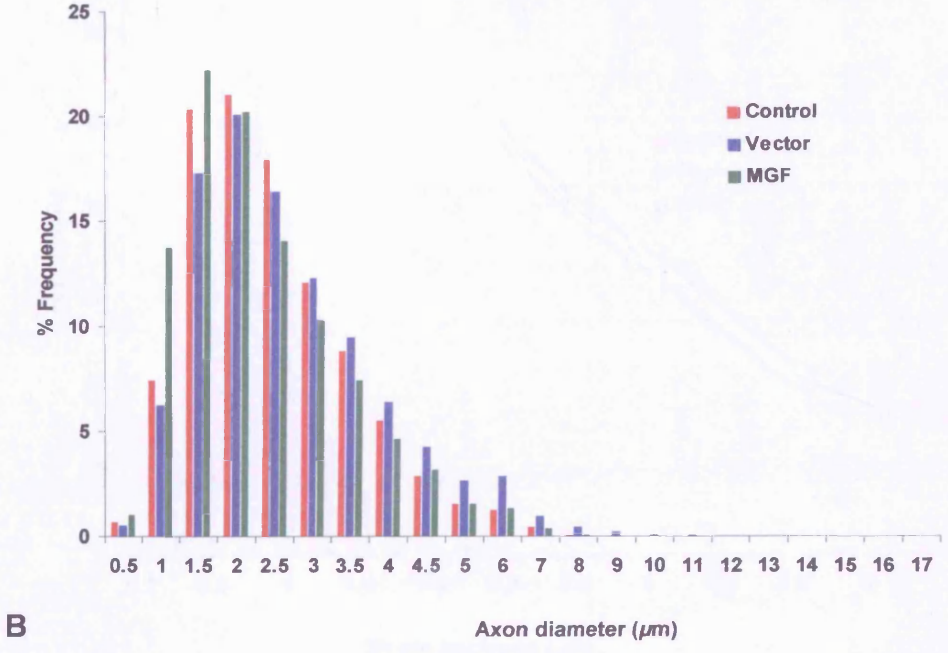

B

Figure 5.5.2 (**A**) Frequency histogram of axon diameter in normal nerve and regenerating nerve 14 weeks following axotomy. In normal nerve a characteristic bimodal distribution of axon diameters is seen whilst in regenerating nerve there is a unimodal distribution concentrated around small diameter axons. On comparing the axotomised control, vector and MGF groups (**B**) the distribution of axon diameters was similar in all regenerating groups (cf. Figure 5.4).

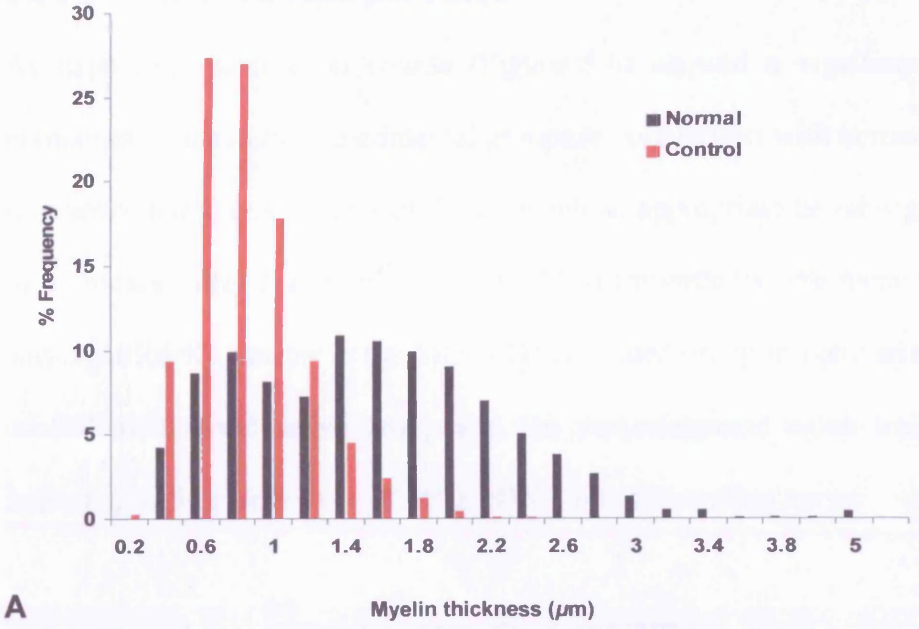

A

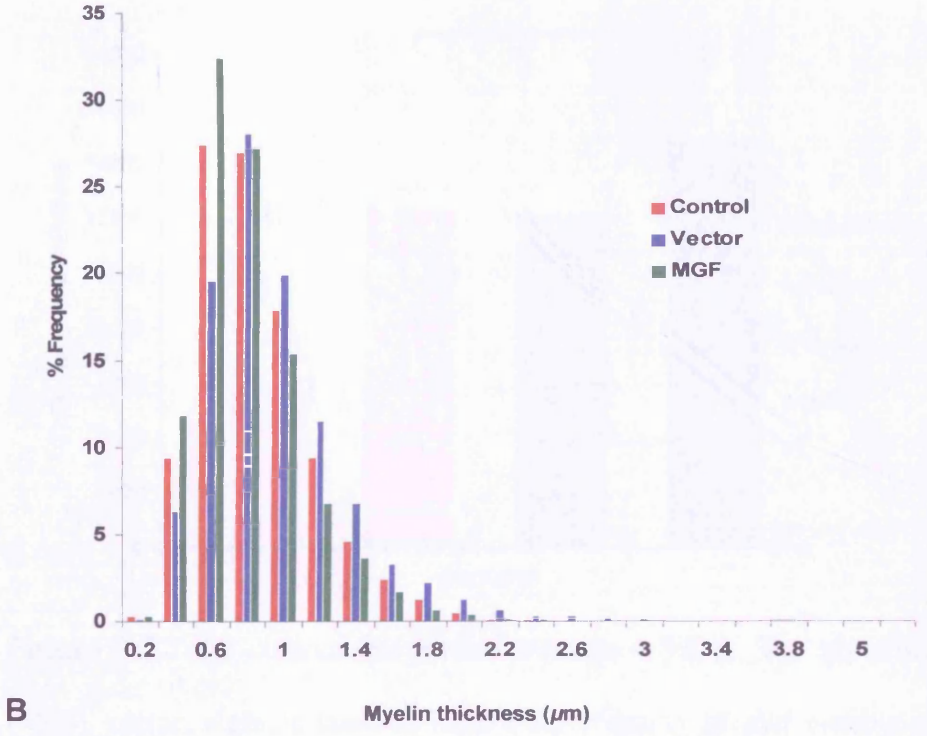

B

Figure 5.5.3 (**A**) Frequency histogram of myelin thickness in normal nerve and regenerating nerve 14 weeks following axotomy. In normal nerve a characteristic bimodal distribution of myelin thickness is seen whilst in regenerating nerve there is a unimodal distribution concentrated around small diameter axons. On comparing the axotomised control, vector and MGF groups (**B**) the distribution of myelin thickness was similar in all regenerating groups (cf. Figure 5.4).

5.3.2.2 Axon number per nerve

As expected, mean axon counts (Figure 5.6) showed a significantly greater number of axons in the experimental groups in comparison with normal nerve. As regeneration matures axons that do not reach an appropriate target organ die back in a process called 'pruning' (cf. 1.3). Most importantly, the mean axon count was significantly greater in the MGF cDNA treated group in comparison with the control axotomised nerve group and the vector/alginate alone treated groups indicating a direct influence of MGF cDNA on regenerating nerve.

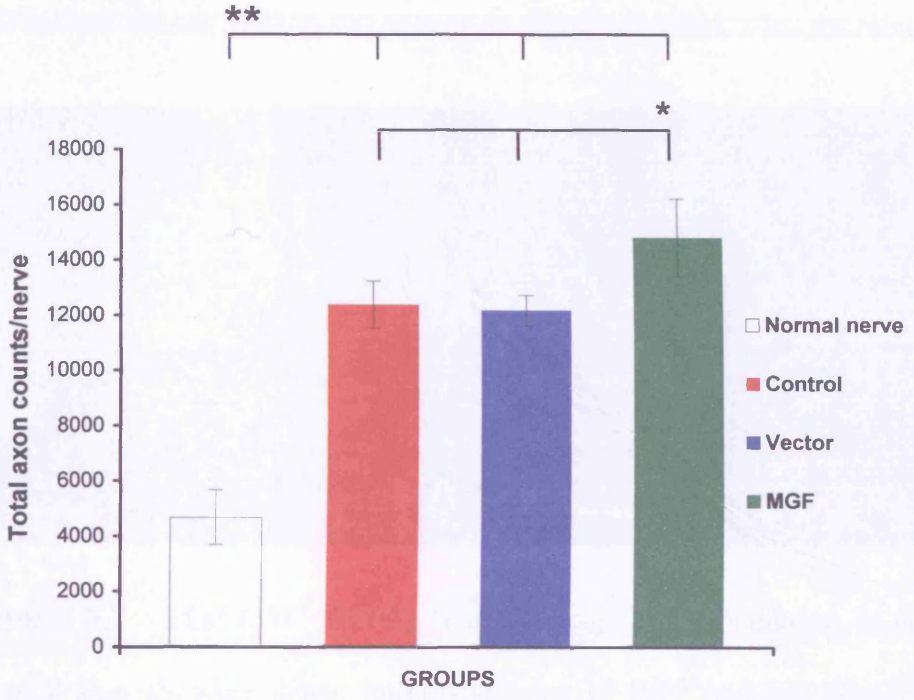

Figure 5.6 Total axon counts per nerve (mean ± S.D.). The experimental groups (MGF, vector, alginate control) have a significantly greater number of axons per nerve than normal nerve (**P<0.001). MGF cDNA treated nerve has a greater number of axons than the vector treated nerve and the alginate control axotomised nerve (*P<0.05).

5.3.3 Skin analysis

Lateral foot pad skin was harvested and prepared for immunohistochemical staining to identify nerve innervation using a PGP primary antibody and an FiTC secondary antibody to give green fluorescence (Figure 5.7). As expected the area of PGP staining was significantly reduced in the denervated groups (alginate control, vector and MGF) in comparison with normal innervated skin (Figure 5.8). There was a slight increase (not significant) in fractional immunostaining in the MGF group in comparison with the control and vector groups (0.046±0.01 *vs.* 0.039±0.007 and 0.036±0.01 respectively).

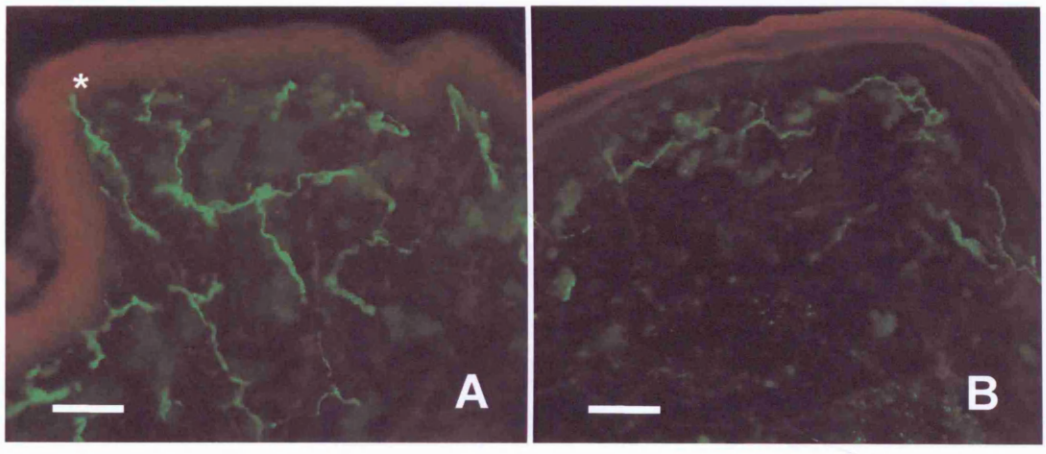

Figure 5.7 PGP-FiTC (green fluorescence) immunostaining of skin. (**A**) Normal skin showing dense immunostaining of PGP positive fibres within the dermis of the skin with extension of fibres into the epidermis (*). (**B**) Skin at 14 weeks following axotomy showing reduced intensity and density of nerve fibres. Scale bar = 40μm.

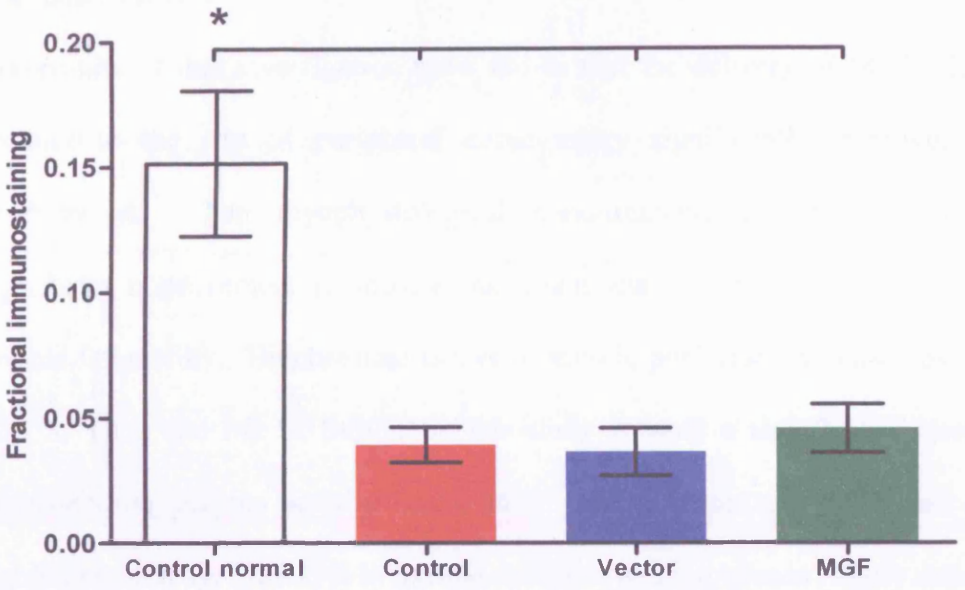

Figure 5.8 Fractional immunostaining (area of PGP staining as a fraction of the total area of staining; mean ± s.d.) in normal skin, control denervated skin and denervated skin in the vector and MGF groups (cf. Figure 5.7). The area of PGP staining in the denervated groups is significantly less in comparison to normal skin. There was a slight increase (not significant) in fractional immunostaining in the MGF group in comparison with the control and vector groups (0.046±0.01 *vs.* 0.039±0.007 and 0.036±0.01 respectively). * $P < 0.001$.

5.4 Discussion

The results of this investigation have shown that the delivery of MGF via gene transfer to the site of peripheral nerve injury significantly improves nerve regeneration. The myophysiological measurements performed showed a significant improvement in muscle maximum tetanic force and a reduction in muscle fatigability. Biochemical assays of muscle performed by co-investigators (Dr. S. Yang and Mr D. Sutton) in this study showed a significant increase in mitochondrial enzyme activity in the MGF cDNA treated group. There was a significant increase (229.2%) in muscle succinate dehydrogenase (SDH) activity in the MGF group over contralateral innervated control. SDH activity in vector only and alginate only groups were found to be 128.5% and 127.2% respectively. The functional improvement in muscle activity was corroborated by the histological quantification of nerve tissue distal to the conduits that identified a significant improvement in the number of regenerating axons present (19.7%). A smaller increase (non-significant) was seen in skin re-innervation in the footpad skin. These results lead to the conclusion that early restoration of muscle function has been as a result of improved axonal regeneration. The specific mechanism of action of MGF cDNA is however unclear. Whilst anterograde and retrograde transport of molecules along an axon may lead to the theory that MGF cDNA could be transported to muscle and neuronal cell bodies for translation and transcription it is not clear as to the mechanism in this model. Following axotomy Wallerian degeneration leads to complete autolysis of the entire course of the distal nerve stump leading to interruption of the anterograde transport pathway. With respect to retrograde transport, preliminary data has shown that MGF RNA

does not appear in tissue harvested from the dorsal root ganglia corresponding to an axotomised nerve transfected with MGF cDNA (labelled with a GFP exon). However Aperghis et al. (2004) have found that both MGF and IGF-I Ea cDNA constructs when injected into rat facial muscle were neuroprotective following avulsion of the facial nerve. In addition it has been reported that DNA constructs such as adeno-associated virus (AAV) vector can be retrogradely transported efficiently from muscle to motor neuron cell bodies in the spinal cord (Kaspar et al. 2002).

There is a possibility that MGF cDNA primarily acts at the site of injury. IGF-1 has been shown to have a mitogenic effect on Schwann cells (SCs) *in vitro* (Cheng et al. 1996) and has a potent neurotrophic effect both *in vitro* (Akahori & Horie, 1997) and *in vivo* following nerve injury (Skottner et al. 1987), therefore its MGF isoform is likely to have a similar effect although this has not been studied. SCs are known to secrete IGF-1 up to 7 days following nerve injury after which IGF-1 is produced by infiltrating macrophages (Cheng et al. 1996). In this study the delivery of MGF cDNA may have a direct and indirect action on stimulating nerve regeneration, both of which mediated by local SCs. Transfection of local SCs with MGF cDNA may lead to production of MGF peptide that in turn stimulates SC proliferation, thereby improving the environment for nerve regeneration. SC production of MGF may also directly stimulate nerve regeneration. In summary, MGF has a potential therapeutic role as an adjuvant treatment for peripheral nerve injuries and secondly, the use of a gene transfer technique has been shown to be efficacious method of providing prolonged delivery of growth factor.

Chapter 6

Modulation of PHB Nerve Conduits with Extracellular Matrix Macromolecules

6.1 Introduction

The major constituents of the peripheral nerve include Schwann cells (SCs), axons and the extracellular matrix (ECM). The ECM is comprised of basal lamina sheets that surround individual axon-Schwann cell units and collagen fibrils. The ECM is composed from 3 major classes of macromolecules: glycoproteins, collagens and proteoglycans. The ECM regulates cell morphology and tissue organization, SC and axon migration, SC proliferation and myelination (Reviewed by Chernousov & Carey, 2000). The major glycoproteins include laminin, fibronectin and tenascin. Laminin is a large glycoprotein consisting of 3 disulphide-linked polypeptide chains, α, β, and γ, and is the major constituent of the basal lamina. SCs secrete laminin-2 which they deposit into the ECM both *in vitro* and *in vivo* (Cornbrooks et al. 1983; Jaakkola et al. 1993 263). Fibronectin is a multidomain glycoprotein secreted into the ECM by SCs. It is found in the endoneurium of peripheral nerves in areas surrounding axon-Schwann cell units (Cornbrooks et al. 1983). A large number of collagens are secreted by SCs both *in vitro* and *in vivo* including collagen I and III which are involved in fibril formation; collagen IV, which is a structural constituent of the basal lamina, and collagen V which is prominent in developing nerve and has a high affinity for heparan sulphate (Chernousov et al. 1999). The proteoglycans are a more heterogeneous group of molecules which include: perlecan, a heparan sulphate proteoglycan which is found in the SC basal lamina and which binds to other ECMMs such as laminin, fibronectin and collagen (Fujiwara et al. 1984); agrin, a heparan sulphate proteoglycan (Tsen et al. 1995); collagen XVIII (Halfter et al. 1998); and the chondroitin sulphate proteoglycans (Braunewell et al. 1995).

A number of studies have identified the benefit of augmenting bio-engineered nerve conduits with individual components of the ECM. Mosahebi et al. (2003) showed that the addition of fibronectin to an alginate-Schwann cell matrix suspension improved regeneration across a 1cm nerve gap spanned by a PHB conduit. Laminin-coated poly-L-lactide filaments have been shown to induce uni-directional neurite outgrowth *in vitro* (Rangappa et al. 2000). Tong et al. (1994) demonstrated significant axonal regeneration through 10mm collagen tubes loaded with unidirectional collagen fibres coated with laminin and fibronectin.

Axonal and SC regeneration responds to both trophic and physical cues. Contact guidance has been demonstrated *in vitro* on micropatterned surfaces for both neurite outgrowth (Miller et al. 2001) and SC proliferation (Miller et al. 2000). This study aimed to investigate the ability of unidirectional dissociated PHB fibres within a PHB conduit to support nerve regeneration via contact guidance and secondly to investigate whether these fibres could act as a matrix for transplanted SCs (Figure 6.1). To augment axonal and SC regeneration the effect of coating these fibres with ECMMs was also studied. *In vitro* studies were first performed to characterise the effect of ECMM sustrata on SC growth on tissue culture plastic and pre-coated PHB fibres, followed by *in vivo* studies to investigate nerve regeneration through PHB conduits containing PHB fibres pre-coated with ECMMs and seeded with GFP-labelled SCs.

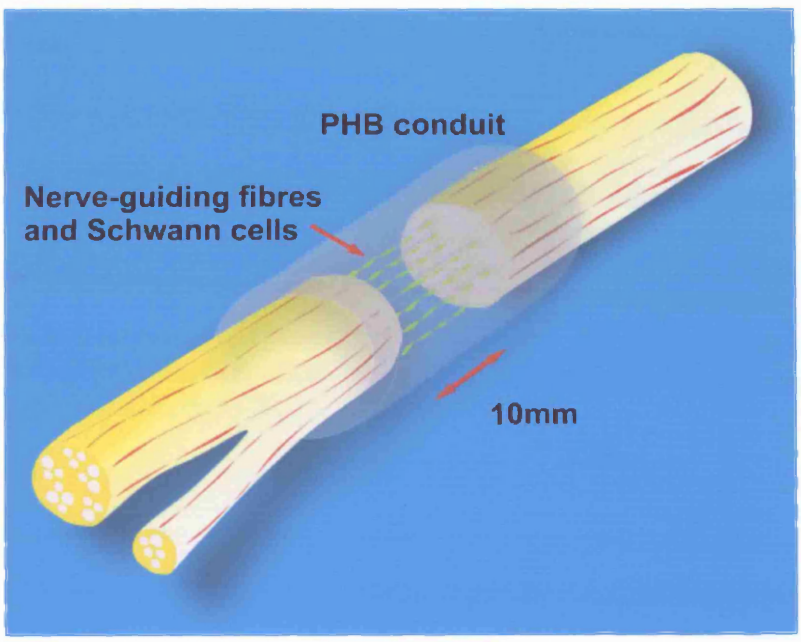

Figure 6.1 Schematic diagram representing a model of unidirectional intraluminal PHB fibres acting as a matrix for transplanted Schwann cells within a PHB conduit spanning a 1cm nerve gap in the rat sciatic nerve.

6.2 Materials and Methods

6.2.1 *In vitro* study 1 – Schwann cell growth on ECMM substrata

Tissue culture plates (24-well) were coated with either laminin, fibronectin or collagen (Appendix B) at the concentrations given in Table 6.1. A poly-D-lysine (PDL) coated plate was used as a control. Schwann cells (SCs) were seeded on the plates at a concentration of 1 X 10^5 cells/ml/well and incubated at 37°C, 5% CO_2. SC growth curves on each substrata were subsequently constructed using the protocol described in section 2.7. The growth curves for each ECMM substrata were repeated by coating 24-well plates with either laminin, fibronectin and collagen on plates initially coated with PDL.

ECMM	*Concentration*
Laminin 2	$2\mu g/cm^2$
Fibronectin	$2\mu g/cm^2$
Collagen 5	$5\mu g/cm^2$
Collagen 10	$10\mu g/cm^2$

Table 6.1 Concentrations of ECMM substrata used to coat tissue culture plastic. Two concentrations of collagen were used as no optimal concentration was recommended in the manufacturer's guidelines (Sigma) or published literature on SC culture.

6.2.2 *In vitro* study 2 – Schwann cell metabolic activity on ECMM pre-coated PHB fibres

Dissociated PHB fibres were pre-coated with either laminin, fibronectin or collagen at the concentrations given in Table 6.1, following which 1cm^2 squares of PHB were placed in each well of a 24-well plate. A suspension of SCs (1 X10^5 cells/ml/well) was then added to each well and incubated at 37°C, 5% CO_2. After 24hrs the medium was replaced with SC growth medium containing 10% alamar Blue™ indicator solution. The cultures were placed in the incubator and the medium was sampled each day for 7 days to measure metabolic activity (cf. 2.6). Cultures were immunostained with an S100-Cy3 conjugate to assess SC attachment to PHB fibres (cf. 2.13.3).

6.2.3 Intraluminal PHB fibres

Polyhydroxybutyrate (PHB) conduits were constructed as described in section 2.8. Dissociated PHB fibres were used as a matrix for transplanted SCs by threading PHB fibres through conduits prior to transplantation (cf. 2.10.3). To determine a suitable density of fibres a number of conduits were constructed and sectioned in transverse and cross-sectional directions (Figure 6.6). Conduits containing 0.35mg dissociated fibres per conduit were chosen on an arbitrary basis. Low PHB fibre concentrations were excluded as these were expected to be ineffectual as a matrix for capturing transplanted SCs. Similarly, high concentrations were excluded as these were thought to be likely to cause obstruction.

6.2.3.1 Pilot *in vivo* testing of intraluminal PHB fibres within a PHB conduit

Prior to a full scale *in vivo* experiment, a PHB conduit containing 0.35mg dissociated PHB fibres was grafted into a 1cm gap in the rat sciatic nerve. The conduit was seeded with cultured rat primary SCs at a concentration of 80 X 10^6cells/ml suspended in SC growth medium by injecting 30μL of cell suspension into one end of the conduit using a Hamilton syringe. The conduit was harvested at 2 weeks and prepared for immunohistochemical staining to assess transplanted SC capture (cf. 2.13.1).

6.2.3.2 *In vivo* assessment of intraluminal PHB fibres pre-coated with ECMMs

An *in vivo* experiment was performed to determine the ability of dissociated intraluminal PHB fibres to act as a matrix for transplanted SCs within a PHB conduit spanning a 1cm gap in the rat sciatic nerve. In addition fibres were pre-coated with either laminin, fibronectin or collagen (c.f. 6.2.2). Groups (n=5) were constructed as follows:

Group 1 : Control (uncoated fibres)

Group 2 : Laminin-coated fibres (2μg/cm^2)

Group 3 : Fibronectin-coated fibres (2μg/cm^2)

Group 4 : Collagen-coated fibres (5μg/cm^2)

Operative and anaesthetic procedures were carried out according to the protocols described in section 2.11. Following grafting of the conduits SC (transduced with

GFP) suspensions were transplanted into the conduits (cf. 6.2.3.1). Nerve conduits, together with proximal and distal stumps, were harvested at 2 weeks and fixed in preparation for immunohistochemical staining (cf. 2.12). Nerves were immunostained stained with PGP9.5 antisera to detect axonal regeneration and S100 antisera to detect Schwann cell regeneration (cf. 2.13.1). Axonal and Schwann cell regeneration distances were quantified (cf. 2.14.1) and compared using ANOVA.

6.3 Results

6.3.1 *In vitro* assessment of Schwann cell growth on ECMM substrata

Initial studies of SC growth on ECMM substrata (Figure 6.2) showed improved growth at all time points for SCs grown on laminin, fibronectin and poly-D-lysine (PDL). Collagen substrata at 5 and 10 $\mu g/cm^2$ performed unexpectedly poorly. It was noticed that a large number of cells failed to adhere to the tissue culture plastic in the collagen substrata groups. The experiment was repeated, however the protocol was altered by pre-coating all tissue culture plastic with PDL followed by the application of either laminin, fibronectin or collagen. The resulting growth curves (Figure 6.3) showed increased cell numbers at all time points for PDL-laminin, PDL-fibronectin and PDL-collagen (5 and 10 $\mu g/cm^2$) substrata when compared to substrata not pre-coated with PDL (Figure 6.2). The primary effect of PDL is to remove the electrostatic charge present on tissue culture plastic thereby facilitating SC attachment. Pre-coating with PDL prior to the application of the above ECMMs potentiates their effects by maximising SC

attachment. In addition to their effects on SC growth, laminin and fibronectin may have properties similar to that of PDL whilst collagen does not.

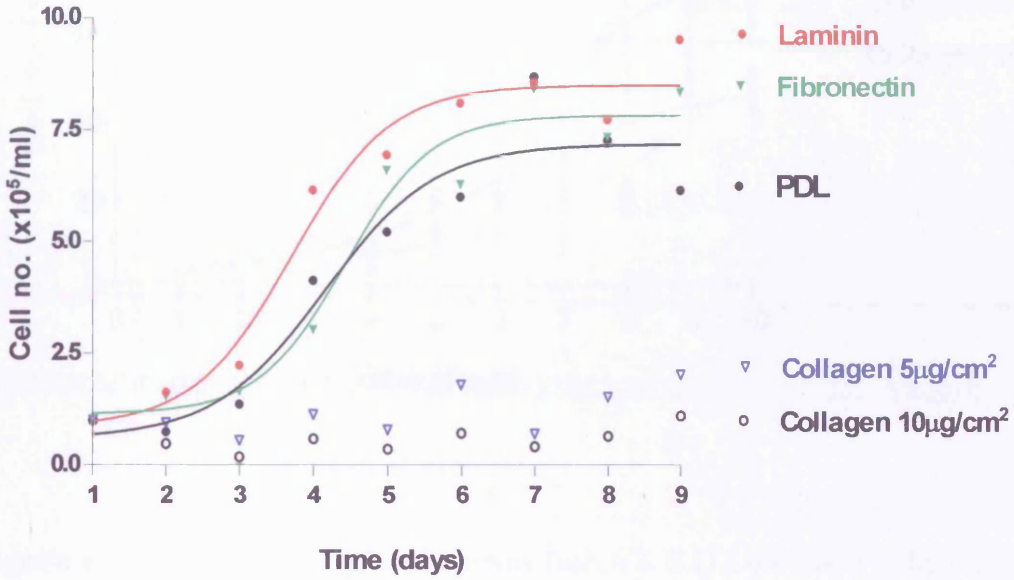

Figure 6.2 Schwann cell growth curves (mean values with non-linear regression curves) on initial testing of laminin, fibronectin, collagen and poly-D-lysine (PDL; control) substrata. Laminin, fibronectin and PDL improve growth over both concentrations of collagen.

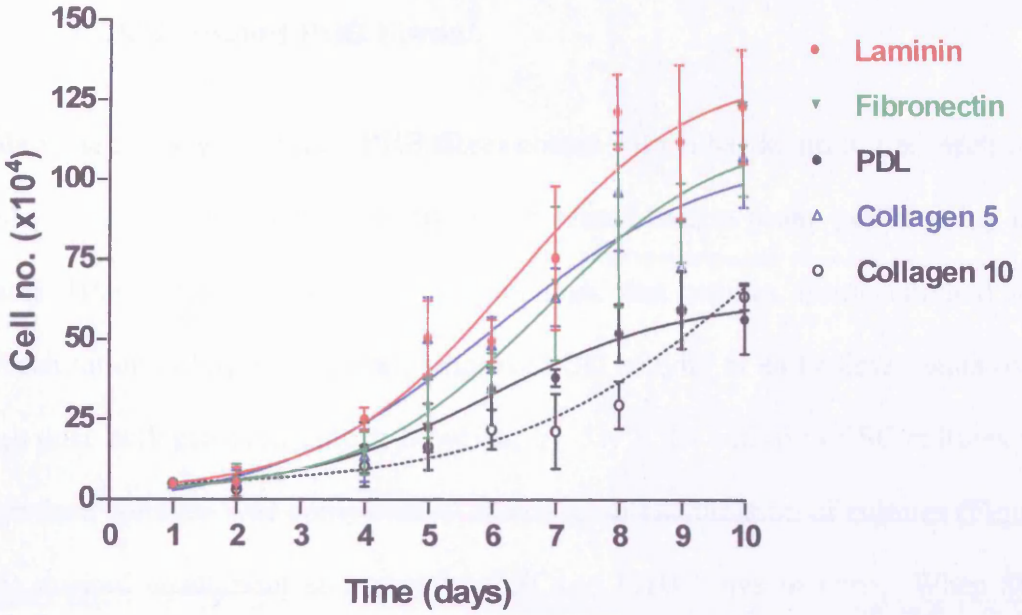

Figure 6.3 Schwann cell growth curves (mean ± S.D.) on tissue culture plastic initially coated with PDL followed by the addition of either laminin, fibronectin or collagen substrata. Pre-coating tissue culture plastic with PDL improved the Schwann cell growth curve of low concentration collagen ($5\mu g/cm^2$) when compared to collagen alone as shown in Figure 6.2. At 10 days there were significantly higher Schwann cell numbers on laminin, fibronectin and collagen ($5\mu g/cm^2$) in comparison with PDL alone and collagen ($10\mu g/cm^2$). The final cell numbers of all groups (with the exception of PDL alone) were higher when tissue culture plastic was initially treated with PDL (cf. Figure 6.2).

6.3.2 *In vitro* assessment of Schwann cell metabolic activity on ECMM-coated PHB fibres

Following seeding of SCs on PHB fibres coated with either laminin, fibronectin or collagen *in vitro* metabolic activity was assessed over a 6 day period using the alamar Blue™ assay (Figure 6.4). It was found that laminin, fibronectin and low concentration collagen ($5\mu g/cm^2$) improved SC activity at early time points over high dose collagen ($10\mu g/cm^2$); however, by day 6 the activity of SC cultures on high dose collagen was comparable. Histological examination of cultures (Figure 7.5) showed attachment and growth of SCs to PHB fibres *in vitro*. When SCs were cultured with uncoated PHB fibres measured metabolic activity was poor although an increase was detectable by day 6. This probably reflects either a sampling error when applying a SC suspension to the uncoated fibres or a temporal delay in SC attachment and growth due to the hydrophobic electrostatic charge present on PHB fibres.

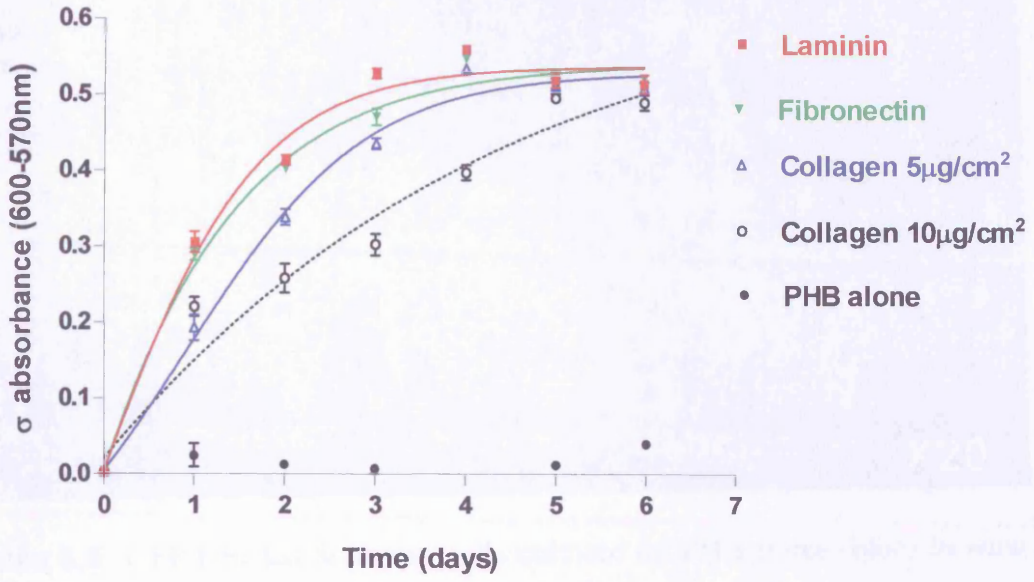

Figure 6.4 Schwann cell metabolic activity (mean ± S.E.M.) when cultured on PHB fibres pre-coated with either laminin, fibronectin or collagen as assessed via the alamar Blue™ assay (cf. 2.6). Schwann cell metabolic activity at day 6 was similar in laminin, fibronectin and collagen pre-coated PHB fibres when compared to uncoated PHB fibres. The poor performance of uncoated PHB fibres was attributed to either the native electrostatic charge of PHB preventing adherence of Schwann cells or more likely a sampling error when initially applying Schwann cells to the PHB fibres at the beginning (day 0) of the experiment. A small increment is seen at day 6 and it is possible that with continued measurement beyond this time point continued metabolic activity would have been identified.

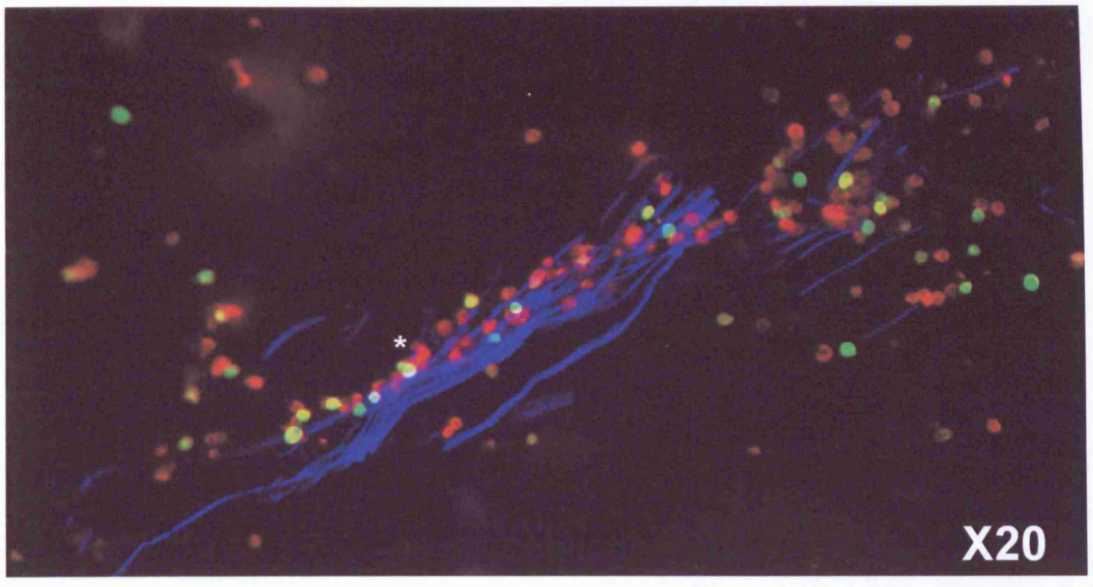

Figure 6.5 GFP-labelled Schwann cells cultured on PHB fibres (blue) *in vitro*. Cultures were stained with an S100-Cy3 conjugate (red) to identify all Schwann cells, co-localisation with GFP fluorescence appears yellow (asterisk). Schwann cells are shown to be concentrated around PHB fibres.

6.3.3 *In vivo* assessment of the dissociated intraluminal PHB fibres as a matrix for transplanted Schwann cells

Four PHB conduits were constructed containing dissociated intraluminal PHB fibres at the concentrations given in Table 6.2. The conduits were embedded in OCT, frozen at –40°C, sectioned at 15μm and examined under phase contrast microscopy (Figure 6.6). Fibre weights per conduit of 0.35mg (Figure 6.6C; ~1015 fibres/conduit) were chosen for the *in vivo* experiment.

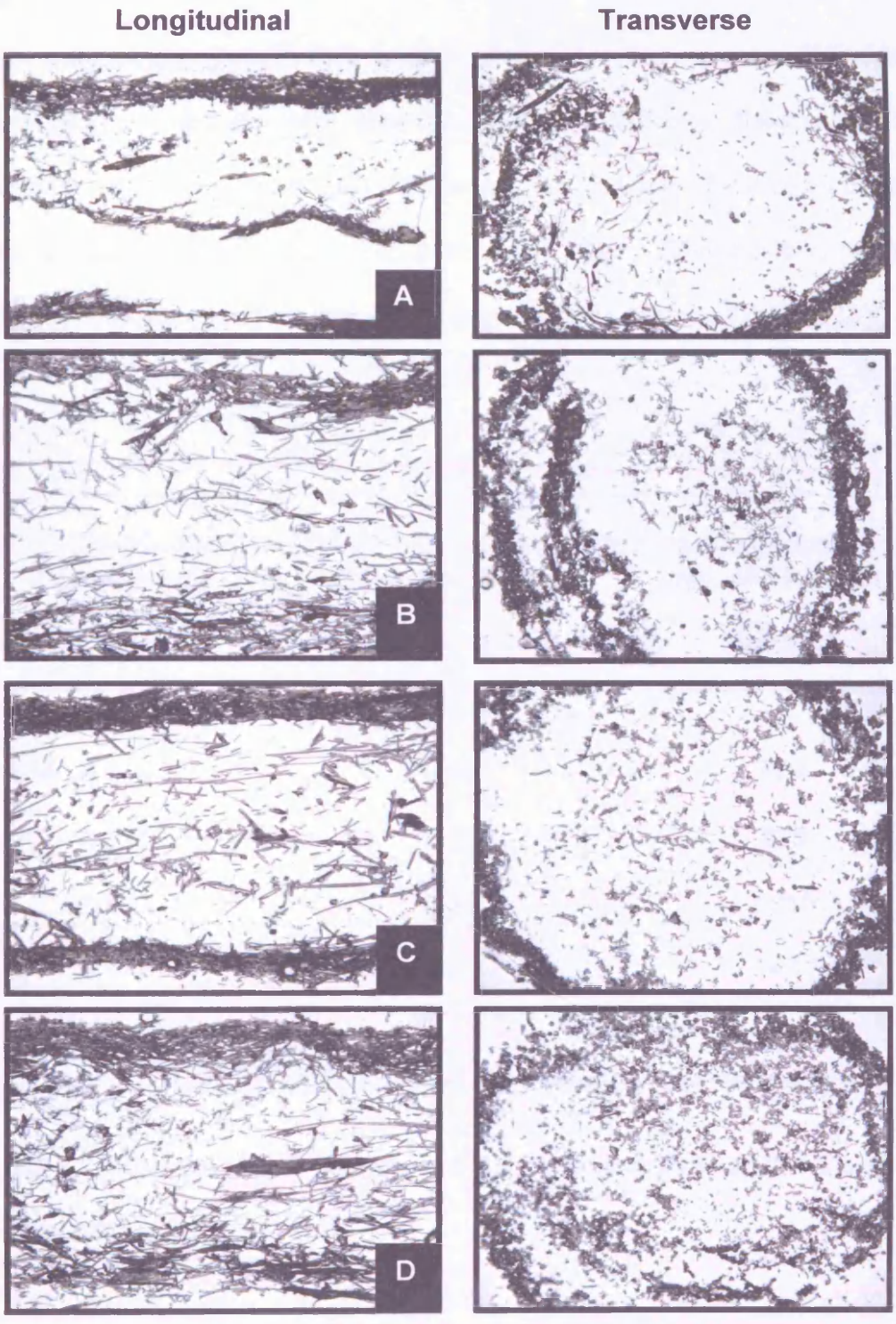

Figure 6.6 See overleaf for detailed legend

Figure 6.6 legend

Phase contrast histology of PHB conduits threaded with dissociated PHB fibres (cf. 2.10.3). Conduits were constructed with 4 different dissociated fibre concentrations (based on weight). Following construction of the conduits they were embedded in OCT, frozen and sectioned at 15μm. Fibre numbers per unit cross-sectional area were counted using image analysis software (Table 6.2).

Figure label	*Fibre weight(mg)*	*No. of fibres per conduit*[3]
6.6 A	0.15	564
6.6 B	0.25	875
6.6 C	0.35	1015
6.6 D	0.50	1471

Table 6.2 Fibre weights and number of fibres per unit cross-sectional area for conduits **6A-6D** (cf. Figure 6.6).

[3] Fibre numbers per cross sectional unit area were counted using image analysis software (ImagePro Plus).

Preliminary *in vivo* testing of a conduit with transplanted SCs showed an even distribution of SCs throughout the length of the conduit. SCs were found to be closely related to the intraluminal PHB fibres (Figure 6.7A, B and C). SCs were also found to be integrated with regenerating axons (Figure 6.8) and host SC regeneration (Figure 6.9) at the regeneration front of the proximal stump.

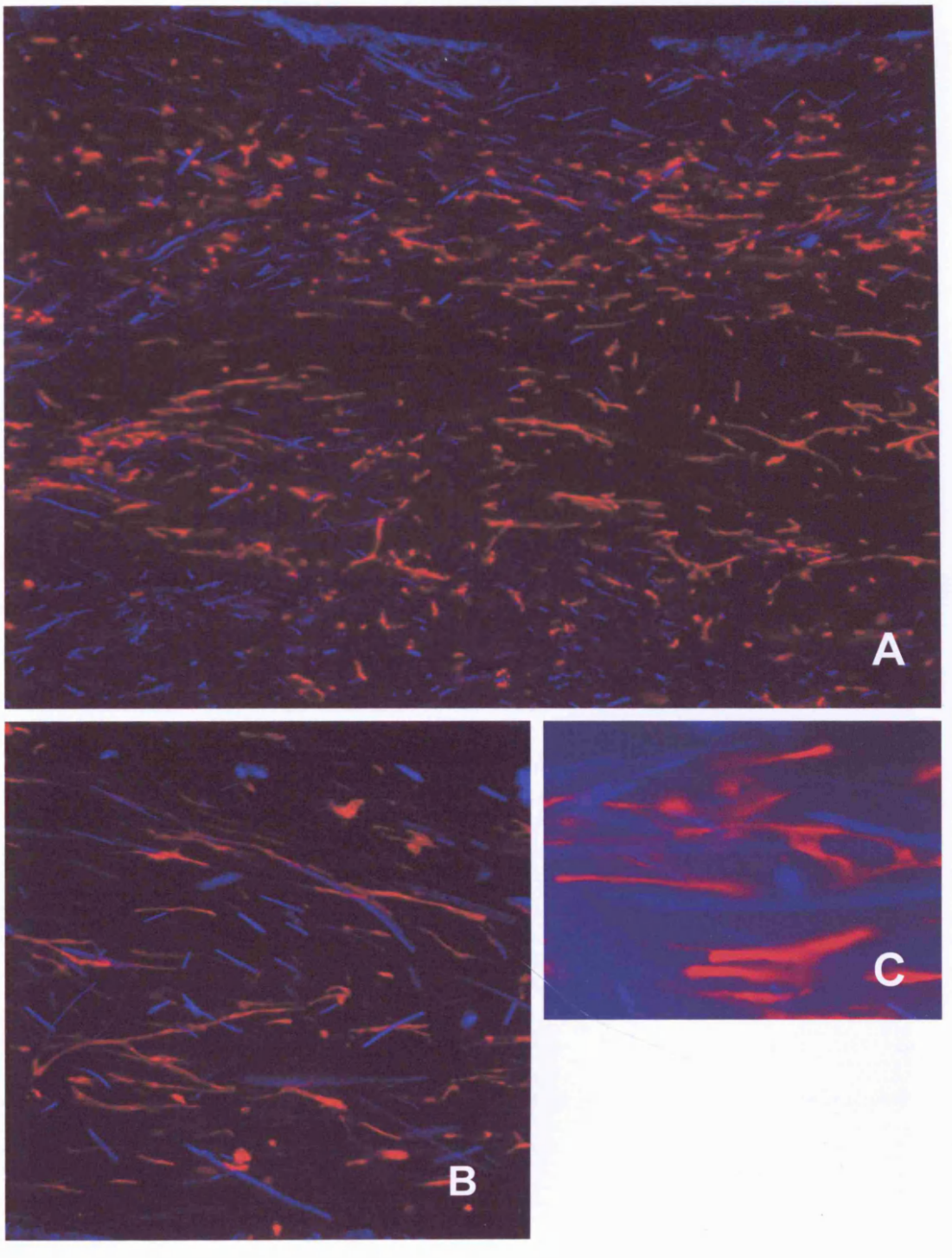

Figure 6.7 Sections of a PHB conduit containing intraluminal PHB fibres (blue) transplanted with Schwann cells and stained with an S100-Cy3 conjugate (red). Schwann cells are clearly seen to be associated with PHB fibres and are evenly distributed throughout the length of the conduit. (**A**, X10; **B**, X20; **C**, X40).

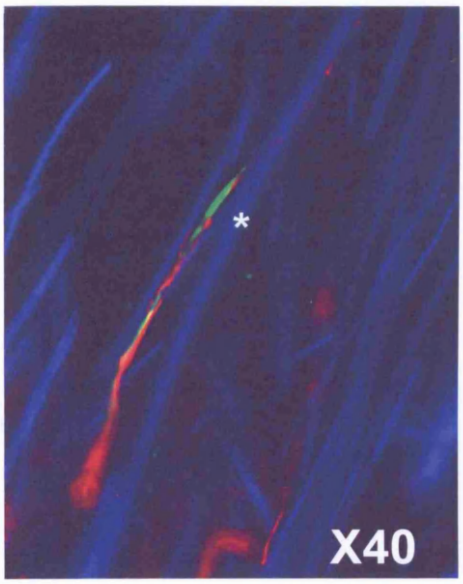

Figure 6.8 Section of an explanted conduit seeded with GFP-Schwann cells. A GFP-Schwann cell (asterisk) is shown associated with a regenerating axon immunostained with a PGP9.5-Cy3 conjugate (red). The axon and Schwann cell are shown to be closely aligned with intraluminal PHB fibres (blue autofluorescence).

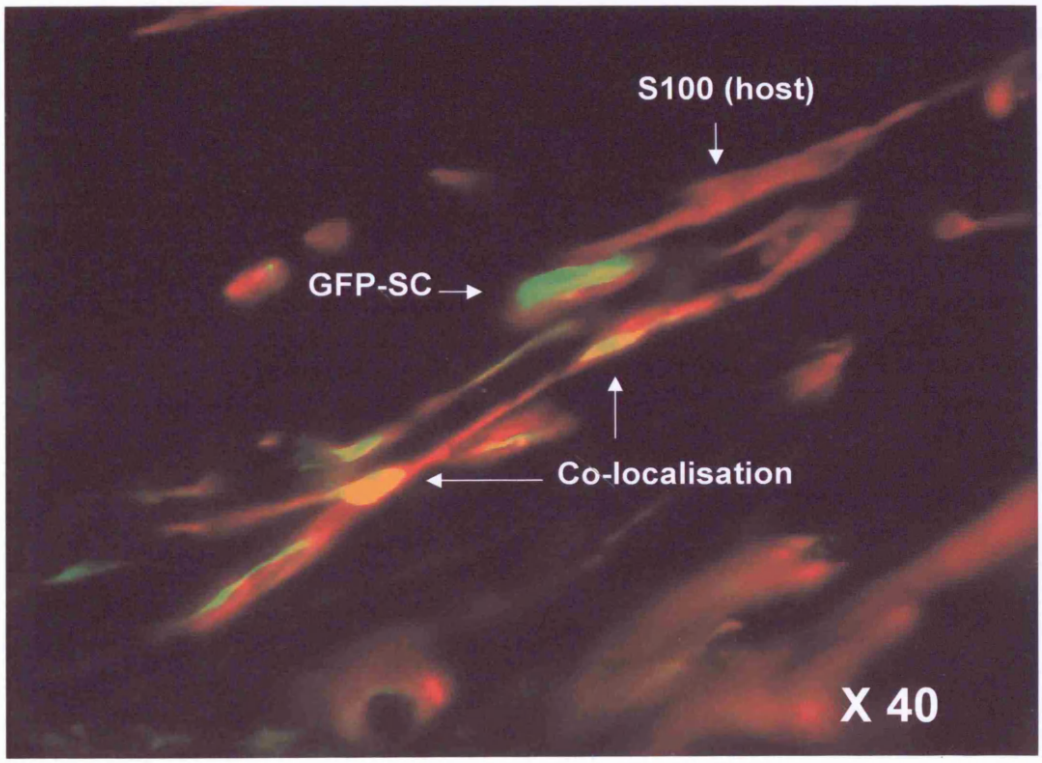

Figure 6.9 Section of a PHB conduit containing GFP-Schwann cells (GFP-SC) immunostained with a S100-Cy3 conjugate (red). Integration of transplanted Schwann cells is clearly shown with host regenerating Schwann cells.

6.3.4 *In vivo* assessment of intraluminal PHB fibres pre-coated with ECMMs

Following the preliminary results discussed in section 6.3.2 an *in vivo* experiment was performed using PHB fibres pre-coated with ECMMs as described in section 6.3.2.1. At 2 weeks the mean Schwann cell regeneration distances were significantly greater in the laminin and fibronectin coated groups in comparison with the uncoated control ($P<0.05$; Figure 6.10), with the distances between laminin and fibronectin being comparable. Similarly, mean axonal regeneration distances were significantly greater in the laminin and fibronectin groups when compared to the uncoated control group ($P<0.05$; Figure 6.11). Mean axonal regeneration distance was slightly better in the laminin coated group when compared to the fibronectin coated group although this was not statistically significant.

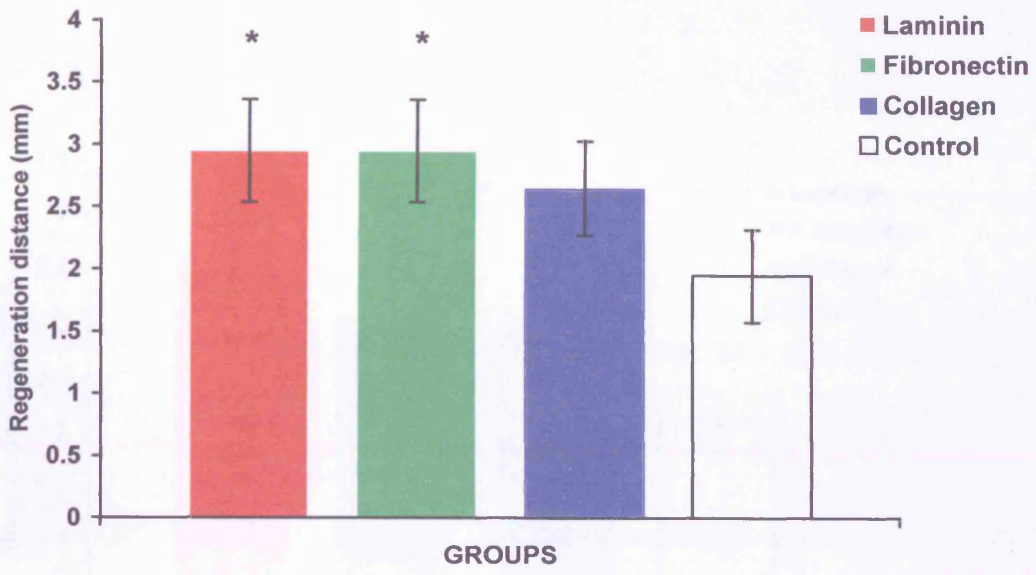

Figure 6.10 Schwann cell regeneration distances (mean ± S.D.). Distances were measured from the insertion of the proximal stump to the tip of the most distal regenerating fibre. Regeneration distances were significantly greater in the laminin and fibronectin groups when compared to the control group (uncoated fibres). *P<0.05; ANOVA.

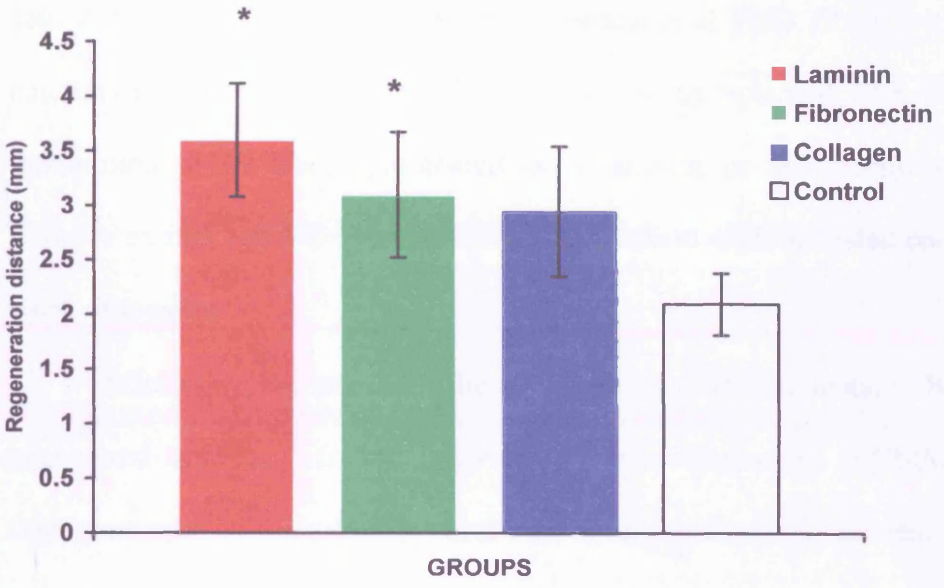

Figure 6.11 Axonal (measured via PGP9.5 immunoreactivity) regeneration distances (mean ± S.D.). Distances were measured from the insertion of the proximal stump to the tip of the most distal regenerating fibre. Regeneration distances were significantly greater in the laminin and fibronectin coated groups when compared to the uncoated control group. *P<0.05; ANOVA.

6.4 Discussion

This study has shown that (a) laminin, fibronectin and to a lesser extent collagen, promote SC growth *in vitro* both as tissue culture plastic substrata and when pre-coated on PHB fibres, (b) dissociated intraluminal PHB fibres within a PHB conduit can successfully act as a matrix for transplanted SCs and (c) that intraluminal PHB fibres pre-coated with laminin or fibronectin significantly improve axonal and SC regeneration in comparison with uncoated controls at a 2 week time point.

Mimicking the internal milieu of any tissue is fundamental to building bio-engineered systems. Extracellular matrix macromolecules (ECMMs) play an important role in the ultra-structure and homeostasis of all tissues. Molecules such as laminin, fibronectin and collagen closely interact with and support cellular elements *in vivo* (Ide, 1996). The beneficial effect of ECMMs on SC proliferation and axonal regeneration within a bio-engineered nerve supports the need for an engineered extracellular matrix. ECMMs are known to promote cellular adhesion and proliferation and to influence the expression of cell adhesion molecules. The component molecules within the matrix do not operate as individual units but as part of a highly organized macromolecular complex. The assembled ECM is likely to have biochemical and physical properties that are not manifested by individual ECM molecules alone (Chernousov & Carey, 2000). Further characterisation of the effect of these molecules at the cellular and molecular level, and further studies involving combinations of molecules, will lead to important information relating to, and advances in, the behaviour of cellular transplants within bio-engineered systems and subsequent regeneration.

Chapter 7

The Effect of Extracellular Matrix Macromolecules on NCAM and N-cadherin Expression in Bioengineered Nerve Constructs

7.1 Introduction

The cellular responses following nerve injury are activated by a complex and heterogeneous array of signalling proteins located in the plasma membrane. Amongst these proteins are the cell adhesion molecules (CAMs). In addition to maintaining tissue architecture through cell-cell and cell-matrix adhesion, CAMs form important signalling interfaces between the environment and the cytoplasmic processes which control nerve development and the response to nerve injury and regeneration. CAMs are expressed in the developing CNS and PNS where they participate in neuronal cell migration, myelination, neurite outgrowth, and axonal guidance and fasciculation (reviewed by Fu and Gordon, 1997). The experiment described in this chapter examines the expression of two important CAMs (neural cell adhesion molecule (NCAM) and N-cadherin) at the regeneration front of a regenerating nerve within a bio-engineered nerve conduit containing a scaffold of fibres coated in various extracellular matrix macromolecules (laminin, fibronectin and collagen). Extracellular matrix macromolecules (ECMMs) are important components of the matrix and have been shown to stimulate neurite extension and modulate CAM expression *in vitro* (cf. chapter 6; Kiryushko et al. 2004; Burgess et al. 2007). Little is known regarding the expression of CAMs at the regeneration front of nerves regenerating through nerve conduits.

A detailed discourse on the molecular biology of CAMs in peripheral nerve regeneration is outside the scope of this thesis. In summary, CAMs are categorised into a number of major classes which include: The cadherins (e.g. N-cadherin); the immunoglobulin superfamily (e.g. NCAM); the integrins (which bind to laminin); and the selectins. Following injury, neurite induction and

sprouting, the extracellular matrix (ECM) has a number of effects on the regeneration front. There are positive cues (permissive or attractive), negative cues (inhibitory or repulsive) or guiding cues (due to the physical environment). These signals come from macromolecules of the ECM, molecules on the surface of cells in the environment and diffusible factors such as growth factors and cytokines. The extent and success of regeneration will therefore depend on the balance between permissive and inhibitory cues (reviewed by Goodman, 1996).

N-cadherin is a transmembrane glycoprotein containing 5 cadherin domains mediating Ca^{2+}-dependent homophilic interaction. N-cadherin interacts intracellularly with α- and β-catenins which in turn interact with the actin cytoskeleton (reviewed by Tepass et al. 2000). N-cadherin is highly expressed by Schwann cell precursors (SCPs) during embryonic nerve development with intense expression being seen at the regeneration front of the developing nerve, however the expression diminishes as SCPs differentiate into mature Schwann cells and as axons reach their target organs (Wanner et al. 2006). This down-regulation appears to coincide with architectural changes in the maturing nerve including increased connective tissue, blood vessel infiltration and the appearance of Schwann cell basal lamina (Wanner & Wood, 2002; Wanner et al. 2006). N-cadherin expression is up-regulated following peripheral nerve injury (Shibuya et al. 1995; Squitti et al. 1999; Thornton et al. 2005). This probably reflects the increased presence of dedifferentiated and immature Schwann cells associated with peripheral nerve regeneration (Mirsky & Jessen 1999). N-cadherin expression is increased during regeneration at axons-Schwann cell interfaces but

is not expressed at points where axons and the basal lamina are in contact (Shibuya et al. 1995).

Neural cell adhesion molecule (NCAM) is a calcium-independent CAM and is comprised of 5 Ig modules and 2 fibronectin type III homology regions (Crossen & Krushel, 2000). Alternative splicing produces a large number of isoforms varying between 120 and 180kDa. NCAM-180 has large cytoplasmic extensions which bind to cytoskeletal proteins. NCAM can contain PSA (polysialic acid) which is highly expressed during development but whose expression diminishes with maturation (Rutishauser & Landmesser, 1996). Neurite extension on NCAM *vs*. NCAM-PSA substrata *in vitro* shows up to 80% increased growth on NCAM-PSA substrata (Doherty et al. 1992). Loss of PSA with maturation in the CNS appears to be associated with the less permissive environment of the CNS to regeneration following injury. The multidomain structure of NCAM leads to multiple binding sites. The extracellular region of NCAM hence mediates homophilic and heterophilic *cis* and *trans* interactions. NCAM is involved in heterophilic binding with heparin sulphate proetoglycans, chondroitin sulphate proteoglycans, laminin, the FGF receptor, integrins and the L1-CAM. NCAM is expressed by small unmyelinated fibres and non-myelinating Schwann cells (Le Forestier et al. 1993). NCAM is believed to be involved axonal network formation in the developing nervous system and is actively expressed in areas undergoing plasticity (e.g. the neurohypophysial system) in the adult brain (Aubert et al. 1998) or the paranodal areas of peripheral nerve (Rios et al. 2000). The addition of soluble forms of NCAM to Schwann cell cultures promotes cell migration, indicating that homophilic binding is likely to play an

important role in the interaction between axons and Schwann cells following injury (Thomaidou et al. 2001), however the addition of antibodies to NCAM has been shown to have little inhibitory effect on neurite extension (Bixby et al. 1988). Following injury NCAM levels rise in the immediate zone of injury, in the dorsal root ganglia and anterior horn of the spinal cord, and at the neuromuscular junction of denervated muscle (Daniloff et al. 1986; Saito et al. 2005). Tacke and Martini (1990) have shown that NCAM mRNA expression increases in the distal stump 2-3 weeks following transection. Thorton et al. (2007) have found that the administration of neurotrophins to the site of a peripheral nerve axotomy effect NCAM and N-cad expression at the proximal stump and that this coincides with an increase of respective mRNA expression in dorsal root ganglia. Following peripheral nerve injury myelinating Schwann cells dedifferentiate and start to express NCAM (Martini & Schachner, 1988). Saito et al. (2005) found that NCAM expression was initially high after transection but had fallen after 7 days.

Regenerating axons use adhesion molecules to navigate through the ECM and to extend along the Schwann cell column during regeneration. The experiment described aimed to investigate the expression of NCAM and N-cadherin at the regeneration front of regenerating nerves within bio-engineered polyhydroxybutyrate (PHB) nerve conduits pre-coated with either laminin, fibronectin or collagen. Quantitative assessment of CAM expression was performed using fluorescent immunohistochemical techniques previously optimised in our laboratory (Thornton et al. 2005). The expression levels were correlated with the regeneration distances measured in these nerve grafts (cf. chapter 6).

7.2 Materials and Methods

In chapter 6 axonal and Schwann cell regeneration through nerve conduits containing PHB fibres coated with extracellular matrix macromolecules and seeded with cultured Schwann cells was measured at 2 weeks following axotomy and grafting. Using the same tissue from this previous experiment, further sections were collected and subjected to immunofluorescent histochemical analysis to quantify the expression of NCAM and N-cadherin in the 4 experimental groups. The groups (n=5) were constructed as follows:

Group 1: Control (uncoated fibres)

Group 2: Laminin-coated fibres ($2\mu g/cm^2$)

Group 3: Fibronectin-coated fibres ($2\mu g/cm^2$)

Group 4: Collagen-coated fibres ($5\mu g/cm^2$)

7.2.1 *In vivo* expression of NCAM and N-cadherin

Nerve-conduit constructs were harvested, processed and cryosectioned as described in section 2.12.1. Nerves were immunostained to detect NCAM and N-cadherin expression (cf. 2.13.1). NCAM and N-cadherin expression was quantified at the proximal stump, regeneration front and distal stump using Image-Pro Plus image analysis software (Media Cybernetics, UK) as described in 2.14.2. NCAM and N-cadherin expression was quantified as intensity/unit area in arbitrary units (Thornton et al. 2005). Statistical analysis was performed using Sigmastat® software (SPSS Science, USA). Kruskal-Wallis one-way ANOVA on ranks was used to analyse the median values of intensity/ unit area of adhesion molecule expression in the proximal stump, regeneration front and distal stump. Experimental and control groups were compared using Dunn's multiple comparisons test.

7.2.2 Quantification of NCAM and N-cadherin expression

NCAM and N-cadherin expression was quantified as intensity of staining per unit area. All images were taken in monochrome to minimise loss of signal. Images were taken within 48 hours of staining to minimise decay. Exposure of each section to fluorescent light was kept to an absolute minimum to prevent photo bleaching. At a set distance from the tip of the regenerating front images were captured at the regeneration front, proximal stump and distal stump (Figures 2.24 and 2.25). The image capture region corresponding to the regeneration front was a point 2mm from the most distal regenerating fibre (as determined by co-staining with S100) and that corresponding with the proximal stump was 4mm from the

most distal regenerating fibre. The distal stump capture area was a point 2mm from the distal stump axotomy.

7.3 Results

7.3.1 NCAM expression

The expression of NCAM was examined at the proximal stump (PS), regeneration front (RF) and distal stump (DS) within each group to identify a trend in the expression across the nerve construct, and between each experimental group at each point (PS, RF, DS) to identify the effect of the addition of ECMMs on NCAM expression.

Within each group there was a generalised reduction in the mean and median values of NCAM expression between the PS and the RF, and between the RF and the DS (Figure 7.2). In all groups the reduction in expression between the PS and DS was significant. There was a significant reduction between the PS and the RF in the control and fibronectin groups. There were no significant differences between the RF and DS in any of the groups.

On looking at the variation of NCAM expression at the PS between each group (Figure 7.2) there was a significant increase in the median values in the laminin and fibronectin groups in comparison with the control group but not with the collagen group. This is consistent with the increased PGP and S100 regeneration distances seen in these groups (cf. chapter 6). At the RF there was a significant increase in the range of NCAM expression in the laminin group in comparison with the control and fibronectin groups, although the median value of NCAM expression in the laminin group was comparable with these groups the

mean value was increased (Figure 7.2). There were no significant differences in NCAM expression between each group at the distal stump.

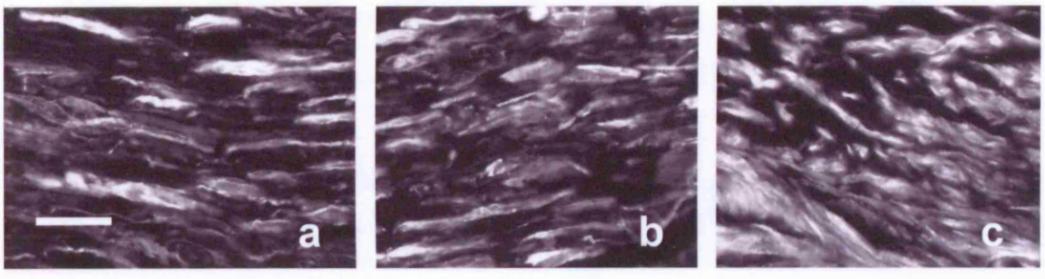

Figure 7.1 NCAM staining at the proximal stump (a,), regeneration front (b) and distal stump (c). All images are X40 magnification. Scale bar = 50μm.

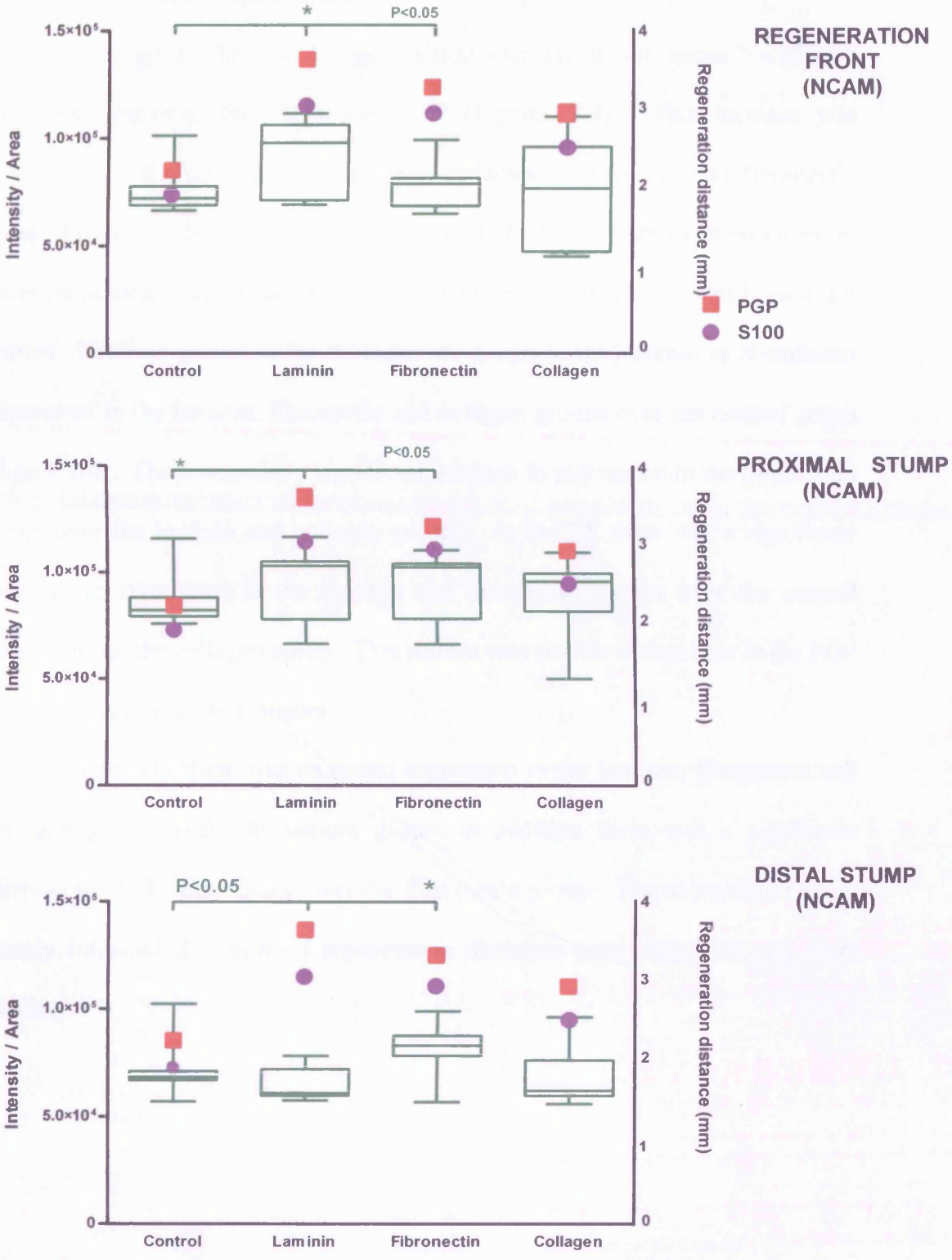

Figure 7.2 NCAM expression (mean ± s.d.) at the regeneration front, proximal stump and distal stump in each experimental group. PGP and S100 regeneration distances (mean values; cf. chapter 6) superimposed for comparison.

7.3.2 N-cadherin expression

Within each group there was a generalised increase in the mean N-cadherin expression between the PS and the RF (Figures 7.4). This increase was significant in the control, laminin (most pronounced increase) and fibronectin groups but not in the collagen group. Between the RF and DS there was a slight decrease in mean and median N-cadherin expression in the control and fibronectin groups. Between groups at the PS there was a significant increase in N-cadherin expression in the laminin, fibronectin and collagen groups over the control group (Figure 7.4). There was also a significant increase in expression in the fibronectin group over the laminin and collagen groups. At the RF there was a significant increase in expression in the laminin and fibronectin groups over the control group but not the collagen group. This pattern was similar to that seen in the PGP and S100 regeneration distances.

At the DS there was increased expression in the laminin, fibronectin and collagen groups over the control group, in addition there was a significant increase in the laminin group over the fibronectin group. The expression pattern closely followed the order of regeneration distances seen with PGP and S100 staining.

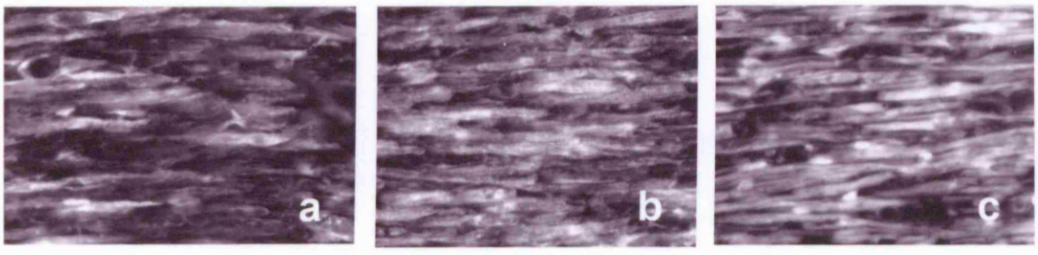

Figure 7.3 N-cad staining at the proximal stump (**a**), regeneration front (**b**) and distal stump (**c**). All images are X40 magnification.

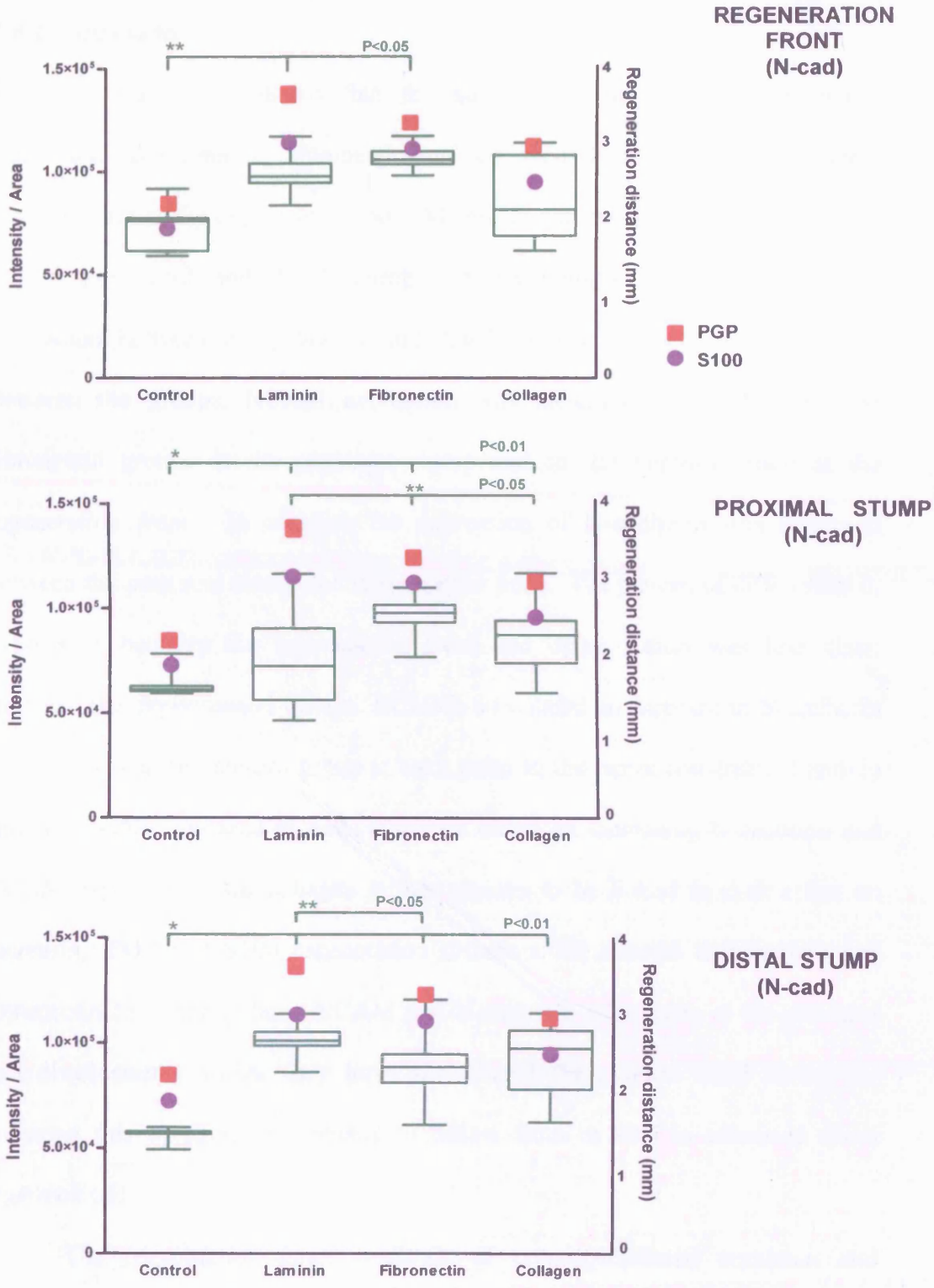

Figure 7.4 N-cad expression (median ± 25-75 percentile range) at the regeneration front, proximal stump and distal stump in each experimental group. PGP and S100 regeneration distances (mean values; cf. chapter 6) superimposed.

7.4 Discussion

This experiment has shown that the addition of the extracellular matrix macromolecules laminin, fibronectin and collagen to a bioengineered nerve construct effects the expression of NCAM and N-cadherin on the proximal stump, regeneration front and distal stump. A generalised reduction in NCAM expression between the proximal and distal stumps was seen in all groups. Between the groups, NCAM expression was increased in the laminin and fibronectin groups at the proximal stump and in the laminin group at the regeneration front. In contrast, the expression of N-cadherin was increased between the proximal stump and regeneration front. The pattern of differences in expression between the regeneration front and distal stump was less clear. Between the experimental groups, ECMMs stimulated an increase in N-cadherin expression over the control group at each point in the nerve construct. Laminin and fibronectin appeared to have a greater effect on increasing N-cadherin and NCAM expression than collagen which appears to be linked to their effect on increasing PGP and S100 regeneration distances. It appears that laminin and fibronectin have upregulated NCAM and N-cadherin expression at the proximal and distal stump, whilst they have not altered the general trend across the construct this upregulation appears to follow from or lead to enhanced nerve regeneration.

The regeneration front responds to contact-mediated attraction and repulsion (physical cues from tissue architecture) and chemo-attraction and chemo-repulsion (from growth factors and cytokines). This experiment has attempted to synthesize an environment containing physical and molecular cues

within a nerve conduit which may promote nerve regeneration. Poly-hydroxybutyrate fibres have been used within the conduit to act as a scaffold along which axons may regenerate, this scaffold has been supplemented with extracellular matrix macromolecules to provide molecular cues to encourage regeneration (cf. chapter 6). Neurite outgrowth triggered by extracellular matrix macromolecules (ECMMs) is a result of both modulation of cell surface adhesion to the ECM and activation of cell surface receptors initiating intracellular signalling cascades. Increased expression of N-cadherin in the regeneration front of axons exposed to ECMMs indicates either a secondary response to regeneration or activation by shared common messenger systems (reviewed by Maness & Schachner, 2007).

The coating of substrata with ECMMs has been shown to enhance neurite outgrowth *in vitro* (Niere et al. 2005) and stimulates SC proliferation (cf. chapter 6). Similarly, substrata containing synthesized CAMs support cell adhesion, migration and neurite outgrowth (Feri et al. 1992). *In vitro* studies have shown that as a substrata, laminin is superior to L1 (Niere et al. 2005), however laminin is a complex macromolecule that will potentiate other cell types which may not be necessarily beneficial for nerve regeneration (e.g. fibroblasts), laminin may also be difficult to manufacture in a form of sufficient quality for bio-engineered nerve constructs. In contrast, CAMs can be manufactured using recombinant technology, are highly nerve specific and therefore would be an appropriate alternative to ECMMs. Nerve conduits coated with the L1-CAM have demonstrated increased regeneration (Xu et al. 2004).

A traditional view of CAMs is that cell-cell and cell-matrix interactions mediated by these molecules establish a physical anchorage of these cells to their environment necessary for proliferation, growth and migration of cells. It is now established that CAMs can initiate intracellular signalling cascades (Kamiguchi & Lemmon, 2001). Adhesion and signalling therefore seem to be mutually interdependent. All NCAM isoforms can mediate *cis*-, *trans*-, homo-, and heterophilic interactions (Kiss et al. 2001) with NCAM interactions at the cell surface activating intracellular signalling cascades (reviewed by Manness and Schachner, 2007).

The method incorporated to quantify NCAM and N-cadherin expression is novel and subject to a number of factors which can adversely influence the results. The protocol for tissue collection, staining, image capture and quantification was previously developed and optimised in our laboratory by Thornton et al. (2005). Whilst it has been shown that immunoflorescent histochemical techniques can be successfully used to assess CAM expression both qualitatively and quantitatively, they are not sufficient on their own. Thornton et al. 2007 confirmed that NCAM, N-cadherin and L1 mRNA expression follows a similar pattern to that seen at the proximal stump following neurotrophin delivery at the site of an axotomy. Indicating a retrograde passage of neurotrophin and possibly anterograde delivery of cell adhesion molecule mRNA to the regeneration front.

Chapter 8

General Discussion

Engineering the ideal nerve graft requires optimisation of the key elements of the construct i.e. the conduit, the matrix, transplanted cells and/or growth factors. It is envisaged that ultimately an 'off-the-shelf' graft will be available in specialist centres for the reconstruction of peripheral nerve injuries. The ideal conduit material must be practical for use in the clinical setting, non-immunogenic, and biodegradable, however this may not be an absolute pre-requisite if its persistence does not interfere with function. Poly-hydroxy-butyrate (PHB) appears to satisfy most of these requirements when used in our animal model. A limited clinical evaluation in the human has been performed with sheets of PHB being used as a 'wrap around' repair around injured nerves. The number of patients recruited has been small as numerous criteria must be met before entry into the study, however initial results have not revealed any significant problems with rejection of PHB or detriment in recovery in comparison with patients treated with direct apposition of nerve stumps.

An additional structural component of the nerve graft of importance is the matrix within the conduit. The matrix provides signal inputs from the extracellular space and not only supports transplanted cells and growth factors but also provides mechanical cues which aid axonal growth. It has been shown that the matrix can influence axonal growth and the expression of cell adhesion molecules at the regeneration front. The complex molecular events occurring at the regeneration front during regeneration are slowly coming to light (reviewed by Maness & Schachner, 2007) and it is undoubted that understanding these events will lead to the design of more sophisticated matrices capable of supporting sustained regeneration.

The goal of augmenting peripheral nerve regeneration is to enhance the speed of regeneration so that target organs can be re-innervated before permanent atrophic changes develop. The source of this support may either be derived from the addition of growth factors, SCs or stem cells. Cellular transplants may be genetically engineered to act a platform for the increased production of growth factors. Alternatively genetic constructs may be delivered directly to the site of injury which, following uptake by local cells lead to the temporary production of growth factors. SCs are the ideal cell to transplant into a nerve conduit however their harvesting and culture is time-consuming and impractical for the acute clinical setting. Results involving marrow stromal cells have been encouraging; these cells are accessible, abundant and relatively easy to culture. The future may involve harvesting and separation of these cells for transplantation at the time of nerve repair or banks of tissue-typed cells may be made available for immediate transplantation. The possibility of bone marrow stromal cells as an alternative cellular transplant to Schwann cells is receiving concentrated attention. Initial evidence of trans-differentiation towards a SC lineage and a beneficial effect following transplantation (Tohill et al. 2004) has been corroborated by a number of studies. These include studies of morphological and phenotypical differentiation (Caddick et al. 2006) and studies assessing regeneration following transplantation in a rat model (Mimura et al. 2004; Keilhoff et al. 2006) and in a primate model (Hu et al. 2007). It is likely that SC harvesting, culturing, and transplantation will cease to be seen as a practical therapeutic tool but as a control against which MSC trans-differentiation and transplantation will assessed.

Histological examination will always remain an important part of assessing regeneration. As research focuses on cellular transplantation it is important that these cells can be tracked to evaluate their survival and integration. Fluorescent protein technology has great potential for the study of bio-engineered cellular systems. Developments have been aimed at producing a range of spectrally distinct fluorescent proteins to allow simultaneous multicolour tracking of separate genes, fusion proteins or labelled cells. Mutants of GFP are now available with enhanced fluorescence (EGFP) and emission spectra corresponding to blue (BFP), cyan (CYP) and yellow light (YFP) (Zimmer, 2002). The discovery of DsRed, a red fluorescent protein cloned from *Discosoma* coral significantly improves multicolour tracking due its much longer emission maxima of 558 and 583nm (Matz et al. 1999). Such a red-shift in emission spectra in comparison with GFP (509nm) not only improves spectral separation from autofluorescence and other fluorescent proteins but the longer wavelength also aids tissue penetration (Baird et al. 2000). More than 25 fluorescent proteins have been isolated from different marine organisms (Labas et al. 2002; Labas et al. 2002). These technologies have far-reaching applications for the study of bio-engineered nerve grafts. For example, cells could be labelled with one fluorescent protein for cell tracking following transplantation whilst secondary proteins could be tagged to a particular growth factor(s) enabling the measurement of gene expression within transplanted cells. New developments in imaging (Lippincourt-Schwartz & Patterson, 2003) will allow real time study of intracellular protein traffic *in vitro* revealing new insights into the complexities of Schwann cell-neuronal interactions and variations in gene regulation induced by growth factors.

This approach would therefore simplify the complex process of *in-situ* hybridisation or northern blotting for measuring gene expression. Whilst a number of studies have described the use of viral-based transduction for labelling SCs with GFP (Tohill et al. 2004; Bachelin et al. 2005; Schaal et al. 2007) the development of transgenic animals expressing GFP (Radtke et al. 2005) will simplify transplantation studies.

The experiments described in this thesis used a 2 week time point to assess regeneration activity with the exception of the experiment described in Chapter 6 which involved a 14 week time point. The aims of many studies related to peripheral nerve regeneration are to assess the ability of novel techniques to enhance regeneration but also to answer questions relating to the pathophysiology of nerve injury and regeneration. To assess the effect of an adjuvant treatment on the active regeneration front we have found that a 2 week time point is optimal because at this time the regeneration front is usually midway through a 1cm conduit. This allows the determination of the quality and quantity of regeneration, the expression of molecules known to play an important role in nerve regeneration and the integration of transplanted cells within the regenerating front. Indirect comparative analysis is also possible with previous studies from our laboratory incorporating the same model and time points (Mosahebi et al. 2001). The aims of experiments utilising longer time points have different objectives in that there is greater emphasis on defining the advantage conferred on functional outcome following axotomy and repair. The ideal assessment of regeneration involves a combination of qualitative and quantitative histological analysis correlated to measurements of functional outcome. Measurements of functional outcome

involve relatively simplistic parameters such as wet muscle weights, unreliable assessments e.g. walking track patterns, and the gold standard - measurements of neuro- and myophysiological function. Long time points are necessary when assessing functional outcome to allow time for regenerating axons to re-innervate their end organs, i.e. muscle and skin.

Long term animal experiments are expensive, it is therefore important that experiments planned for these studies are based on sound preliminary findings that justify initiating a full study. A preliminary study was performed to assess regeneration at a 2 month time point involving SC transplantation within a 1cm PHB or silicone conduit grafted into the rat sciatic nerve. Dissociated PHB fibres (cf. Chapter 7) or collagen gel was used as a matrix to support transplanted cells (cf. 2.8-2.10; 2.11.3). In collaboration with Miss Jenny Caddick (Blond McIndoe Laboratories) regeneration was determined via immunohistochemical techniques to determine S100 (Schwann cell) and PGP9.5 (axonal) staining at the proximal, middle and distal areas within the nerve conduit (cf. 2.13.1). Semithin sections from the distal stump were also examined to determine the degree of successful cross-over regeneration (cf. 2.12.2). It is not technically possible to cut and immunostain longitudinal sections of silicone conduits due to the nature of the material, therefore to assess regeneration semithin sections of the distal stump were used alone in these groups.

The study was limited as there was a higher than expected rate of autophagy of denervated limbs, this is a recognised complication of experiments involving axotomy of the sciatic nerve in the rat. It was necessary to perform premature termination of these animals to prevent undue suffering. This limited

animal numbers and therefore made the interpretation of results difficult. Regeneration in the distal stump was found to be better in nerves grafted with silicone conduits in comparison with those grafted with PHB conduits. This may be due to the impervious nature of silicone providing an enclosed environment which concentrates local growth factors and molecules responsible for stimulating regeneration. A surprising finding was that conduits containing transplanted SCs displayed reduced regeneration in comparison to those without SCs. As the numbers in these groups were small (n=3) these findings must be interpreted with caution as they may either represent natural variation within the group or they may be due to an unexpected adverse effect of transplanted SCs over long periods of time. This may be due to an immune reaction as although the cells were all derived from the same inbred strain complete allogenicity cannot be guaranteed. It is also possible that there has been an adverse interaction between the collagen matrix (Vitrogen) and the transplanted SCs as detailed study of the vitality and viability of these cells within this gelled matrix were not performed *in vitro*. There is also the possibility that there was a technical error in SC preparation and transplantation at the time of grafting. It has therefore not been possible to draw an accurate conclusion from this preliminary long term experiment, further refinement of the model is necessary to optimise the conduit, matrix and cellular transplantation.

Successful nerve regeneration depends on the intrinsic growth capacity of the peripheral nervous system in addition to the permissive environment of the peripheral nerve (in comparison with the central nervous system). Peripheral

nerve has the ability to regenerate however this is frequently ineffectual in the clinical setting. Further understanding of the pathophysiology of degeneration and regeneration, in addition to advances in conduit and matrix technology, growth factor delivery and stem cell biology will lead to advances in the treatment of peripheral nerve injury.

BIBLIOGRAPHY

Afting M, Stock UA, Nasseri B, Pomerantseva MD, Seed B, Vacanti JP. Efficient and stable retroviral transfection of ovine endothelial cells with green fluorescent protein for cardiovascular tissue engineering. *Tissue Engineering* 2003;**9**:137-41.

Ahmed Z, Brown RA. Adhesion, alignment, and migration of cultured Schwann cells on ultrathin fibronectin fibres. *Cell Motility and the Cytoskeleton* 1999;**42**:331-43.

Akahori Y, Horie H. IGF-1 enhances neurite regeneration but is not required for its survival in adult DRG explant. *Neuroreport* 1997;**8**:2265-9.

Akiyama Y, Radtke C, Honmou O, Kocsis JD. Remyelination of the Spinal Cord Following Intravenous Delivery of Bone Marrow Cells. *GLIA* 2002;**39**:229-36.

Alison MR, Poulsom R, Forbes S, Wright NA. An introduction to stem cells. *Journal of Pathology* 2002;**197**:419-23.

Anderson DJ, Gage FH, Weissman IL. Can stem cells cross lineage boundaries? *Nature* 2001;**7**:393-5.

Andree C, Voigt M, Wenger A, Erichsen T, Bittner K, Schaefer D *et al.* Plasmid gene delivery to human keratinocytes through a fibrin-mediated transfection system. *Tissue Engineering* 2003;**7**:757-66.

Aphergis P, Johnson IP, Cannon J, Yang SY, Goldspink G. Different levels of neuroprotection by two insulin-like growth factor-I splice variants. *Brain Research* 2004;**1009**:213-8.

Artavanis-Tsakonas S, Rand MD, Lake RJ. Notch signalling: Cell fate control and signal integration in development. *Science* 1999;**284**:770-6.

Aubert J, Ridet JL, Schachner M, Rougan G, Gage FH. Expression of L1 and PSA during sprouting and regeneration in the adult hippocampal formation. *Journal of Comparative Neurology* 1998;**399**:1-19.

Azizi SA, Stokes D, Augelli BJ, DiGirolamo C, Prockop DJ. Engraftment and migration of human bone marrow stromal cells implanted in the brains of albino rats-similarities to astrocyte grafts. *Proceedings of the National Academy of Sciences* 1998;**95**:3908-13.

Bachelin C, Lachapelle F, Girard C, Moissonnier P, Suerguera-Lagache C, Mallet J *et al.* Efficient myelin repair in the macaque spinal cord by autologous grafts of Schwann cells. *Brain* 2005;**128**:540-9.

Bailey SB, Eichler ME, Villadiego A, Rich KM. The influence of fibronectin and laminin during Schwann cell migration and peripheral nerve regeneration through silicone chambers. *Journal of Neurocytology* 1993;**22**:176-84.

Baird GS, Zacharias DA, Tsien RY. Biochemistry, mutagenesis, and oligomerization of DsRed, a red fluorecent protein from coral. *Proceedings of the National Academy of Sciences* 2000;**97**:11984-9.

Barbash IM, Chouraqui P, Baron J, Feinberg MS, Etzion S, Tessone A *et al.* Systemic delivery of bone-marrow derived mesenchymal stem cells to the infarcted myocardium. *Circulation* 2003;**108**:863-8.

Baron-Von Evercooren A, Kleinman HK, Seppa HE, Rentier B, Dubois-Dalcq M. Fibronectin promotes rat Schwann cell growth and motility. *Journal of Cell Biology* 1982;**93**:211.

Bartholomew A. Mesenchymal stem cells suppress lymphocyte proliferation in vitro and prolong skin graft survival in vivo. *Experimental Haematology* 2002;**30**:42-8.

Bartholomew A, Patil S, Mackay A, Nelson M, Buyaner D, Hardy W *et al.* Baboon mesenchymal stem cells can be genetically modified to secrete human erythropoietin in vivo. *Human Gene Therapy* 2001;**12**:1527-41.

Beresford JN, Bennett JH, Devlin C, Leboy PS, Owen ME. Evidence for an inverse relationship between the differentiation of adipocytic and osteogenic cells in rat marrow stromal cell cultures. *Journal of Cell Science* 1992;**102**:341-51.

Bianco P, Riminucci M, Gronthos S, Gehron Robey P. Bone marrow stromal stem cells: nature, biology, and potential applications. *Stem Cells* 2001;**19**:180-92.

Billinton N, Knight AW. Seeing the wood through the trees: a review of techniques for distinguishing green fluorescent protein from endogenous autofluorescence. [Review] [119 refs]. *Anal.Biochem.* 2001;**291**:175-97.

Bixby JL, Harris WA. Molecular mechanism of axon growth and guidance. *Annual Review of Cell Biology* 1991;**7**:117-59.

Bixby JL, Jhablava P. Extracellular matrix molecules and cell adhesion molecules induce neurites through different mechanisms. *Journal of Cell Biology* 1990;**111**:2725-32.

Bixby JL, Lilien J, Reichardt LF. Identification of the major proteins that promote neuronal process outgrowth on Schwann cells in vitro. *The Journal of Cell Biology* 1988;**107**:353-61.

Bokman SH, Ward WW. Renaturation of *Aequorea* green fluorecent protein. *Biochemical and Biophysical Research Communications* 1981;**101**:1372-80.

Brandt KE, Mackinnon SE. Microsurgical repair of peripheral nerve injuries and nerve grafts. In Aston SJ, Beasley RW, Thorne CH, eds. *Grabb and Smith's Plastic Surgery*, pp 79-89. Philadelphia: Lippincott-Raven, 1997.

Braunewell KH, Pesheva P, McCarthy JB, Furcht LT, Schmitz B, Schachner M. Functional involvement of sciatic nerve-derived versican- and decorin-like molecules and other chondroitin sulphate proteoglycans in ECM-mediated cell adhesion and neurite outgrowth. *European Journal of Neuroscience* 1995;**7**:805-14.

Brockes JP, Fields KL, Raff MC. Studies on cultured rat Schwann cells. I. Establishment of purified populations from cultures of peripheral nerve. *Brain Research* 1979;**165**:105-18.

Brockes JP, Lemke GE, Balzer DR, Jr. Purification and preliminary characterization of a glial growth factor from the bovine pituitary. *Journal of Biological Chemistry* 1980;**255**:8374-7.

Bunge RP. Expanding roles for the Schwann cell: ensheathment, myelination, trophism and regeneration. *Current Opinion in Neurobiology* 1993;**3**:805-9.

Burgess A, Weng YQ, Ypsilanti AR, Cui X, Caines G, Aubert I. Polysialic acid limits septal neurite outgrowth on laminin. *Brain Research* 2007;**1144**:52-8.

Caddick J, Kingham PJ, Gardiner NJ, Wiberg M, Terenghi G. Phenotypical and functional characteristics of mesenchymal stem cells differentiated along a Schwann cell lineage. *GLIA* 2006;**54**:840-9.

Caplan AI. Mesenchymal stem cells. *Journal of Orthopaedic Research* 1991;**9**:641-50.

Caplan AI. The mesengenic process. *Clinical Plastic Surgery* 1994;**21**:429-35.

Caroni C, Grandes P. Nerve sprouting in innervated adult skeletal muscle induced by exposure to elevated levels of insulin-like growth factors. *Journal of Cell Biology* 1990;**110**:1307-17.

Chalfie M, Euskirchen G, Ward WW, Prasher DC. Green fluorescent protein as a marker for gene expression. *Science* 1994;**263**:802-5.

Chamberlain LJ, Yannus IV, Hsu H-P, Strichartz G, Spector M. Collagen-GAG substrate enhances the quality of nerve regeneration through collagen tubes up to level of autograft. *Experimental Neurology* 1998;**154**:315-29.

Chang A, Yannas IV, Perutz S, Loree H, Sethi RR, Krarup C *et al.* Electrophysiological study of recovery of peripheral nerves regenerated by a collagen-glycosaminoglycan copolymer matrix. In Gebelein CG, Dunn RL, eds. *Progress in Biomedical Polymers*, pp 107-19. New York: Plenum Press, 1990.

Cheng H-L, Feldman EL. Insulin-like growth factor-I (IGF-I) and IGF binding protein-5 in Schwann cell differentiation. *Journal of Cell Physiology* 1997;**171**:161-7.

Cheng H-L, Randolph A, Yee D, Delafontaine P, Tennekoon G, Feldman EL. Characterization of Insulin-Like Growth Factor-I and Its Receptor and Binding Proteins in Transected Nerves and Cultured Schwann Cells. *Journal of Neurochemistry* 1996;**66**:525-36.

Chernousov MA, Carey DJ. Schwann cell extracellular matrix molecules and their receptors. *Histology and Histopathology* 2000;**15**:593-601.

Chernousov MA, Scherer SS, Stall RC, Carey DJ. p200, a collagen secreted by Schwann cells, is expressed in developing nerves and in adult nerves following axotomy. *Journal of Neuroscience Research* 1999;**56**:284-94.

Conget PA, Minguell JJ. Phenotypical and functional properties of human bone marrow mesenchymal progenitor cells. *Journal of Cell Physiology* 1999;**181**:67-73.

Cornbrooks CJ, Carey DJ, McDonald JA, Timpl R, Bunge RP. *In vivo* and *in vitro* observations on laminin production by Schwann cells. *Proceedings of the National Academy of Sciences* 1983;**80**:3850-4.

Crossen KL, Krushel LA. Cellular signalling by neural cell adhesion molecules. *Developmental Dynamics* 2000;**218**:260-79.

Cubitt AB, Heimm R, Adams SR, Boyd AE, Gross LA, Tsien RY. Understanding, improving and using green fluorescent proteins. *TIBS* 1995;**20**:448-55.

Cubitt AB, Woollenweber LA, Heim R. Understanding structure-function relationships in the Aequorea victoria green fluorescent protein. [Review] [37 refs]. *Methods Cell Biol.* 1999;**58**:19-30.

Cuevas P, Carceller F, Dujovny M, Garcia-Gomez I, Cuevas B, Gonzalez-Corrochan R *et al.* Peripheral nerve regeneration by bone marrow stromal cells. *Neurological Research* 2002;**24**:634-8.

Daniloff JK, Levi G, Grumet M, Rieger F, Edelman GM. Altered expression of neuronal cell adhesion molecules induced by nerve injury and repair. *The Journal of Cell Biology* 1986;**103**:929-45.

de Pablo F, de la Rosa EJ. The developing CNS: a scenario for the action of proinsulin, insulin and insulin-like growth factors. *Trends in Neuroscience* 1995;**18**:143-50.

Deans RJ, Moseley AB. Mesenchymal stem cells: biology and potential clinical uses. *Experimental Haematology* 2000;**28**:875-84.

Dezawa M, Takahashi I, Esaki M, Takano M, Sawada H. Sciatic nerve regeneration in rats induced by transplantation of *in-vitro* differentiated bone marrow stromal cells. *European Journal of Neuroscience* 2001;**14**:1771-6.

Doherty P, Moolenaar C, Ashton SV, Michalides R, Walsh FS. The VASE exon downregulates the neurite growth-promoting activity of NCAM140. *Nature* 1992;**356**:791-3.

Doherty P, Walsh FS. Cell adhesion molecules, second messengers and axonal growth. *Current Opinion in Neurobiology* 1992;**2**:595-601.

Donovan PJ, Gearhart J. The end of the beginning for pluripotent stem cells. *Nature* 2001;**414**:92-7.

Duvivier-Kali VF, Omer A, Parent RJ, O'Neill JJ, Weir GC. Complete protection of islets against allorejection and autoimmunity by a simple barium-alginate membrane. *Diabetes* 2001;**50**:1698-705.

Erlanger J, Gasser HS. The compound nature of the action current of nerves as disclosed by the cathode ray oscillograph. *American Journal of Physiology* 1924;**70**:624.

Evans GRD. Peripheral Nerve Injury: A Review and Approach to Tissue Engineered Constructs. *The Anatomical Record* 2001;**263**:396-404.

Feri T, vonBohlen und Halbach F, Willie W, Schachner M. Different extracellular domains of the neural cell adhesion molecule (N-CAM) are involved in different functions. *Journal of Cell Biology* 1992;**118**:177-94.

Ferrari F, DeCastro Rodrigues A., Malvezzi C.K., Dal Pai Silva M, Padovani CR. Inside-out vs. standard vein graft to repair a sensory nerve in rats. *Anatomical Record* 1999;**256**:227-32.

Ferrari G, Cusella-De Angelis G, Coletta M, Paolucci E, Storniuolo A, Cossu G *et al.* Muscle Regeneration by Bone Marrow-Derived Myogenic Progenitors. *Science* 1998;1528-30.

Freshney RI. Culture of animal cells: a manual of basic technique. Wiley-Liss, 2000.

Fu SY, Gordon T. The cellular and molecular basis of peripheral nerve regeneration. *Molecular Neurobiology* 1997;**14**:67-116.

Fuchs E, Segre JA. Stem cells: A New Lease on Life. *Cell* 2000;**100**:143-55.

Fujiwara S, Wiedemann H, Timpl R, Lustig A, Engel J. Structure and interactions of heparan sulfate proteoglycans from a mouse tumor basement membrane. *European Journal of Biochemistry* 1984;**143**:145-57.

Funakoshi H, Friesen J, Barbany G, Timmusk T, Zachirsson O, Verge VM. Differential expression of mRNA for neurotrophins and theri receptors after axotomy of the sciatic nerve. *Journal of Cell Biology* 1993;**123**:455-65.

Gatlin J, Melkus MW, Padgett A, Petroll WM, Cavanagh HD, Garcia JV *et al. In vivo* fluorescent labelling of corneal wound healing fibroblasts. *Experimental Eye Research* 2003;**76**:361-71.

Gentili C, Bianco P, Neri M, Malpeli M, Campanile G, Castagnola P *et al.* Cell proliferation, extracellular matrix mineralisation, and ovotransferrin transient expression during in vitro differentiation of chick hypertrophic chondrocytes into osteoblast-like cells. *Journal of Cell Biology* 1993;**122**:703-12.

Geuna S, Borrione P, Fornaro M, Giacobini-Robecchi MG. Neurogenesis and stem cells in adult mammalian dorsal root ganglia. *Anatomical Record* 2000;**261**:139-40.

Glasby MA, Gschmeissner SE, Huang CL, De Souza BA. Degenerated muscle grafts used for peripheral nerve repair in primates. *Journal of Hand Surgery - British Volume* 1986;**11**:347-51.

Gojo S, Gojo N, Mori T, Abe H, Kyo S, Hata J *et al.* In vivo cardiovasculogeneis by direct injection of isolated adult mesenchymal stem cells. *Experimental Cell Research* 2003;**288**:51-9.

Goldspink G. Changes in muscle mass and phenotype and the expression of autocrine and systemic growth factors by muscle in response to stretch and overload. *Journal of Anatomy* 1999;**194**:323-34.

Goodman CS. Mechanisms and molecules that control growth cone guidance. *Annual Review of Neuroscience* 1996;**19**:341-77.

Gravel C, Gõtz R, Lorrain A, Sendtner M. Adenoviral gene transfer of ciliary neurotrophic factor and brain-derived neurotrophic factor leads to long-term survival of axotomised motor neurons. *Nature Medicine* 1997;**3**:765-70.

Gritti A, Parati EA, Cova L, Frolichsthal P, Galli R, Wanke E *et al.* Multipotential stem cells from the adult mouse brain proliferate and self-renew in response to basic fibroblast growth factor. *Journal of Neuroscience* 1996;**16** :1091-100.

Gronthos S, Simmons PJ. The growth factor requirements of STRO-1-positive human bone marrow stromal precursors under serum-deprived conditions in vitro. *Blood* 1995;**85**:929-40.

Groves MJ, Christopherson T, Giometto B, Scaravilli F. Axotomy-induced apoptosis in adult rat primary sensory neurons. *Journal of Neurocytology* 1997;**26**:615-24.

Guenard V, Schweitzer B., Flechsig E., Hemmi S., Martini R., Suter U. Effective gene transfer of lacZ and P0 into Schwann cells of P0 deficient mice. *GLIA* 1999;**25**:165-78.

Guenard V, Kleitman N, Morrissey TK, Bunge RP, Aebischer P. Syngeneic Schwann cells derived from adult nerves seeded in semi-permeable guidance channels enhance peripheral nerve regeneration. *Journal of Neuroscience* 1992;**12**:3310-20.

Hainfellner JA, Voitlander T, Strobel T, Mazal PR, Madalena AS, Aguz A *et al.* Fibroblasts can express glial fibrillary acidic protein (GFAP) *in vivo*. *Journal of Neuropathology and Experimental Neurology* 2001;**60**:449-61.

Halfter W, Dong S, Schurer B, Cole GJ. Collagen XVIII is a basement membrane heparan sulphate proteoglycan. *Journal of Biological Chemistry* 1998;**273**:25404-12.

Hall S. The effect of inhibiting Schwann cell mitosis on the reinnervation of acellular autografts in the peripheral nervous system of the mouse. *Neuropathology and Applied Neurobiology* 1986;**12**:401-14.

Hall S. Observations on the progress of Wallerian degeneration in transected peripheral nerves of C57BL/Wld mice in the presence of recruited macrophages. *Journal of Neurocytology* 1993;**22**:480-90.

Hall S. Nerve repair: A neurobiologists view. *The Journal of Hand Surgery* 2001;**26B**:129-36.

Hameed M, Orrell RWCM, Goldspink G, Harridge SDR. Expression of IGF-1 splice variants in young and old human skeletal muscle after high resistance exercise. *Journal of Physiology* 2003;**547**:247-54.

Hansson H-A. Insulin like growth factors and nerve regeneration. *Annals of the New York Academy of Sciences* 1993;**692**:161-71.

Hart AM, Brannstorm T, Wiberg M, Terenghi G. Primary sensory neurons and satellite cells after peripheral axotomy in the adult rat: time course of cell death and elimination. *Experimental Brain Research* 2002;**142**:308-18.

Hazari A, Wiberg M, Johansson-Ruden G, Green C, Terenghi G. A resorbable nerve conduit as an alternative to nerve autograft in nerve gap repair. *British Journal of Plastic Surgery* 1999;**52**:653-7.

Heim R, Prasher DC, Tsien RY. *Proceedings of the National Academy of Sciences U.S.A.* 1994;**91**:12501-4.

Henderson ST, Gao D, Lambie EJ, Kimble J. lag-2 may encode a signalling ligand for the GLP-1 and LIN-12 receptors of C. elegans. *Development* 1994;**120**:2913-24.

Heumann R, Korshing S, Bandtlow C, Thoenen H. Changes of nerve growth factor synrthesis in non-neuronal cells in response to sciatic nerve transection. *Journal of Cell Biology* 1987;**104**:1623-31.

Hinks GL, Chari DM, O'Leary MT, Zhao HS, Keirstead HS, Blakemore WF *et al.* Depletion of endogenous oligodendrocyte progenitors rather than increased availability of survival factors is a likely explanation for enhanced survival of transplanted oligodendrocyte progenitors in X-irradiated compared to normal CNS. *Neuropathology and Applied Neurobiology* 2003;**27**:59-67.

Hofstetter CP, Schwarz EJ, Hess D, Widenfalk J, El Manira A, Prockop DJ *et al.* Marrow stromal cells form guiding strands in the injured spinal cord and promote recovery. *Proceedings of the National Academy of Sciences* 2002;**99**:2199-204.

Hori J, Ng TF, Shatos M, Klassen H, Streilein JW, Young MJ. Neural progenitor cells lack immunogenicity and resist destruction as allografts. *Stem Cells* 2003;**21**:405-16.

Hou SY, Zhang HY, Quan DP, Liu XL, Liu XL, Zhu JK. Tissue-engineered peripheral nerve grafting by differentiated bone marrow stromal cells. *Neuroscience* 2006;**140**:101-10.

Hu J, Zhu QT, Liu XL, Xu YB, Zhu JK. Repair of extended peripheral nerve lesions in Rhesus monkeys using acellular allogeneic nerve grafts implanted with autologous mesenchymal stem cells. *Experimental Neurology* 2007;**204**:658-66.

Ide C. Peripheral nerve regeneration. *Neuroscience Research* 1996;**25**:101-21.

Ikawa M, Yamada S, Nakanishi T, Okabe M. Green fluorescent protein (GFP) as a vital marker in mammals. [Review] [76 refs]. *Current Topics in Developmental Biology* 1999;**44**:1-20.

Inouye S, Tsuji F. Evidence for redox forms of the Aequorea green fluorescent protein. *FEBS Letters* 1994;**341**:277-80.

Ishii DS, Glazner GW, Whalen LR. Regulation of peripheral nerve regeneration by insulin-like growth factors. *Annals of the New York Academy of Sciences* 1993;**692**:172-82.

Iwashita Y, Crang A., Blakemore W. Redistribution of bisbenzimide Hoechst 33342 from transplanted cells to host cells. *Neuroreport* 2000;**11**:1013-6.

Jaakkola S, Savunen O, Halme T, Uitto J, Peltonen J. Basement memebranes during development of human nerve: Schwann cells and perineural cells display marked changes in their expression profiles for laminin subunits and beta 1 and beta 4 integrins. *Journal of Neurocytology* 1993;**22**:215-30.

Jacque CM, Suard IM, Collins VP, Raoul MM. Interspecies identification of astrocytes after intercerebral transplantation. *Developmental Neuroscience* 1986;**8**:142-9.

Jan YN, Jan LY. Asymmetric cell division. *Nature* 1998;**392**:775-8.

Jensen UB, Lowell S, Watt FM. The spatial relationship between stem cells and their progeny in the basal layer of human epidermis - a new view based on whole-mount labelling and lineage analysis. *Development* 1999;**126**:2409.

Jessen KR, Mirsky R. Schwann cells and their precursors emerge as major regulators of nerve development. *Trends in Neurosciences* 1999;**22**:402-10.

Jessen KR, Mirsky R, Morgan L. Myelinated, but not unmyelinated axons, reversibly downregulate in Schwann cells. *Journal of Neurocytology* 1987;**16**:681-8.

Jiang Y, Jahagirdar BN, Reinhardt RL, Schwartz RE, Keene CD, Ortiz-Gonzalez XR *et al.* Pluripotency of mesenchymal stem cells derived from adult marrow. *Nature* 2002; **418**:41-9.

Jockusch H, Voigt S, Eberhard D. Localisation of GFP in frozen sections: immobilization of a highly soluble marher protein by formaldehyde vapour. *Journal of Histochemistry Cytochemistry* 2003;**51**:401-4.

Kamiguchi H, Lemmon V. IgCAMs:bidirectional signals underlying neurite growth. *Current Opinion in Cellular Biology* 2001;**12**:598-605.

Kanje M, Skottner A, Sjoberg SA, Lundborg G. Insulin-like growth factor I (IGF-I) stimulates regeneration of the rat sciatic nerve. *Brain Research* 1989;**486**:396-8.

Kaplan DR, Hempstead BL, Martin-Zanca D, Chao M, Parad LF. The trk protooncogene product: a signal transducing receptor for nerve growth factor. *Science* 1991;**252**:554-8.

Kaspar BK, Erickson D, Schaffer D, Hinh L, Gage FH, Peterson DA. Targeted retrograde gene delivery for neuronal protection. *Molecular Therapeutics* 2002;**5**:50-6.

Kater SB, Mills LR. Regulation of growth cone behaviour by calcium. *Journal of Neuroscience* 1991;**11**:891-9.

Keilhoff G, Goihl A, Langnäse K, Fansa H, Wolf G. Transdifferentiation of mesenchymal stem cells into Schwann-like myelinating cells. *European Journal of Cell Biology* 2006;**85** :11-24.

Keilhoff G, Goihl A, Stang F, Wolf G, Fansa H. Peripheral nerve tissue engineering: autologous Schwann cells vs. transdifferentiated mesenchymal stem cells. *Tissue Engineering* 2006;**12**:1451-65.

Keilhoff G, Stang F, Goihl A, Wolf G, Fansa H. Transdifferentiated mesenchymal stem cells as alternative therapy in supporting nerve regeneration and myelination. *Cellular and Molecular Neurobiology* 2006;**26**:1235-52.

Kim BJ, Seo JH, Bubien JK, Young SO. Differentiation of adult bone marrow stem cells into neuroprogenitor cells in vitro. *Neuroreport* 2002;**13**:1185-8.

Kiryushko D, Berezin V, Bock E. Regulators of neurite outgrowth - role of cell adhesion molecules. *Annals of the New York Academy of Sciences* 2004;**1014**:140-54.

Kiss JZ, Troncoso E, Djebbarra Z, Vutskits L, Muller D. The role of neural cell adhesion molecules in plasticity and repair. *Brain Research* 2001;**36**:175-84.

Klein R, Lamballe F, Bryant S, Barbacid M. The trkB tyrosine protein kinase is a receptor for neurotrophin-4. *Neuron* 1992;**8**:947-56.

Kopan R, Nye JS, Weintraub H. The intracellular domain of mouse Notch: a constituitively activated repressor of myogenesis directed at the basic helix-loop-helix region of MyoD. *Development* 1994;**120**:2385-96.

Kopen GC, Prockop DJ, Phinney DG. Marrow stromal cells migrate throughout forebrain and cerebellum, and they differentiate into astrocytes after injection into neonatal mouse brains. *Proceedings of the National Academy of Sciences* 1999;**96**:10711-6.

Krekoski CA, Parhad IM, Clark AW. Attenuation and recovery of nerve growth factor receptor mRNA in dorsal root ganglion following recovery. *Journal of Neuroscience Research* 1996;**43**:1-11.

Kurek JB. Up-regulation of leukaemia inhibitory factor and interleukin-6 in transected sciatic nerve and muscle following denervation. *Neuromuscular disorders* 1996;**6**:105-14.

Labas YA, Gurskaya NG, Yanushevich YG, Fradkov AF, Lukyanov KA, Lukyanov SA *et al.* Diversity and evolution of the green fluorescent protein family. *Proceedings of the National Academy of Sciences* 2002;**99**:4256-61.

Lagasse E, Connors H, Al-Dhalimy M, Reitsma M, Dohse M, Osbourne L *et al.* Purified haematopoietic stem cells can differentiate into hepatocytes in vivo. *Nature* 2000;**6**:1229-34.

Lamballe F, Klein R, Barbacid M. trk C, a new member of the trk family of tyrosine protein kinases, is a receptor for neurotrophin-3. *Cell* 1991;**66**:967-79.

Le Douarin N. Glial cell lineages in the neural crest. *GLIA* 1991;**4**:175-84.

Letourneau PC, Condic ML, Snow DM. Interactions of developing neurons with the extracellular matrix. *Journal of Neuroscience* 1994;**14**:915-28.

Letourneau PC, Shattuck TA, Roche FK, Takeichi M, Lemmon V. Nerve growth cone migration onto Schwann cells involves the calcium-dependent adhesion molecule, N-cadherin. *Developmental Biology* 1990;**138**:430-42.

Levi AD, Guenard V, Aebischer P, Bunge RP. The functional characteristics of Schwann cells cultured from human peripheral nerve after transplantation into a gap within the rat sciatic nerve. *Journal of Neuroscience* 1994;**14**:1309-19.

Lippincourt-Schwartz J, Patterson GH. Development and use of fluorescent protein markers in living cells. *Science* 2003;**300**:87-91.

Ljungberg C, Novikov L, Kellerth J-O, Ebendal T, Wiberg M. The neurotrophins NGF and NT-3 reduce sensory neuronal loss in adult rat after peripheral nerve lesion. *Neuroscience Letters* 1999;**262**:29-32.

Loeffler M, Potten CS. Stem cells and cellular pedigrees - a conceptual introduction. *Stem Cells*, pp 1-27. Academic Press Ltd., 1997.

Lorenz WW, McCann RO, Longiaru M, Cormier MJ. Isolation and expression of cDNA encoding *Renilla reniformis* luciferase. *Proceedings of the National Academy of Sciences* 1991;**88**:4438-42.

Lumsden A, Cohen J. Axon guidance in the vertebrate central nervous system. *Current Opinion in Genetics and Development* 2004;**1**:230-5.

Lundborg G. The Nerve Trunk. In Lundborg G, ed. *Nerve Injury and Repair*, pp 32-63. New York: Churchill Livingstone, 1988.

Lundborg G, Dahlin LB, Danielson N, Nachemson AK. Tissue specificity in nerve regneration. *Scandinavian Journal of Plastic and Reconstructive Surgery* 1986;**20**:279-83.

Lundborg G, Gelberman RH, Longo FM, Powell HC, Varon S. In vivo regeneration of cut nerves encased in silicone tubes: growth across a six-millimeter gap. *Journal Neuropathology and Experimental Neurology.* 1982;**41**:412-22.

Mackinnon SE, Dellon AL. A comparison of nerve regeneration across a sural nerve graft a vascularized pseudosheath. *Journal of Hand Surgery - American Volume* 1988;**13**:935-432.

Mahanthappa NK, Anton ES, Matthew WD. Glial growth factor 2, a soluble neuregulin, directly increases Schwann cell motility and indirectly promotes neurite outgrowth. *Journal of Neuroscience* 1996;**16**:4673-83.

Maness LM, Kastin AJ, Weber JT, Banks WA, Beckman BS. The neurotrophins and their receptors: structure, function and neuropathology. *Neuroscience and Biobehavioural Review* 1994;**18**:143-59.

Maness P, Schachner M. Neural recognition molecules of the immunoglobulin superfamily:signalling transducers of axon guidance and neuronal migration. *Nature Neuroscience* 2007;**10**:19-26.

Marshak DR, Gottlieb D, Gardner RL. Introduction: Stem Cell Biology. *Stem Cell Biology*, pp 1-16. Cold Spring Harbor Laboratory Press, 2001.

Martini R. Expression and functional roles of neural cell surface molecules and extracellular matrix components during development and regeneration of peripheral nerves. *Journal of Neurocytology* 1994;1-28.

Martini R, Schachner M. Immunoelectron microscopic localisation of neural cell adhesion molecules (L1, NCAM and myelin-associated glycoprotein) in regenerating adult mouse sciatic nerve. *Journal of Cell Biology* 1988;**106**:1735-46.

Matsumoto K, Ohnishi K, Sekine T, Ueda H, Yamamoto Y, Kiyanotani T *et al.* Peripheral nerve regeneration across an 80-mm gap bridged by a polyglycolic acid (PGA)-collagen tube filled with laminin-coated collagen fibers: a histological and electrophysiological evaluation of regenerated nerves. *Brain Research* 2000;**868**:315-28.

Matz MV, Fradkov AF, Labas YA, Savitsky AP, Zaraisky AG, Markelov ML *et al.* Fluorescent proteins from nonbioluminescent Anthozoa species. *Nature Biotechnology* 1999; **17**:969-73.

Maurel P, Salzer JL. Axonal regulation of Schwann cell proliferation and survival and the initial events of myelination requires PI-3 kinase activity. *Journal of Neuroscience* 2000;**20**:4635-45.

McAllistair RMR, Gilbert SEA, Calder JS, Smith PJ. The epidemiology and management of upper limb peripheral nerve injuries in modern practice. *Journal of Hand Surgery (British and European Volume)* 1996;**21B**:4-13.

McKoy G, Ashley W, Mander J, Yang S-Y, Williams N, Russell B *et al.* Expression of insulin growth factor-1 splice variants and structural genes in rabbit skeletal muscle induced by stretch and stimulation. *Journal of Physiology* 1999;**516**:583-92.

McLaren A. Ethical and social considerations of stem cell research. *Nature* 2000;**414**:129-31.

McMahon SB, Armanini MP, Ling LH, Philipps HS. Expression and coexpression of trk receptors in subpopulations of adult primary sensory neurons projected to identified peripheral targets. *Neuron* 1994;**12**:1161-71.

Mezey E, Chandross KJ, Harta G, Maki RA, McKercher SR. Turning blood into brain: cells bearing neuronal antigens generated in vivo from bone marrow. *Science* 2000;**290**:1779-82.

Miller C, Jeftinija S, Mallapragada S. Micro-patterned Schwann cell-seeded biodegradable polymer substrates significantly enhance neurite alignment and outgrowth. *Tissue Engineering* 2001;**7**:705-15.

Miller C, Shanks H, Witt A, Rutkowski G, Mallapragada S. Orientated Schwann cell growth on micropatterned biodegradable polymer substrates. *Biomaterials* 2000;**22**:1263-9.

Mimura T, Dezawa M, Kanno H, Sawada H, Yamamoto I. Peripheral nerve regeneration by transplantation of bone marrow stromal cell-derived Schwann cells in adult rats. *Journal of Neurosurgery* 2004;**101**:806-12.

Minghetti L, Goodearl ADJ, Mistry K, Stroobant P. Glial growth factors I-III are specific mitogens for glial cells. *Journal of Neuroscience Research* 1996;**43**:684-93.

Mirsky R, Jessen K. The neurobiology of Schwann cells. *Brain Pathology* 1999;**9**:293-311.

Mohanna P-N, Terenghi G, Wiberg M. Composite PHB-GGF conduit for long nerve gap repair: a long-term evaluation. *Scandinavian Journal of Plastic and Reconstructive Surgery and Hand Surgery* 2005;**39**:129-37.

Mohanna P-N, Young R.C., Wiberg M, Terenghi C. A composite poly-hydroxybutyrate-glial growth factor conduit for long nerve gap repairs. *Journal of Anatomy* 2003;**203**:553-65.

Morin JG, Hastings JW. Energy transfer in a bioluminescent system. *Journal of Cellular Physiology* 1971;**77**:313-8.

Morise H, Shimomura O, Johnson FH, Winant J. *Biochemistry* 1974;**13**:2656-62.

Morrison SJ, Prowse KR, Ho P, Weissman IL. Telomerase activity of haematopoietic cells is associated with self-renewal potential. *Immunity* 1996;**5**:207-16.

Morrison SJ, Shah NM, Anderson DJ. Regulatory mechanisms in stem cell biology. *Cell* 1997;**88**:287-98.

Morrison SJ, White PM, Zock C, Anderson DJ. Prospective identification, isolation by flow cytometry, and in-vivo self-renewal of multipotent mammalian neural crest stem cells. *Cell* 1999;**96**:737-49.

Mosahebi A, Woodward B, Green C, Martin R, Terenghi G. Long-term effect of vital labelling on mixed Schwann cell cultures. *The Histochemical Journal* 2000;**32**:337-43.

Mosahebi A, Fuller P, Wiberg M, Terenghi G. Effect of allogeneic Schwann cell transplantation on peripheral nerve regeneration. *Experimental Neurology* 2002;**173**:213-23.

Mosahebi A, Wiberg M, Terenghi G. Addition of Fibronectin to Alginate Matrix Improves Peripheral Nerve Regeneration in Tissue-Engineered Conduits. *Tissue Engineering* 2003;**9**:209-18.

Mosahebi A, Woodward B, Wiberg M, Martin R, Terenghi G. Retroviral labeling of Schwann cells: In vitro characterization and in vivo transplantation to improve peripheral nerve regeneration. *GLIA* 2001;**34**:8-17.

Munson JB, McMahon SB. Effects of GDNF on axotomised sensory and motor neurons in adult rats. *European Journal of Neuroscience* 1997;**9**:1126-9.

Muraglia A, Cancedda R, Quarto R. Clonal mesenchymal progenitors from human bone marrow differentiate in vitro according to a hierarchial model. *Journal of Cell Science* 2000;**113**:1161-6.

Murakami T, Fujimoto Y, Yasunaga Y, Ishida O, Tanaka N, Ikuta Y *et al.* Transplanted neuronal progenitor cells in a peripheral nerve gap promote nerve repair. *Brain Research* 2003;**974**:17-24.

Navarro X, Valero A, Guidino G, Fores J, Rodriguez FJ, Verdu E *et al.* Ensheathing glia transplants promote dorsal root regeneration and spinal reflex restitution after multiple rhizotomy. *Annals of Neurology* 1999;**45**:207-15.

Neff NT, Prevette D, Houenou L, Lewis MD, Glicksman MA, Yin QW. Insulin-like growth factors: Putative muscle-derived trophic agents that promotes motoneuron survival. *Journal of Neurobiology* 1993;**24**:1578-88.

Neugebauer KM, Tomaselli KJ, Reichardt LF. N-cadherin, N-CAM and integrin promote retinal neurite outgrowth on astrocytes in vitro. *Journal of Cell Biology* 1988;**107**:1177-89.

Neumann P, Bradke F, Tessier-Lavigne M, Basbaum AI. Regeneration of sensory axons within the injured spinal cord induced by intraganglionic cAMP elevation. *Neuron* 2002;**34**:893.

Niere M, Gass R, Sturany S, Volkmer H. Combination of engineered neural cell adhesion molecules and GDF-5 for improved neurite extension in nerve guide concepts. *Biomaterials* 2005;**27**:3432-40.

Noble J, Munro CA, Prasad VS, Midha R. Analysis of Upper and Lower Extremity Peripheral Nerve Injuries in a Population of Patients with Multiple Injuries. *The Journal of Trauma: Injury, Infection, and Critical Care* 1998;**45**:116-22.

Novikova L, Novikov L, Kellerth JO. Effects of neurotransplants and BDNF on the survival and regeneration of injured adult spinal motoneurons. *European Journal of Neuroscience* 1997;**9**:2774-7.

O'Leary MT, Blakemore WF. Use of a rat Y chromosome probe to determine the long-term survival of glial cells transplanted into areas of CNS demyelination. *Journal of Neurocytology* 1997;**26**:191-206.

Obremski VJ, Bunge MB. Addition of purified basal lamina molecules enables Schwann cell ensheathment of sympatheic neurites in culture. *Developmental Biology* 1995;**168**:124-37.

Orlic D, Kajstura J, Chimenti S, Jakoniuk I, Anderson SM, Li B *et al.* Bone marrow cells regenerate infarcted myocardium. *Nature* 2001;**410**:701-5.

Owen ME, Friedentstein AJ. Cell and molecular biology of vertebrate hard tissues. 1988.

Pellegrino RG, Spencer PS. Schwann cell mitosis in response to regenerating peripheral axons in vivo. *Brain Research* 1985;**341**:16-25.

Penn RD, Kroin JS, York MM, Cederbaum JM. Intrathecal ciliary neurotrophic factor delivery for treatment of amyotrophic lateral sclerosis (phase I trial). *Neurosurgery* 1997;**40**:94-9.

Pittenger MF, Mackay AM, Beck SC, Jaiswal RK, Douglas R, Mosca JD *et al.* Multilineage potential of adult human mesenchymal stem cells. *Science* 1999;**284**:143-7.

Popov S. Forward plasma membrane flow in growing nerve processes. *Science* 1993;**259**:244-6.

Prasher DC. Using GFP to see the light. *Trends in Genetics* 1995;**11**:320-3.

Prasher DC, Eckenrode VK, Ward WW, Prendergast FG, Cormier MJ. Primary structure of the *Aequorea victoria* green fluorescent protein. *Gene* 1992;**111**:229-33.

Prockop DJ. Marrow stromal cells as stem cells for non-haematopoietic tissues. *Science* 1997;**276**:71-4.

Quesenberry PJ, Becker PS. Stem cell homing: Rolling, crawling and nesting. *Proceedings of the National Academy of Sciences U.S.A.* 1998;**95**:15155.

Rabinovsky ED, Gelir E, Gelir S, Lui H, Kattash M, Demayo FJ *et al.* Targeted expression of IGF-I transgene to skeletal muscle accelerates muscle and motor neuron regeneration. *FASEB Journal* 2003;**17**:53-5.

Radtke C, Akiyama Y, Langford KL, Vogt PM, Krause DS, Kocsis JD. Integration of engrafted Schwann cells into injured peripheral nerve: axonal association and nodal formation on regenerated axons. *Neuroscience Letters* 2005;**387**:85-9.

Raivich G, Bohatschek M, Da Costa C, Iwata O, Galiano M. The AP-1 transcription factor c-Jun is required for efficient axonal regeneration. *Neuron* 2004;**43**:57-67.

Ramon-Cueto A, Avila J. Olfactory ensheathing glia: properties and function. *Brain Research Bulletin* 1998;**46**:175-87.

Ramon-Cueto A, Nieto-Sampedro M. Regeneration into the spinal cord of transected dorsal root axons is promoted by ensheathing glia transplants. *Experimental Neurology* 1994;**127** :232-44.

Rangappa N, Romeo A, Nelson KD, Eberhart RC, Smith GM. Laminin-coated poly(L-lactide) filaments induce robust neurite growth while providing directional orientation. *Journal of Biomedical Materials Research* 2000;**51**:625-34.

Rathjen FG. A neurite out-growth promoting molecule in developing fibre tracts. *Trends in Neuroscience* 1988;**11**:183-4.

Reichardt LF, Tomaselli KJ. Extracellular matrix macromolecules and their receptors: Functions in neuron development. *Annual Review of Neuroscience* 1991;**14**:531-70.

Reynolds BA, Weiss S. Generation of neurons and astrocytes from isolated cells of the adult mammalian central nervous system. *Science* 1992;**255**:1707-10.

Reynolds BA, Weiss S. Clonal and population analyses demonstrate that an EGF-responsive mammalian embryonic CNS precursor is a stem cell. *Developmental Biology* 1996;**175**:1-13.

Reynolds ML, Woolf CJ. Reciprocal Schwann cell-axon interaction. *Current Opinion in Neurobiology* 1993;**3**:683-93.

Rich KM, Disch SP, Eichler ME. The influence of regeneration and nerve growth factor on the neuronal cell body reaction to injury. *Journal of Neurocytology* 1989;**18**:567.

Rifle G, Mousson C. Donor-derived haematopoietic cells in organ transplantation: a major step towrads allograft tolerance? *Transplantation* 2003;**75**:3S-7S.

Rios JC, Melendez-Vasquez CV, Einheber S, Lustig M, Grumet M, Hemperly J *et al.* Contactin-associated protein (Caspr) and contactin form a complex that is targeted to the paranodal junctions during myelination. *Journal of Neuroscience* 2000;**20**:8354-64.

Rodriguez FJ, Verdu E, Ceballos D, Navarro X. Nerve guides seeded with autologous Schwann cells improve nerve regeneration. *Experimental Neurology* 2000;**161**:571-84.

Rutishauser U, Landmesser L. Polsialic acid in the vertebrate nervous system: a promoter of plasticity in cell-cell interactions. *Trends in Neuroscience* 1996;**19**:422-7.

Saffell J, Walsh FS, Doherty P. Direct activation of second messenger pathways mimics cell adhesion molecule-dependent neurite outgrowth. *Journal of Cell Biology* 1992;**118**:663-70.

Saito H, Nakao Y, Takayama S, Toyama Y, Asou H. Specific expression of HNK-1 carbohydrate epitope and NCAM on femoral nerve Schwann cells in mice. *Neuroscience Research* 2005;**53**:322.

Saito T, Kuang JQ, Bittra B, Al-Khaldi A, Chin RC. Xenotransplant cardiac chimera: immune tolerance of adult stem cells. *Annals of Thoracic Surgery* 2002;**74**:19-24.

San Pietri RM, Prendergast FG, Ward WW. *Photochemistry and Photobiology* 1993;**57**:63S.

Sanchez-Ramos J, Song S, Cardozo-Pelaez F, Hazzi C, Stedeford T, Willing A *et al.* Adult bone marrow stromal cells differentiate into neural cells in vitro. *Experimental Neurology* 2000;**164**:247-56.

Santos-Silva A, Calvacante LA. Expression of the non-compact myelin protein 2'-3'-cyclic nucleotide 3'-phosphodiesterase (CNPase) in olfactory bulb ensheathing glia from explant cultures. *Neuroscience Research* 2001;**40**:189-93.

Santos X, Rodrigo J, Hontanilla B, Bilbao G. Evaluation of peripheral nerve regeneration by nerve growth factor locally administered with a novel system. *Journal of Neuroscience Methods* 1998;**85**:119-27.

Sayers ST, Khan N, Ahmed Y, Shahid R, Khan T. Preparation of brain-derived neurotrophic factor and neurotrophin-3-Secreting Schwann cells by infection with a retroviral vector. *Journal of Molecular Neuroscience* 1998;**10**:143-59.

Scarpini E, Baron P, Scarlatto G. Human Schwann cells in culture. In Gorio A, ed. *Neuroregeneration*, pp 123-44. New York: Raven Press, Ltd., 1993.

Schaal SM, Kitay BM, Cho K.S., Lo TP, Barakat DJ, Marcillo AE *et al.* Schwann cell transplantation improves reticulospinal axon growth and forelimb strength after severe cervical spinal cord contusion. *Cell Transplantation* 2007;**16**:207-28.

Schuldiner M, Yanuka O, Itskovitz-Eldor J, Melton D, Benvinisty N. Effects of eight growth factors on the differentiation of cells derived from human embryonic stem cells. *Proceedings of the National Academy of Sciences* 2000;**97**:11307-12.

Seckel BR. Enhancement of peripheral nerve regeneration. *Muscle and Nerve* 1990;**13**:785-800.

Seilheimer B, Schachner M. Studies of adhesion molecules mediating interactions between cells of peripheral nervous systems indicate a major role for L1 in mediating sensory neuron growth on Schwann cells in culture. *Journal of Cell Biology* 1998;**107**:341-51.

Sendtner M, Gotz R, Holtmann B, Thoenen H. Endogenous ciliary neurotrophic factor is a lesion factor for axotomised motoneurons in adult mice. *Journal of Neuroscience* 1997;**17**:6999-7006.

Seydoux G, Mello CC, Pettitt J, Wood WB, Priess JR, Fire A. Repression of gene expression in the embryonic germ lineage of C. elegans. *Nature* 1996;**382**:713-6.

Shah NM, Groves A, Anderson DJ. Alternative neural crest cell fates are instructively promoted by TGFβ superfamily members. *Cell* 1996;**85**:331-43.

Shah NM, Marchionni MA, Stroobant P, Anderson DJ. Glial growth factor restricts mammalian neural crest stem cells to a glial fate. *Cell* 1994;**77**:349-60.

Shapiro HT. Ethical dilemmas and stem cell research. *Science* 1999;**285**:2065.

Sherer RP. The biology and pathobiology of Schwann cells. *Current Opinions in Neurobiology* 1997;**10** :386-97.

Sherley JL. Asymmetric cell kinetics genes: the key to expansion of adult stem cells in culture. *Stem Cells* 2002;**20**:561-72.

Shibuya Y, Mizoguchi A, Takeichi M, Shimada K, Ide C. Localization of N-cadherin in the normal and regenerating nerve fibres of the chicken peripheral nervous system. *Neuroscience* 1995;**67**:253-61.

Shimomura O, Johnson FH, Saiga Y. Extraction, purification, and properties of aequorin, a bioluminescent protein from the luminous hydromedusan. *J.Cell.Comp.Physiol.* 1962;**59**:223-39.

Simmons PJ, Torok-Storb B. Identification of stromal cell precursors in human bone marrow by a novel monoclonal antibody, STRO-1. *Blood* 1991;**78**:55-62.

Skottner A, Kanje M, Widegram D, Lundborg G, Logberg E. Insulin-like growth factor-I (IGF-I) stimulates peripheral nerve regeneration in rats. *Journal of Clinical Investigation* 1987;**10**:25.

Sørensen J, Haase G, Krarup C, Gilgenkrantz H, Kahn A, Schmalbruch H. Gene transfer to Schwann cells after peripheral nerve injury: a delivery system for therapeutic agents. *Annals of Neurology* 1998;**43**:205-11.

Squitti R, De Stefano ME, Edgar D, Toschi G. Effects of axotomy on the expression and ultrastructural localization of N-cadherin and neural cell adhesion molecule in the quail ciliary ganglion: an in vivo model of neuroplasticity. *Neuroscience* 1999;**91**:707-22.

Sterman AB, Delannoy MR. Cell body responses to axonal injury: traumatic axotomy versus toxic neuropathy. *Experimental Neurology* 1985;**89**:408-19.

Sterne GD, Coulton GR, Brown RA, Green CJ, Terenghi G. Neurotrophin-3-enhanced nerve regeneration selectively improves recovery of muscle fibers expressing myosin heavy chains 2b. *Journal of Cell Biology* 1997;**139**:709-15.

Stoll G, Griffin JW, Li C.Y., Trapp BD. Wallerian degeneration in the peripheral nervous system: participation of both Schwann cells and macrophages in myelin degradation. *Journal of Neurocytology* 1989;**18**:671-83.

Studeny M, Marini FC, Champlin RE, Zompetta C, Fidler IJ, Andreeff M. Bone marrow-derived mesenchymal stem cells as vehicles for interferon-beta delivery into tumors. *Cancer Research* 2002;**62**:3603-8.

Sunderland S. Nerves and Nerve Injuries. New York: Churchill Livingstone, 1978.

Syroid DE, Zorick TS, Arbet-Engels C, Kilpatrick TJ, Eckhart W, Lemke G. A role for insulin-like growth factor-I in the regulation of Schwann cell survival. *The Journal of Neuroscience* 1999; **19**:2059-68.

Tacke R, Martini R. Changes in expression of mRNA specific for cell adhesion molecules (L1 and NCAM) in the transected peripheral nerve of the adult rat. *Neuroscience Letters* 1990;**120**:227-30.

Takada T, Iida K, Awaji T, Itoh K, Takahashi R, Shibui A *et al.* Selective production of transgenic mice using green fluorescent protein as a marker. *Nature Biotechnology* 1997;**15**:458-61.

Takeichi M. Cadherin cell adhesion cell receptors as a morphogenic regulator. *Science* 1991;1451-5.

Tepass U, Truong D, Godt D. Cadherins in embryonic and neural morphogenesis. *Nature Reviews Molecular and Cellular Biology* 2000;**1**:91-100.

Terenghi G. Peripheral nerve regenration and neurotrophic factors. *Journal of Anatomy* 1999;**194**:1-14.

Terzis JK, Smith K. The Peripheral Nerve: Structure, Function and Reconstruction. Raven Press, 1990.

Thomaidou D, Coquillat D, Stathis M, Noda M, Rougon G, Matsas R. Soluble forms of NCAM and F3 neuronal cell adhesion molecules promote Schwann cell migration: identification of protein tyrosine phosphatases ζ / β as the putative F3 receptors on Schwann cells. *Journal of Neurochemistry* 2001;**78**:767-78.

Thomas ED. Frontiers in bone marrow transplantation. *Blood Cells* 1991;**17**:259-67.

Thompson DM, Buettner HM. Schwann cell response to micropatterned laminin surfaces. *Tissue Engineering* 2001;**7**:247-65.

Thompson JA, Itskovitz-Eldor J, Shapiro SS, Waknitz MA, Swiergiel JJ, Marshal VS *et al.* Embryonic stem cells derived from human blastocysts. *Science* 1998;**282**:1145-7.

Thompson SWN, Priestly JV, Southall A. gp130 cytokines, leukaemia inhibitory factor and interleukin-6 induce neuropeptide expression in intact adult sensory neurons in vivo: time course, specificity and comparison with sciatic nerve axotomy. *Neuroscience* 1998;**84**:1247-55.

Thornton MR, Mantovani MA, Birchall MA, Terenghi G. Quantification of N-CAM and N-cadherin expression in axotomized and crushed rat sciatic nerve. *Journal of Anatomy* 2005;**206**:69-78.

Thornton MR, Shawcross SG, Mantovani C, Kingham PJ, Birchall MA, Terenghi G. Neurotrophin 3 and neurotrophin 4 differentially regulate NCAM, L1 and N-cadherin expression during peripheral nerve regeneration. *Biotechnology and Applied Biochemistry* 2007;**Epub ahead of print**.

Till JE, McCulloch EA. A direct measurement of the radiation sensitivity of normal mouse bone marrow cells. *Radiation Research* 1961;**14**:1419-30.

Tohill M, Terenghi G. Stem cell therapy for peripheral nerve inhjuries. *Biochemistry and applied biotechnology* 2004;**40**:17-24.

Tohill M, Mann DJ, Mantovani C, Wiberg M, Terenghi G. Green fluorescent protein is a stable morphological marker for schwann cell transplants in bioengineered nerve conduits. *Tissue Engineering* 2004;**10**:1369-7.

Tohill M, Mantovani C, Wiberg M, Terenghi G. Rat bone marrow mesenchymal stem cells express glial cell markers and stimulate nerve regeneration. *Neuroscience Letters* 2004;**362**:200-3.

Toma JG, Akhaven M, Fernandes KJ. Isolation of multipotent adult stem cells from the dermis of mammalian skin. *Nature Cell Biology* 2001;**3**:778-84.

Tomita M, Adachi Y, Yamada H, Takahashi K, Kiuchi K, Oyaizu H *et al.* Bone marrow-derived stem cells can differentiate into retinal cells in injured rat retina. *Stem Cells* 2002;**20**:279-83.

Tong XJ, Hirai K, Shimada H, Mizutami Y, Izumi T, Toda N *et al.* Sciatic nerve regeneration navigated by laminin-fibronectin double-coated biodegradable collagen grafts in rats. *Brain Research* 1994;**663**:155-62.

Tremain N, Korkko J, Kopen GC, DiGirolamo C, Phinney DG. MicroSAGE analysis of 2,353 expressed genes in a single cell-derived colony of undifferentiated human mesenchymal stem cells reveals mRNAs of multiple cell lineages. *Stem Cells* 2001;**19**:408-18.

Tse WT, Pendleton D, Beyer W, D'Andrea A, Guinan EC. Suppression of allogeneic T-cell proliferation by human marrow stromal cells: implications in transplantation. *Transplantation* 2003;**75**:389-97.

Tsen G, Halfter W, Kroger S, Cole GJ. Agrin is a heparan sulphate proteoglycan. *Journal of Biology* 1995;**270**:3392-9.

Tsien RY. The green fluorescent protein. [Review] [114 refs]. *Annual Reviews Biochemistry.* 1998;**67**:509-44.

Tsien RY, Bacskai BJ, Adams SR. FRET for studying intracellular signalling. *Trends in Cell Biology* 1993;**3**:242-5.

Tuszynski MH, Gabriel K, Gage FH, Suhr S, Meyer S, Rosetti A. Nerve Growth Factor Delivery by Gene Transfer Induces Differential Outgrowth of Sensory, Motor, and Noradrenergic Neurites after Spinal Cord Injury. *Experimental Neurology* 1996;**137**:157-73.

Uludag H, De Vos P, Tresco PA. Technology of mammalian cell encapsulation. *Advanced Drug Delivery Reviews* 2000;**42**:29-64.

Verdu E, Navarro X, Gudino-Cabrera G, Rodriguez FJ, Ceballos D, Valero A *et al.* Olfactory bulb ensheathing cells enhance peripheral nerve regeneration. *Neuroreport* 1999;**10**:1097-101.

Verfaillie CM. Soluble growth factors produced by human bone marrow stroma increase cytokine-induced proliferation and maturation of primitive haematopoietic progenitors while preventing their terminal differentiation. *Blood* 1993;**82**:2045-53.

Vergani L, Di Giulio AM, Lossa M, Rossoni G, Muller EE, Gorio A. Systemic administration of insulin-like growth factor decreases motor neuron cell death and promotes muscle reinnervation. *Journal of Neuroscience Research* 1998;**54**:840-7.

Vogel G. Stem cell policy: Can adult stem cells suffice? *Science* 2001;**292**:1820-2.

Waller A. Experiments on the section of the glossopharyngeal and hypoglossal nerves of the frog and observations of the alterations produced thereby in the structure of their primative fibres. *Philosophical Transactions of the Royal Society London (Biology)* 1850;**140**:423-9.

Wanner IB, Guerra N, Mahoney J, Kumar A, Wood PM, Mirsky R *et al.* Role of N-cadherin in Schwann cell precursors of growing nerves. *GLIA* 2006;**54**:459.

Wanner IB, Wood PM. N-cadherin mediates axon-aligned process growth and cell-cell interaction in rat Schwann cells. *Journal of Neuroscience* 2002;**22**:4066-79.

Wekerle T, Blaha P, Koporc Z, Bigenzahn S, Pusch M, Muehlbacher F. Mechanisms of tolerance induction through the transplantation of donor haematopoietic stem cells: central versus peripheral tolerance. *Transplantation* 2003;**75**:21S-5S.

Wewetzer K, Verdu E, Angelov DN, Navarro X. Olfactory ensheathing glia and Schwann cells: two of a kind? *Cell and Tissue Research* 2002;**309**:337-45.

Whitworth IH, Brown RA, Dore C, Green CJ, Terenghi G. Orientated mats of fibronectin as a conduit material for use in peripheral nerve repair. *Journal of Hand Surgery - British Volume* 1995;**20**:429-36.

Whitworth IH, Brown RA, Dore CJ, Anand P, Green CJ, Terenghi G. Nerve growth factor enhances nerve regeneration through fibronectin grafts. *Journal of Hand Surgery* 1996;**21**:514-22.

Williams PL, Hall SM. Prolonged in vivo observations of normal peripheral nerve fibres and their acute reactions to crush and deliberate trauma. *Journal of Anatomy* 1971;**108**:397-408.

Wilson T, Hastings JW. Bioluminescence. [Review] [163 refs]. *Annu.Rev.Cell Dev.Biol.* 1998;**14**:197-230.

Wislet-Gendebien S, Leprince P, Moonen G, Rogister B. Regulation of neural markers nestin and GFAP expression by cultivated bone marrow stromal cells. *Journal of Cell Science* 2003;**116**:3295-302.

Woodbury D, Schwarz EJ, Prockop DJ, Black IB. Adult rat and human bone marrow stromal cells differentiate into neurons. *Journal of Neuroscience Research* 2000;**61**:364-70.

Xu G, Nie DY, Wang WZ, Zhang PH, Shen J, Ang BT. Optic nerve regeneration in polglycolic acid-chitosan conduits coated with recombinant L1-Fc. *Neuroreport* 2004;**15**:2167-72.

Yang SY, Alnaqueeb M, Simpson H, Goldspink G. Cloning and characterization of an IGF-1 isoform expressed in skeletal muscle subjected to stretch. *Journal of Muscle Research and Cell Motility* 1996;**17**:487-95.

Yang SY, Goldspink G. Different roles of the IGF-1 Ec peptide (MGF) and mature IGF-I in myoblast proliferation and differentiation. *FEBS Letters* 2002;**522**:156-60.

Yin Q, Kemp GJ, Yu LG, Wagstaff SC, Frostick SP. Neurotrophin-4 delivery by fibrin glue promotes peripheral nerve regeneration. *Muscle and Nerve* 2001;**24**:345-51.

Yoshii S, Oka M. Peripheral nerve regeneration along collagen filaments. *Brain Research* 2001;**888**:158-62.

Yoshii S, Oka M, Akagi M, Nakamura T. Bridging a peripheral nerve defect using collagen filaments. *Journal of Hand Surgery - American Volume* 2001;**26**:52-9.

Young R, Wiberg M, Terenghi G. Poly-3-hydroxybutyrate (PHB): a resorbable conduit for long-gap repair in peripheral nerves. *British Journal of Plastic Surgery* 2002;**55**:235-40.

Zimmer M. Green fluorescent protein (GFP): applications, structure, and related photophysical behavior. [Review] [258 refs]. *Chem.Rev.* 2002;**102**:759-81.

APPENDIX A

1 Tissue culture

Reagent / Material	Supplier (code) Stock / working solution
Acetic acid	Sigma (46928)
alamarBlue™	Serotec (BUF012A)
Canada Balsalm mounting medium.....	Sigma
Cell filter (70μm).....	Falcon (2350)
Cell freezing medium.....	Cell growth medium + 10% DMSO
Cell growth medium.....	DMEM + 10% FCS + penicillin/streptomycin 100i.u.-100μg
Centrifuge.....	Labnet, USA
Chamber slides (2,4,8 chambers).....	Lab-Tek (Nalge Nunc International)
Class II ventilated laminar flow tissue culture hood.....	MDH, InterMed
CO_2 incubator (37°C).....	Shelab, Model: TC2323, BoroLab
CO_2 incubator (32 °C).....	EcoCell
Collagen (Type I, from rat tail).....	Sigma (27666)
Collagenase I.....	Worthington Biochemicals (CLS-I, 125U/mg) 1% working solution made with DMEM and aliquoted in 300μl, stored at -20°C.
Complement, rabbit anti-mouse.....	Cederlane Labs (CL3051) 2 vials reconstituted at a time, kept on ice at all times, 1ml sterile water added to each vial, filtered through a 0.45 μM filter, stored in liquid nitrogen as 250μl aliquots.
Cryovials.....	Falcon

Cytosine-β-D-arabinofuranoside.....	Sigma (C1768) Stock solution ~ 1mM: 2mg dissolved in 4 ml PBS, filtered 0.2 µm and stored at -20°C, 250µl aliquots
DMEM high glucose (4.5g/L glucose)..	Gibco (31966-021)
DMEM + Glutamax.....	Gibco (21885-025)
DMEM with HEPES.....	Gibco (22320)
DMSO (dimethylsulphoxide).....	Sigma (D2650)
Electronic Pipette Aid.....	IBS, Integra Biosciences
Fetal Calf Serum (FCS).....	Gibco (10108-165) Heat de-activated at 56°C for 35 minutes, stored at -20°C
Fibroblast Growth Factor (FGFb).....	Pepro Tech (100-18B)
Filters: 0.8, 0.45 and 0.2µm.....	Nalgene
Forksolin.....	Calbiochem (344270) 5mM stock solution made by dissolving 2.0525 mg/ml in DMSO, stored at -20°C, 50/100µl aliquots
Gentamicin 50mg/ml.....	Gibco
Glial Growth Factor II (GGF).....	CeNeS Pharmaceuticals Batch no. rhGGF2/030-040
Haemocytometer.....	Weber
Hank's medium (balanced salt soln.)...	Gibco (14170-088)
Hoechst nuclear labelling solution.....	Sigma (H33342)
Isopentane flasks.....	Bicell, Nihon Freezer Company Ltd.
Laminin (mouse).....	Sigma (L2020)
Marrow stromal cell growth medium...	α-MEM + 10% FCS + penicillin/streptomycin 100i.u.-100µg
α-MEM (Modified Eagle's Medium)...	Invitrogen (22571020)
ß-mercaptoethanol.....	Sigma (M7522)
Microscope (inverted tissue culture)....	Nikon
Mouse anti-mouse/rat Thy1.1.....	Serotec (MCA04G)
Needles 19, 21 and 23G.....	Sherwood Medical

Penicillin/Streptomycin.....	Gibco (15070-022) Working solution: 100 iu-100 µg/ml: 2ml of stock solution to 100ml of cell growth medium
Plastic Pipettes: 1,5,10,25 ml.....	Falcon
Plate Reader (96-well).....	Labsystem, MultiSkan MS
Platelet-Derived Growth Factor(PDGF)	Pepro Tech (100-13A)
Poly-D-Lysine.....	Sigma (P7280)
PT67 packaging cells.....	Clontech
PT67 packaging cells (with GFP).....	Miss Dawn Mann, Queen Victoria Hospital, East Grinstead
PT67 packaging cell growth medium....	DMEM(4.5g/L) + 10%FCS + penicillin/streptomycin 100i.u.-100µg
all-trans retinoic acid	Sigma (22301-8)
Schwann cell growth medium.....	Cell growth medium + 5 µM forskolin + GGF 126 ng/ml. To 100ml of cell growth medium 112 µl of forskolin stock 3 µl of GGF added
Syringe: 2, 5, 10ml.....	Becton & Dickenson
Tissue culture flask ($25cm^2$).....	Greiner Labortechnik (690175)
Tissue culture flask ($75cm^2$).....	Greiner Labortechnik (658175)
Tissue Culture Plates (24-well).....	Falcon
Tissue Culture Plates (6-well).....	Falcon
Tissue Culture Plates (96-well).....	Falcon
Trypsin 2.5%; lypophilised.....	Gibco (610-5095 AE) Rehydrated with Dulbecco's Phosphate Buffered Saline (without Ca^{2+} & Mg^{2+}) 800 µl aliquots stored at -20°C
Trypsin 0.25% / EDTA 0.02%.....	Gibco (45300-019)
Universal container 30, 50 ml.....	Falcon
Water, tissue culture grade.....	Sigma (W3500)

2 Matrices

Alginate (LVM / MVM).....	Pronova Biomedical, Oslo, Norway
Autoclave.....	Boxer, Borolabs, UK
Calcium Chloride.....	Sigma
Collagen (Type I, from rat tail).....	Sigma (27666)
Collagen gel (for conduits).....	Vitrogen
Fibronectin (from bovine plasma).....	Sigma (F4759; 1mg) Reconstituted in 1ml of 0.9% NaCl. Store at -20°C
Laminin.....	Sigma (L2020) Stock: 1mg/ml in Tris buffered NaCl stored at -20°C.

3 PHB and silicone conduits

Hamilton syringe (50µl).....	Hamilton, USA
Polyhydroxybutyrate sheets and dissociated fibres (PHB).....	Astra-tech, Sweden
Soldering iron, gas powered.....	Maplin, UK
Silicone conduits.....	Philip Harris Scientific (γ-irradiated)

4 Animal model

Micro-instruments.....	Mercian, UK
Chlorhexidine gluconate 0.5% w/v in 70% IMS.....	Adams Healthcare, UK
Halothane.....	Nicholas, UK
Oxygen.....	BOC, UK
Operating microscope.....	Zeiss, Germany
Rats, male Sprague Dawley, 6-8 weeks old, 200-250gms.....	Harlan, UK
Suture, 9/0 nylon.....	Ethicon, UK (W2898)
Suture, 4/0 vicryl.....	Ethicon, UK (W9825)
Temgesic.....	Phoenix Pharmaceuticals, UK

5 Tissue processing

Cryotome	Bright, UK
Dako hydrophobic pen	Dako (S2002)
Glass slides (+ Vectabond®)	Lab stock
OCT compound	Tissue-tek, Sakura, Japan
Sucrose/PBS	Lab stock
Triton-X	Sigma (X100)
Zamboni's fixative	Lab stock (see Appendix C)

6 Protein Quantitation

NanoOranage® Protein Quantitation Kit	Molecular Probes, Holland
PhastGel electrophoresis system	Pharmacia

7 Immunohistochemistry

7.1 Primary antibodies	Supplier	Dilution / Incubation
Glial fibrillary acidic protein (GFAP; rabbit polyclonal)	Sigma (G9269)	1:80 2hrs RT
Protein gene product (PGP9.5; mouse monoclonal)	Biogenesis, UK	1:2000 2hrs RT
Protein gene product (PGP9.5; rabbit polyclonal)	Affiniti, UK	1:1200 2hrs RT
Neural cell adhesion molecule (NCAM; rabbit polyclonal)	Chemicon, UK	1:500 2hrs RT
N-cadherin (NCAD; rabbit polyclonal	Santa Cruz Biotechnology, USA	1:20 2hrs RT
S100 (mouse monoclonal)	Affiniti (SA2102)	1:500 2hrs RT
S100 (rabbit polyclonal)	Dako (Z311)	1:1000 2hrs RT
Thy 1.1	Serotec (MCA04G)	1:500 2hrs RT

7.2 Secondary antibodies

Cy3 goat anti-mouse.....	Amersham (PA43002)	1:100 2hrs RT
Cy3 goat anti-rabbit.....	Amersham (PA43003)	1:100 2hrs RT
FiTC anti-mouse secondary.....	Vector labs (FI2000)	1:100 2hrs RT
FiTC anti-rabbit secondary.....	Vector labs (FI1000)	1:100 2hrs RT

7.3 Additional materials

Antibody diluent.....	Lab stock
Digital camera.....	Spot™, Diagnostic Instruments Inc., USA
Fluorescence mounting medium (Vectorshield®).....	Vector Labs, UK
Giemsa stain	Sigma (GS-500) Stock 0.4%w/v in phosphate buffered methanol. Working solution: 5% (of stock) in distilled water
Micoscope.....	Olympus BX60, Japan
Normal goat serum.....	Sigma
Normal rabbit serum.....	Sigma
Syringe driver.....	Genie UK

7.4 Software

Image-Pro® Plus version 4.0.....	Media Cybernetics, USA
GraphPad Prism version 4.0.....	GraphPad Software, San Diego, California, USA
Spike 2 program.....	Cambridge Electronic Design Limited, UK

APPENDIX B

Preparation of coated tissue flasks

Poly-D-lysine (PDL)

0.1 mg/ml of PDL (Sigma) was prepared with culture grade distilled water. One ml of PDL solution was put in a $25cm^2$ flask (or 2 ml in a $75cm^2$ flask), the flask was gently shaken to cover the entire surface evenly. The flask was kept flat at room temperature for 15 minutes then washed twice with sterile water and left to dry in the hood. Coating of chamber slides (Lab-Tek, Nalge Nunc International) was similarly carried out, using PDL solution sparingly. The PDL coated flasks were stored at room temperature and used for up to 6 months following coating.

PDL and laminin (double coating)/ Laminin alone

First the culture flask is coated with PDL as above, 20 μg/ml solution of natural mouse laminin (Sigma) was prepared in DMEM, and 0.1 ml solution/cm^2 of the flask was used to coat the surface area. The flask was gently shaken to spread the solution evenly and kept flat in a CO_2 incubator at 37°C, for 45 minutes, without letting the laminin to dry.

Fibronectin

Fibronectin was dissolved in Hank's medium to give a concentration of 20μg/ml. The surface are of the tissue culture plastic to be covered was calculated and the corresponding volume of fibronectin solution added to give a coating of $2\mu g/cm^2$. The plate/flask is then incubated at room temperature for one hour following which the solution is aspirated and washed with distilled water. The plates/flasks are either used immediately or air dried and stored at 2-8°C.

Collagen

For coating tissue culture plastic collagen was dissolved in 0.02N acetic acid to give a concentration of 50μg/ml. The area of the culture dish to be plated was calculated and the corresponding amount of collagen solution was added to give coating at 5μg/cm^2 or 10μg/cm^2. The collagen solution is left on the culture dish for one hour at room temperature. The collagen solution is then aspirated and the culture dish washed with PBS. The dish is then air dried and used immediately or stored under sterile conditions at 2-8°C for up to one week.

APPENDIX C

Silanisation

Growth factors tend to adhere to surfaces by electrostatic interaction, all glassware and plasticware including polypropylene pipette tips and Eppendorfs for handling and storage were silanised to minimise adsorption. The silanisation was carried out by a published methods (Molecular Cloning: A Laboratory Manual, eds: Sambrook, Fritsch & Manniatis):

Put 1 ml of dichlorodimethylsilane in a small bowl inside a large desiccator with the items to be silanised. Attach a vacuum pump to the desiccator in an extraction hood and apply suction until the dichlorodimethylsilane starts to boil and clamp and switch off the pump. Leave for two hours and open the desiccator under an extraction hood. Rinse the items 3 times with distilled water and dry overnight. Sterilise with gamma-irradiation camera.

Vectabond™ coated slides

The slides were treated to improve adhesion of sections and prevent loss of tissue as a result of washes required for immunohistochemistry protocols. Place clean slides in metal slide racks. Immerse slides in acetone for 5 minutes, then remove and drain well. Prepare Vectabond™ reagent treatment solution by adding 7 ml of reagent to 350 ml acetone and mixing well. Immerse slides in Vectabond™ reagent treatment solution for 5 minutes, then remove and drain well. Rinse slides by dipping rack several times into distilled water over 30 seconds. Avoid the creation of bubbles during this process. Tap slide rack before drying to remove excess water droplets. Dry slides at 37°C.

General laboratory solutions

Antibody diluent

0.3% Triton X-100; 0.1% bovine serum albumin (BSA); 0.1% sodium azide.

For 1200ml: 0.1g BSA, 0.1g sodium azide, 30µl Triton X-100.

Dissolve in 100 ml of PBS.

4% Paraformaldehyde

Dissolve 40g of paraformaldehyde in 800 ml PBS at 60°C and stir until solution is clear. If necessary, add a few drops of 10M NaOH to clear the solution. Adjust volume to one litre and allow to cool before use. Store at 4°C and use within 24 hours. Alternatively, divide into aliquots and keep frozen at -20°C until required. Defrost at room temperature or by immersing in a beaker of hot water. Once defrosted, do not re-freeze.

Phosphate buffered saline (PBS)

To make 10 litres:

Add the following to 5 litres of distilled water:

NaCl 87.9g;

KH_2PO_4 2.72g;

$NaHPO_4(H_2O)$ 12: 3.9g.

Stir and leave for 2 hours, then add 5 litres of distilled water. Check pH and adjust to pH 7.3. Use 8 hours after mixing.

Sucrose-PBS

15% sucrose + 0.1% sodium azide in PBS.

For one litre: 150g sucrose; 1g sodium azide.

Dissolve in 700ml PBS and when dissolved make up to 1 litre.

Zamboni's solution

85ml of 2% paraformaldehyde in PBS.

15ml of saturated picric acid.

Dissolve 20g paraformaldehyde in 800ml PBS AT 60°C and stir until solution is clear. Adjust volume to one litre and allow to cool. Add appropriate amount of saturated picric acid and store at 4°C until use.

Haematoxylin and eosin staining

Place slides in haematoxylin for 30 seconds.

Rinse in tap water.

Wash in tap water.

Place in 0.15M eosin for 6 minutes.

Wash in tap water.

Place in 70% IMS for one minute, 100% IMS for one minute, and xylene for one minute. Mount with DPX and a coverslip.

Giemsa stain

Wash chamber slide with PBS. Remove rubber gasket before exposure to alcohol. Fix in 100% IMS for 6 minutes and air dry. Stain in Giemsa solution (see Appendix A) for 15-60mins. Wash in de-ionised water and air dry. Mount with DPX and a coverslip.